The use of stable isotopes and chloride to assess evaporation and transpiration impacts from flood irrigation

Submitted by

Jason van den Akker
B.Sc

As a requirement in full for the degree of
Master of Science

In the

School of the Environment
Flinders University

10 September 2010

Summary

Flood irrigation is traditionally believed to be particularly inefficient in terms of its salinity impact on the aquifer due to evaporation of the surface water from delivery channels and flood irrigation bays. During flood irrigation the loss of water to the atmosphere occurs through evaporation and transpiration. Both processes concentrate salts of irrigation and soil waters, however evaporation can be managed and is the undesirable component of water loss from any irrigation practice. In principle, the higher the proportion of water loss by transpiration through crop plants relative to evaporation, the higher the efficiency of water use.

Whilst transpiration by a crop can be reasonably estimated using the standard FAO56 Pan evaporation methodology, the evaporation of both irrigation water and shallow soil water at different points in a flood irrigation network can be much more difficult to quantify.

Enrichment of stable isotopes δ^2H and δ^{18}O in residual irrigation and soil waters can provide a sensitive indicator of evaporation losses, exclusive of transpiration and thus provide a parameter relevant to water use efficiency in flood irrigation systems. Isotopic techniques for measuring evaporation from lakes is theoretically sound (Dincer, 1968; Gonfiantin, 1986; Gat 1981, 1991; Simpson et al., 1987, Froechlich et al., 2005) but few applications to irrigation waters are reported.

The body of this research aims to address: 1) the development of new techniques on the basis of stable isotopes δ^2H and δ^{18}O to quantify evaporations losses from flood irrigation and 2) increase the understanding of the sources of salinity via assessment of the independent impacts evaporation and transpiration have on infiltrating irrigation waters. It does so by examining the isotopic and chloride signatures of irrigation water, soil water, groundwater and rainfall at four flood irrigation study sites in the South East of South Australia.

This research begins with the trail of two analytical models to determine evaporation rates from a variety of flood irrigation settings, on the basis of stable isotopes and calibrated against Class A pan experiments conducted in parallel. The isotopic models applied in this setting were previously developed to calculate evaporation from lakes and river systems, and the validity of applying the two

models in this setting was achieved by comparison with conventional non-isotopic methods. In contrast to nearly all of the established empirical techniques employed in agricultural water budgets which lump E and T together, the approaches applied here offers a method to quantify E losses, independent from T in a flood irrigation setting.

Results showed that heavy isotope enrichment of applied irrigation waters varied between each of the study sites. Isotope enrichment was notably different between irrigation bays that drained rapidly (+0.05 ‰ to +0.18 ‰ for $\delta^{18}O$ and +1.7 ‰ to +2 ‰ for $\delta^{2}H$) to those where ponding occurred for up to 18 h post application (+1 ‰ to +2 ‰ for $\delta^{18}O$ and +2 ‰ to 7.5 ‰ for $\delta^{2}H$). When compared to local pan enrichment, these isotope enrichments corresponded to evaporation losses of 0.2 % to 2.7 % (0.5 mm to 4 mm) and 2 % to 5 % (4.5 mm to 7 mm) respectively per irrigation.

This work was then extended to consider and quantify the independent impacts transpiration and evaporation have on infiltrating irrigation waters and residual soil waters. This research has provided new insights into the sources of salinity during flood irrigation. The combination of $\delta^{2}H$, $\delta^{18}O$ and chloride measurements of irrigation water and soil water, along with soil moisture monitoring post irrigation, was successful in identifying transpiration as the dominant cause of water loss from flood irrigation. Results showed that transpiration amounted to 88% of atmospheric losses and the largest contributor to salinity impacts during flood irrigation. The salinity impact (accumulation of salts in the soil) as a result of transpiration was 3 to 50 times greater than the salinity impacts caused by evaporation, and was therefore the dominant mechanism responsible for groundwater salinity increase beneath flood irrigated areas.

In the final stages of this research a Local Meteoric Water Line for the South East of South Australia was developed, to which a qualitative comparison of evaporation rates from the soil zone and irrigation waters could be compared. The LMWL developed here represents the first published LMWL based on direct precipitation for any location in the South East of South Australia.

This thesis presents the first fully integrated assessment of evaporation and transpiration in a flood irrigation setting. Ultimately this research assists in the understanding of these processes during flood irrigation and valuable new insights

into evaporation losses and sources of salinity across different flood irrigation systems and thus suggests which management strategies are more likely to improve water use efficiency and water quality.

Declaration of Originality

I hereby declare that this thesis does not include (without acknowledgment) any material previously submitted for a degree or diploma in any university other than Flinders; and that to the best of my knowledge it does not contain material published or written by another person (except where reference is made in the text).

Jason van den Akker

Acknowledgements

My special thanks go to my supervisors Dr John Hutson and Professor Craig Simmons from the School of the Environment and the National Centre for Groundwater Research and Training, Flinders University, for their guidance, inspiration and motivation.

The cooperation of the flood irrigators from the townships of Padthaway and Keith who participated in this study is acknowledged, with thanks for permission to conduct this research on their property.

The South East Natural Resource Management Board (SENRM) and The Department for Water (DFW) are acknowledged for funding this research.

Contents

Appendices

Notations

I	Irrigation	mm
P	Precipitation	mm
D	Drainage	mm
ΔS	Change in soil water content	mm
ET	Crop Evapotranspiration	mm day^{-1}
E	Actual Evaporation	mm day^{-1}
E_p	Potential Evaporation	mm day^{-1}
E_{pan}	Pan Evaporation	mm day^{-1}
E_a	Isothermal Evaporation rate	(kg/m^2s)
K_c	Crop Coefficient	-
K_p	Pan Coefficient	-
Δ	Slope of saturation vapor pressure curve	kPa $°C^{-1}$
R_n	Net radiation	MJ m^{-2} day^{-1}
G	Soil heat flux	$MJm^{-2}day^{-1}$
γ	Psychrometric constant	kPa $°C^{-1}$
λ	Latent heat of vaporization	MJ kg^{-1}
E_f	Enrichment factor	-
δ_i	Isotopic composition of input water or irrigation water	Per mil (‰)
δ_s	Isotopic composition of ponded irrigation water or surface water	Per mil (‰)
δ_s	Isotopic composition of amospheric vapour	Per mil (‰)
ϵ^*	Equilibrium fractionation factor	-
ϵ	Kinetic enrichment factor and $\epsilon = \epsilon^*-1$	-
h	Mean relative humidity	%
Δsal_{sw}	Change in soil water salinity	mg/l
Δsal_{IW}	Change in irrigation water salinity	mg/l
SI	Salinity Impact	t/h/y
TDS	Total Dissolved Salts	mg/l
$\delta^{18}O$	Oxygen isotope	Per mil (‰)
$\delta^{2}H$	Hydrogen isotope	Per mil (‰)
SL	Suction Lysimeter	-
LMWL	Local Meteoric Water Line	-
LEL	Local Evaporation Line	-

CHAPTER 1

Introduction

Background

The Padthaway and the Hundred of Stirling areas are important irrigation districts in the South East of South Australia. Groundwater for irrigation is extracted from a high yielding unconfined limestone aquifer that occurs at shallow depths throughout the main irrigation areas. Groundwater salinity in the unconfined aquifer below both irrigation regions has been increasing (10 to >100 mg/L/y) since monitoring began in the 1970s, threatening the long-term viability of the irrigation industries.

The increase in groundwater salinity is thought to be partly due to pumping in excess of vertical recharge, and re-cycling of the irrigation water, resulting in accession of the salt back to the unconfined aquifer.

Flood irrigation makes up a significant proportion of irrigation in both regions and is traditionally believed to be particularly inefficient in terms of its salinity impact on the aquifer. This is due to excessive evaporation of the surface water from delivery channels and flood irrigation bays, however, little is understood about the actual impacts evaporation has on infiltrating irrigation waters.

Problem

During flood irrigation, water loss to the atmospheres occurs through Evaporation (E) and transpiration (T). Both processes concentrate salts in irrigation water, however evaporation can be managed and is the undesirable component of water loss from any irrigation practice.

In addition little is understood about the independent contributions these two processes (E and T) have on increasing the concentration of salts in the soil zone beneath a flood irrigation setting.

In water balance studies evaporation and transpiration are often lumped together as one output component, evapotranspiration (ET). Whilst transpiration by a crop can be reasonably estimated using the standard FAO Pan evaporation methodology (Allen et al., 1998, Equation 1), the evaporation of both surface water and shallow soil water at different points in a flood irrigation network can be much more difficult to quantify.

$$ET = f_c.C_p.E_{pa} \quad (1)$$

Where ET = Crop Evapotranspration (mm day^{-1}), f_c = Crop coefficient, C_p = Pan coefficient and E_{pan} = Pan Evaporation (mm day^{-1}).

It is considered that proper quantification of the surface water evaporation component of the water balance could improve our understanding of the salinity impacts from flood irrigation. In particular, understanding at what point in the operation excess surface water evaporation occurs may help in developing benchmark irrigation practices for flood irrigation in the Padthaway and Hundred of Stirling areas.

General Approach and Aims

Enrichment of stable isotopes δ^2H and $\delta^{18}O$ and conservative tracers such as chloride in residual irrigation and soil waters as the result of evaporation and transpiration can provide a sensitive indicator of water loss by these processes in flood irrigation systems.

Isotopic techniques for measuring evaporation from lakes is theoretically sound (Dincer, 1968; Gonfiantin, 1986; Gat 1981, 1991; Simpson et al., 1987, Froechlich et al., 2005), but few applications to irrigation waters are reported. In addition few studies have highlighted the potential utility of coupling isotopic techniques to independently assess salinisation from evaporation and transpiration, particularly from flood irrigation. One way of doing this is by using conservative traces such as chloride concentrations of irrigation water and soil water, which can be conjunctively used with δ^2H and $\delta^{18}O$ to separate the salinsation impacts of transpiration and evaporation.

The aim of this study was to:

- trial a new approach via the use of stable isotope δ^2H and δ^{18}O to quantify and compare evaporation losses during flood irrigation, across four flood irrigation sites which differ in soil type, irrigation delivery and crop type. Two analytical models, previously developed to estimate evaporation from lakes, were applied to a flood irrigation setting.

- couple stable isotopes techniques with conservative tracers such as the chloride ion to separate evaporation and transpiration in the water balance and determine which process is the major contributor to salinity impact.

It is intended that these method will provide new insights into the sources of salinity and improve our understanding of factors that contribute to excessive surface water evaporation from flood irrigation. These methods have broad applications in irrigation trials directed towards minimising evaporation, which represents the largest non-productive loss of water in flood irrigation in this climate.

Objectives

The overall objectives of this study were to:

1. Evaluate the use of analytical models which use stable isotopes δ^2H and δ^{18}O to quantify the amount of irrigation water evaporated at different stages during irrigation delivery at a range of flood irrigated sites, and to validate the applicability of these models to a flood irrigation setting by comparison with traditional methods.

2. Evaluate the use of stable isotopes δ^2H and δ^{18}O as a tool for assessing efficiency of the irrigation network across a number of sites and understand how various parameters (soil type, irrigation delivery, timing of irrigation and crop type/cover) control evaporation and salinity impacts.

3. Use stable isotopes δ^2H and δ^{18}O and the chloride ion, measured in irrigation water and soil water to quantify salinity impact from irrigation and to identify the dominant cause of water loss (evaporation or

transpiration) and therefore the major contributor to salinity impact under each field site.

4. Develop a Local Meteoric Water Line (LMWL) for the South East of South Australia, to which δ^2H and $\delta^{18}O$ values of soil water, irrigation water and groundwater can be compared against.

Outline of Thesis

This thesis consists of three research projects untaken in parallel to address the project objectives. The background, methodology, results and conclusion of each project are reported as separate papers (Chapters 3, 4 and 5) of this thesis. The papers each contain literature reviews within their introductory sections.

Two papers (Chapters 3 and 4) were submitted to the Journal of Irrigation and Drainage Engineering on the 7th and 15th of July 2010. Chapter 3 (van den Akker, et al 2011a) was accepted for publication on the 23 of February 2011 and posted ahead of print on 4 March 2011. Chapter 4 (van den Akker et al 2011b) was accepted for publication on the 29 of March 2011.

This thesis is structured as follows:

- **Chapter 1** outlines the background, problem definition and project objectives.

- **Chapter 2** describes the existing environment, site selection, including a description of the instrumentation used in this study.

- **Chapter 3** details the study: *The use of stable isotopes deuterium and oxygen-18 to derive evaporation from flood irrigation on the basis of pan evaporation techniques*, and addresses Objectives 1 and 2 of this study.

- **Chapter 4** details the study: *Salinity impacts from evaporation and transpiration under flood irrigation*, and addresses Objective 3 of this study.

- **Chapter 5** Details the study: *The hydrogen and oxygen isotopic composition of rainfall and evaporated irrigation water in the South East of South Australia,* and addresses Objective 4 of this study.

Supporting data (isotope, chloride, meteorological and analytical models) relevant to all three experiments (Chapters 3 to 5) are presented in Appendices A to C.

Outline of Chapters 3 to 5

The following abstracts provide an outline of the content from each of the three chapters.

Chapter 3: The use of stable isotopes deuterium and oxygen-18 to derive evaporation from flood irrigation on the basis of pan evaporation techniques.

The loss of water to the atmosphere during flood irrigation occurs through evaporation and transpiration. Whilst transpiration can be estimated via the FAO56 methodology, actual evaporation is difficult to quantify in water balance studies. In this study we applied two analytical models, previously developed to quantify evaporation from lakes on the basis of stable isotopes, to determine evaporation losses from four flood irrigation sites of varied characteristics. Evaporation losses were determined by empirical relationships derived between heavy isotope enrichment and percent water loss in evaporation pan experiments. Validation of the two isotopic models in this setting was achieved by comparison with conventional non-isotopic methods, carried out in parallel. Results showed that heavy isotope enrichment of applied irrigation waters varied between each of the study sites. Isotope enrichment was notably different between irrigation bays that drained rapidly (+0.05 ‰ to +0.18 ‰ for $\delta^{18}O$ and +1.7 ‰ to +2 ‰ for $\delta^{2}H$) to those where ponding occurred for up to 18 h post application (+1 ‰ to +2 ‰ for $\delta^{18}O$ and +2 ‰ to 7.5 ‰ for $\delta^{2}H$). When compared to local pan enrichment, these isotope enrichments corresponded to evaporation losses of 0.2 % to 2.7 % (0.5 mm to 4 mm) and 2 % to 5 % (4.5 mm to 7 mm) respectively. This study demonstrated that the use of stable isotope data for irrigation waters provided valuable new insights into evaporation losses across different flood irrigation systems. The use of these techniques may be useful in suggesting which management strategies are most effective in improving water use efficiency and water quality.

Chapter 4: Salinity impacts from evaporation and transpiration under flood irrigation.

Transpiration and evaporation rates from irrigated pastures can be adequately assessed by conventional methods and in more recent times, by the use of stable isotopes δ^2H and $\delta^{18}O$. However, the salinity impacts these two processes have on infiltrating irrigation waters and residual soil waters have not been independently assessed in a flood irrigation setting. In this study, oxygen-18, deuterium and chloride concentrations of irrigation water, soil water and groundwater were monitored along with soil water content over time, to independently assess the salinisation impacts of evaporation and transpiration. This study was carried out across four flood irrigation sites which overlay a heterogeneous loam-sand and limestone vadose zone. Results showed that minor evaporation losses were detected across most flood irrigation sites through the use of stable isotopes δ^2H and $\delta^{18}O$. The associated increase in chloride concentration of irrigation water as a result of evaporation (minor fractionating water loss) was low (0 mg/l to 129 mg/l) compared to the chloride increase as a result of transpiration (170 mg/l to 3070 mg/l), noted in shallow soil water. Across all sites, the fractionating water loss detected in soil water was minor (<1‰ $\delta^{18}O$ from the source), with isotopic signatures reflecting partially evaporated irrigation waters. The high soil water chloride concentrations, minor fractionating loss and corresponding decrease in soil water content suggests that transpiration is the dominant cause of water loss and therefore the largest contributor to salinity impacts during flood irrigation. Salinity impacts caused by transpiration (0.4 to 2.6 t/ha) were 3 to 50 times greater than the salinity impacts caused by evaporation from irrigation and soil waters (0.01 to 0.3 t/ha).

Chapter 5: The hydrogen and oxygen isotopic composition of rainfall and evaporated irrigation water in the South East of South Australia.

Stable isotope ratios of hydrogen and oxygen in shallow groundwater, soil water and irrigation were measured at four flood irrigation sites, to assess the degree of evaporation by plotting δ^2H and $\delta^{18}O$ values relative to the Local Meteoric Water Line (LMWL). The LMWL developed from local monthly rainfall data collected in the South East of South Australia during 2003 - 2006 gave the following regression; $\delta^2H = 7.65\ \delta^{18}O + 10.14$, a slope somewhat consistent to the world MWL ($\delta^2H = 8.0\ \delta^{18}O + 10$) and the LWML developed from the long term station

at Adelaide ($\delta^2H = 7.44\ \delta^{18}O + 9.2$). The regressions developed here represent the first published LMWLs based on direct precipitation for any location in the South East of South Australia. In comparison, the δ^2H and $\delta^{18}O$ compositions of irrigation waters plot to the right of the LMWL, signifying the effects of evaporation. The slope and deviation of δ^2H and $\delta^{18}O$ values from the LMWL varied across each site according to factors such as (i) day or night irrigation, (ii) soil type, (iii) irrigation application rate and (iv) % crop cover (open water vs crop cover) at time of irrigation. The δ^2H and $\delta^{18}O$ of waters undergoing evaporation plot on lines defined by variable slopes ranging from 4.2 to 3.64, consistent with slopes generated from evaporation of free water surfaces. In comparison, slopes (7) closer to that of the LMWL were produced from irrigation waters applied to bays; (i) over rapid draining soils or (ii) under dense crop cover. Linear regressions through the isotopic composition of soil water ($\delta^2H = 6.43\ \delta^{18}O + 0.36$) and groundwater ($\delta\ \delta^2H = 6.49\ \delta^{18}O + 1.65$) collected 1 - 6 days post irrigation also plotted slightly to the right of the LMWL, however exhibited slopes that reveal evaporation of open surface water bodies (5), indicating that soil water was not subject to evaporation post irrigation.

CHAPTER 2

Description of the Study Area

General

The four irrigation study sites lie within the inter-dunal flats of Padthaway and Tatiara Prescribed Wells Areas (PWA's) in the South East of South Australia (Figure 1).

The Padthaway PWA was proclaimed in 1976 following concern that increased irrigation activity may lower the water table. It covers an area of 700 km^2 and is divided by topography into a low lying inter-dunal flat to the west and a remnant dune ridge to the east that rises up to 60 m above the flat. The two terrains are separated by the Kanawinka fault, which runs through the middle of the PWA in a NW-SE direction. Irrigation is concentrated on the inter-dunal flat, due to the combination of suitable soil types, good quality shallow groundwater and high well yields. Here, groundwater flows through two sub-aquifers of the unconfined aquifer system: the Padthaway Formation sub-aquifer which is present only on the flat and the underlying Bridgewater formation sub-aquifer. In the ranges to the east, the Bridgewater formation sub-aquifer is the main source of groundwater. The principal irrigated industry in the Padthaway PWA is viticulture. There are also substantial areas of irrigated pasture, hay and seed production, cereals and canola.

The Tatiara Prescribed Wells Area was proclaimed in 1984 and its area was further extended in 1986 following the interstate agreement to manage groundwater resources along the South Australia – Victoria border. It covers an area of 3500 km^2 and is divided topographically into two discrete landforms, a low lying coastal plain to the west (where the study sites are located) and the uplifted highlands of the Pinnaroo Block to the east. A scarp referred to as the Marmom Jabuk Fault to the north of the PWA and the Kanawinka Fault to the south separates the two terrains. The major irrigated crop in the Tatiara PWA area is lucerne seed. Other irrigated crops include irrigated pasture, grape vines, pasture seed (mostly clovers), potatoes and oil seeds.

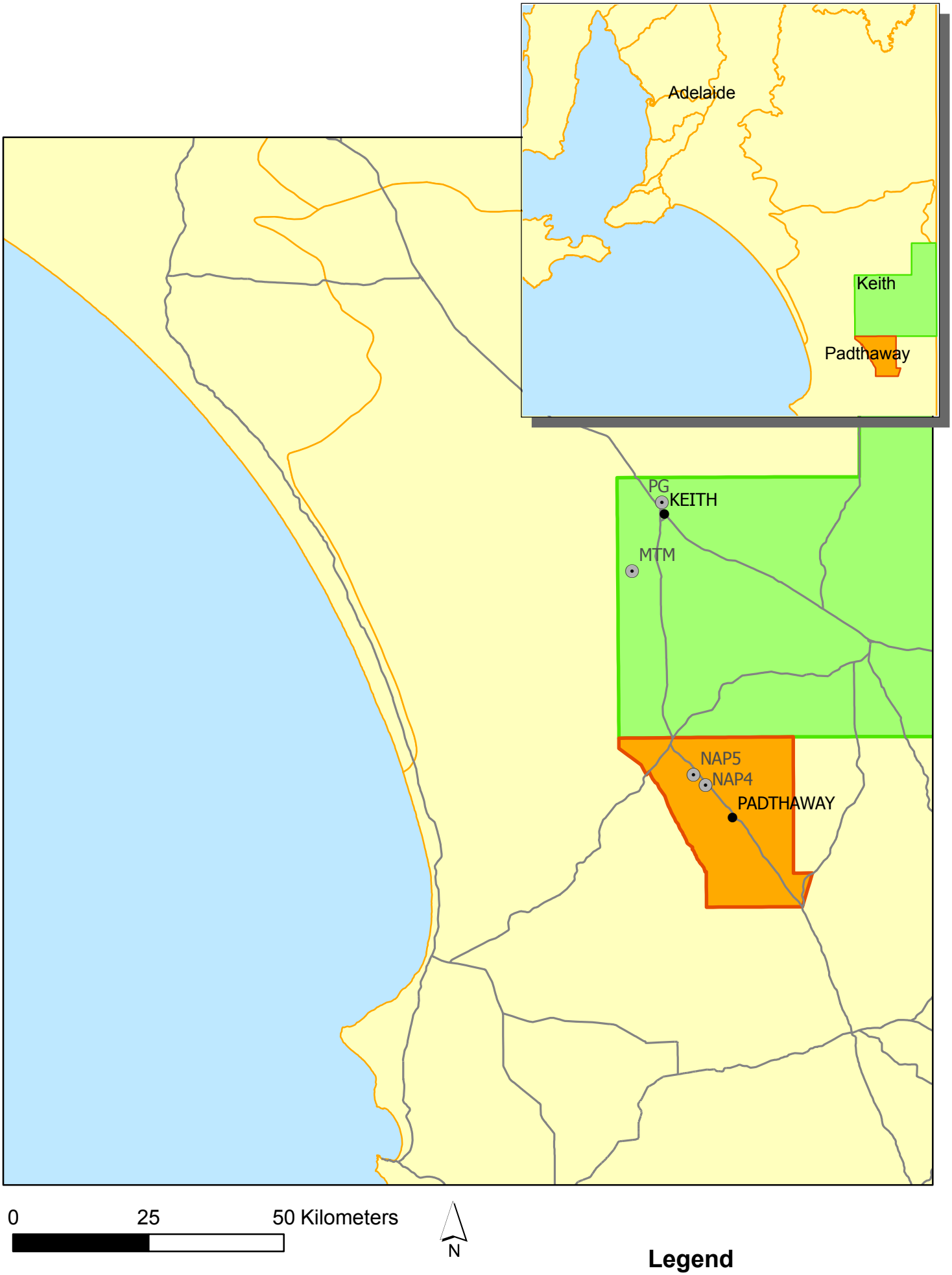

Figure 1 Site Location

Soil

Soils under each field site vary from loam in the northern portion of the Padthaway PWA to sand in the Hundred of Stirling Management Area. Soil profiles consist of a shallow top soil (sand or loam), which overlays marly limestone (Padthaway Formation). Soil profiles are presented in Plate 1.The particle size distribution in the top soil at each flood irrigation site was determined previously (Harrington et al. 2004 and Wohling, 2007). In Padthaway the top soil is 70 % sand, 7 % silt, 21 % clay, compared to soil at the Hundred of Stirling which is 87 % sand 4 % silt, 9 % clay. The topsoil is often shallow < 0.50 m and overlies a shallow calcrete topped limestone aquifer known as the Padthaway Formation. The overlying calcrete is a hard 2 - 5 cm thick layer and in some cases has been ripped to allow drainage (see Plate 1).

Hydrogeology

The Padthaway Formation is one of the main unconfined aquifer systems in the region. Due to the secondary porosity of the limestone, bore yields are highly variable and can range from 0.2 L/s to 300 L/s (Harrington et al., 2004). Depth to water in bores below the inter-dunal flats range between 3 to 7 m, and groundwater salinity ranges from 1000 to 3000 mg/l in Padthaway and from 2000 to 8000 mg/L within the Hundred of Stirling irrigation district.

Across the Padthaway Flats, where irrigation is concentrated, groundwater salinity increase down gradient from 1000 mg/l in the south, to 3000 mg/l in the north of the area. On average, groundwater salinity is rising at a rate of 10 to 20 mg/l/y. The significant rising trend is attributed to two basic mechanisms, the recycling of irrigation water and the movement of salt fluxes down gradient from the ranges in the east (Harrington et al., 2004).

Across the Tatiara PWA, the groundwater salinity ranges from ~1000 mg/l in the east to > 8500 mg/l in the north west portion of the Stirling irrigation area. It is evident that areas of higher groundwater salinity and areas where irrigation exceeds vertical recharge, notably the Stirling irrigation area, exhibit a greater annual salinity increase due to the large salt load leaching from the unsaturated zone into the water table by the recycling of irrigation water. In parts of the Stirling irrigation area, where the salinity of the groundwater exceeds 7000 mg/l, the salinity is increasing at a rate of 50 to >100 mg/l/y for the majority of observation wells (van den Akker et al., 2004).

a) 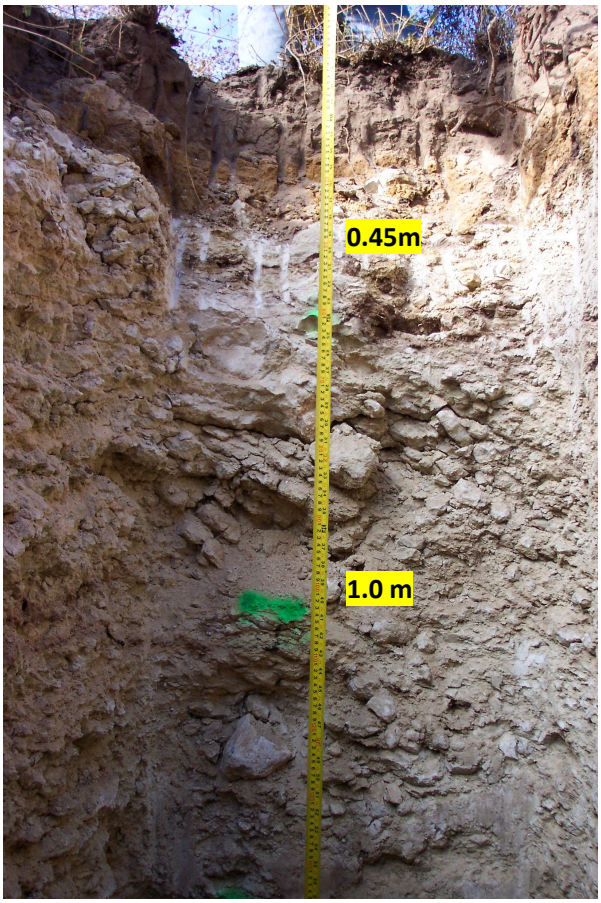

b) 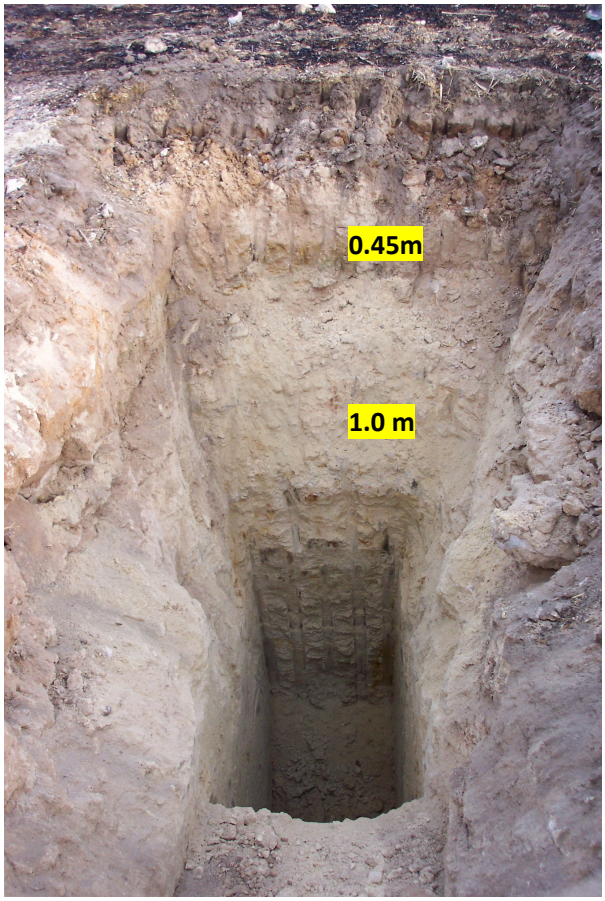

c) 

d) 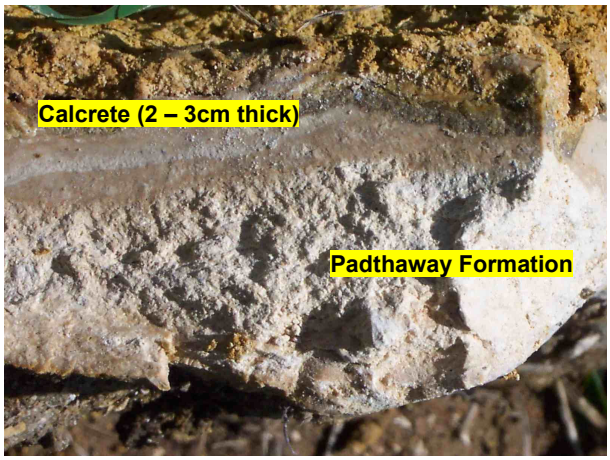

Plate 1. Soil pits excavated at a) MTM, b) PG, c) shallow depth to calcrete commonly encountered across Padthaway and d) calcrete layer overlying the Padthaway Formation.

Climate

The climate within the study areas is typical of a Mediterranean climate, with warm to hot dry summers and cool wet winters. Climate data is available via the Bureau of Meteorology website which commenced in 1977. Monthly averages for rainfall, evaporation and temperature are presented in Figure 2. A mean daily minimum temperature of 5°C occurs in July and mean daily maximum of 29°C occurs in February. The highest and lowest recorded temperatures at Padthaway are - 4°C and 44°C respectively. A rainfall gradient exists across the study area, with average annual rainfall being slightly higher in Padthaway at 509 mm/y to 462 mm/y in Keith. Rainfall in concentrated during the cooler months (June - September). Annual potential evaporation is 1600 mm/y and 1700 mm/y for Padthaway and Keith respectively.

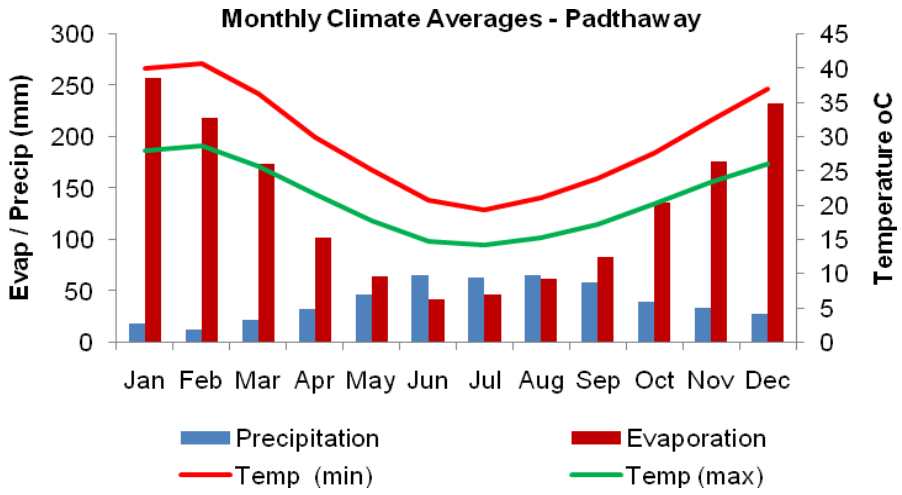

Figure 2 Mean monthly climatic data for upper South East of South Australia

Site Selection

Four flood irrigation sites were established with detailed monitoring equipment in the main Padthaway Flats and Hundred of Stirling irrigation areas to determine evaporation and salt accession impacts (Figure 1). Each irrigation site was selected on the basis of differences in soil type/thickness, irrigation bay design (width/length of bay, laser levelled or not), crop type, and irrigation delivery (pump rate, length and head of delivery channel). The characteristics of the four flood irrigation sites are summarised in Table 1.

Instrumentation

Instrumentation installed at each site was designed to measure all components of the water and salt balance, of a flood irrigation site. Figures 3 to 6 show the location of the instrumentation at each study area and Plate 2 shows the typical instrumentation installed at each flood instrumentation sites, the function of which is summarised as follows:

- **Piezometers** - to measure changes in isotopic and Cl^- signatures of groundwater beneath the flood irrigation bays, post irrigation (Plate 2a).
- **Rain capturing devices** - 6 capturing devices, distributed across the region, to characterise the Cl^- and isotopic composition of rainfall, in order to establish a LMWL for the region (Plate 2b).
- **Flow meter** (Mace Agrilflow) on irrigation bores and **shaft encoder** (Dataflow Systems 392 depth loggers) - to measure the volume pumped from the irrigation bore and volume applied to the irrigation bay from the channel, to which the fraction of evaporated water can be calculated (Plate 2c).
- **Capacitance Probe** (Agrilink C - Probe) - Installed beneath the flood irrigation bays, to monitor changes in soil moisture at various depths over time as a result of evaporation, transpiration (root activity) and drainage (Plate 2a).
- **Suction lysimeters** - Installed vertically at nominal depths of 0.3 to 3.5 m, beneath the flood irrigation bays to measure the change in Cl^-, TDS and isotopic composition of soil water in and beneath the root zone after irrigation (Plate 2d).
- **Class A evaporation Pan** - to monitor evaporation losses and evolution of salinity and isotopic signatures of pan water over time.

Table 1 Flood bay characteristics

	Soil and crop type			Irrigation application				Dimensions of irrigation bay				Channel
Site	Top soil	Soil thickness (m)	Crop Type	Pump Rate (Ml/h)	Duration (h)	Ml/ha	Ponding duration (h)	Width (m)	Length (m)	Area (ha)	Laser levelled	length (m from bore)
NAP4	Loam	0.35 - 0.5	Pasture	0.55	10	1.10	24 - 28	125	200	2.50	N	180
NAP5	Loam	0.1	Clover	0.46	8	1.47	18 - 22	50	500	2.50	Y	620
MTM	Sand	<0.30	Lucerne	0.48	2.5	2.00	6 - 15	20	300	0.60	Y	500
PG	Sand	<0.30	Lucerne	0.55	6	1.55	8	50	425	2.13	Y	105

Figure 3 . Site plan of instrumentation and sampling locations at flood irrigation site NAP5

Figure 4. Site plan of instrumentation and sampling locations at flood irrigation site NAP4

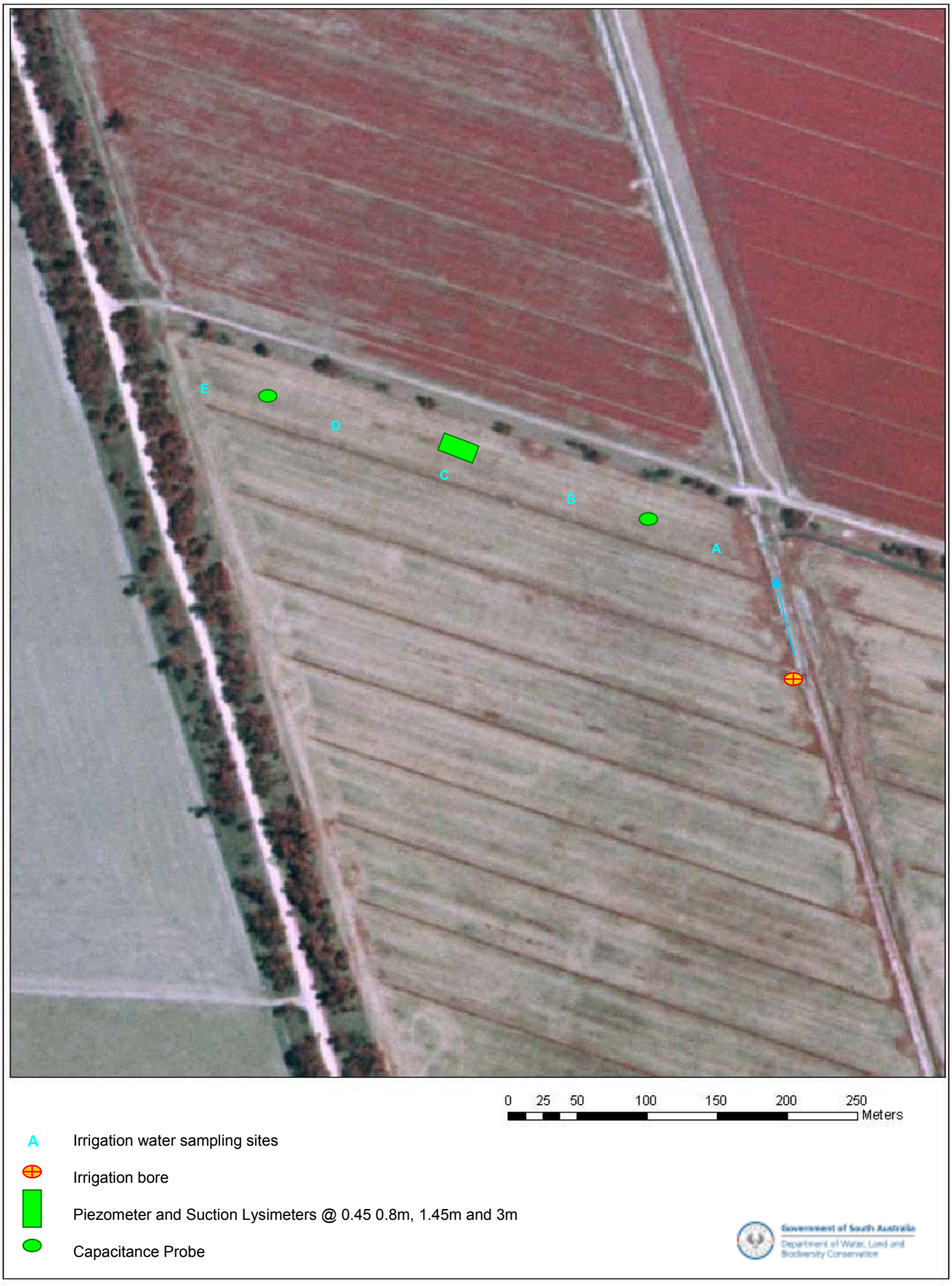

Figure 5. Site plan of instrumentation and sampling locations at flood irrigation site PG

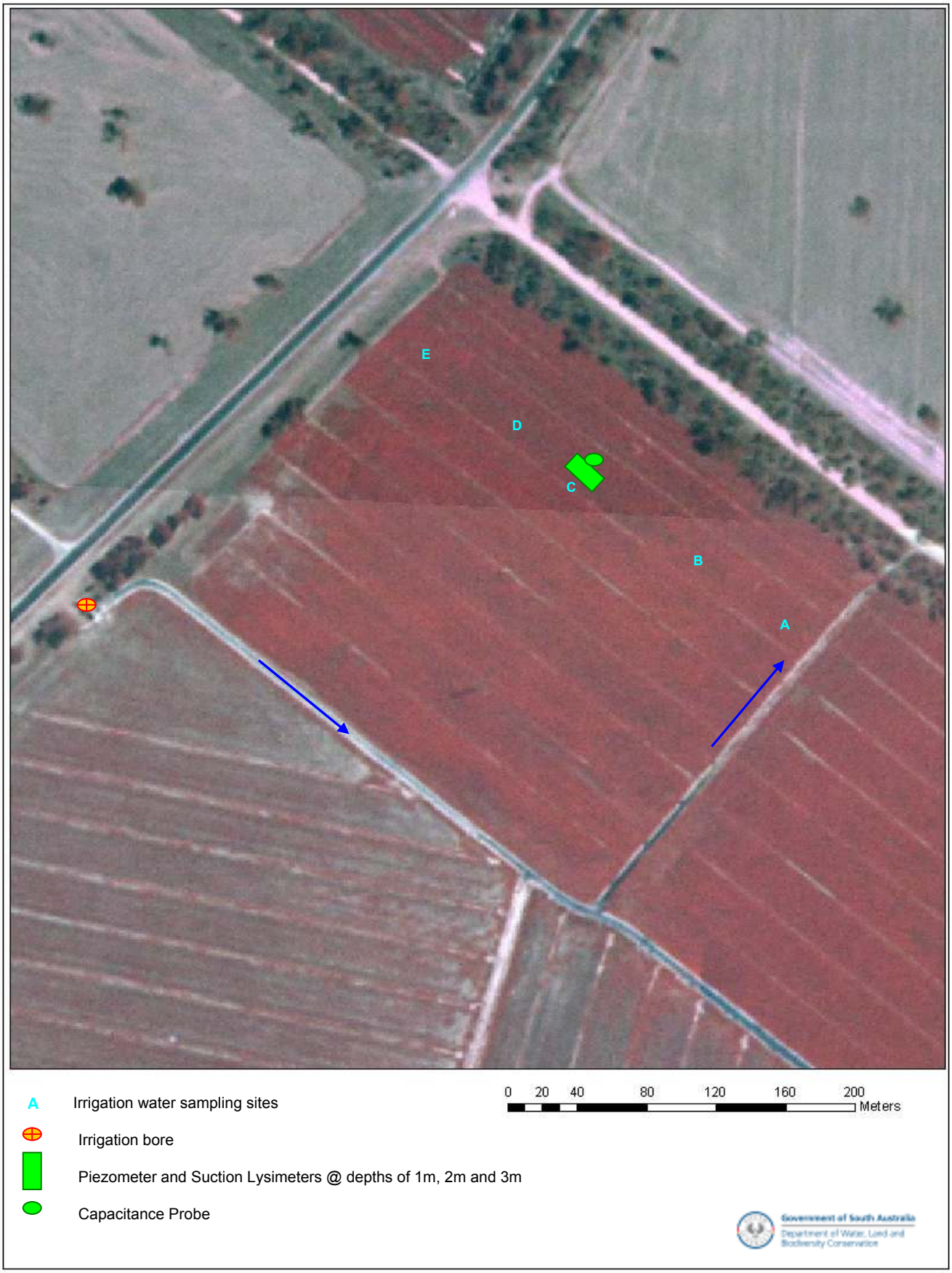

Figure 6. Site plan of instrumentation and sampling locations at flood irrigation site MTM

a)

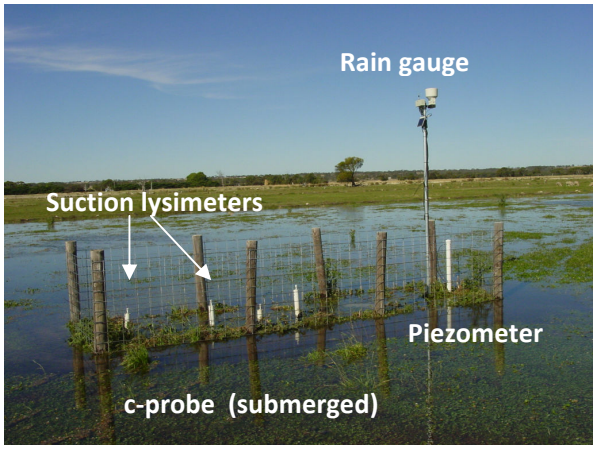

b)

c)

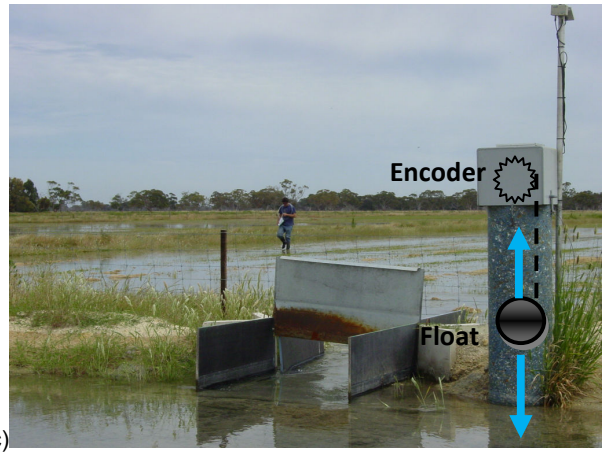

d)

e)

Plate 2. a) Instrumentation at NAP5, b) rain collection container for isotopic analysis, c) shaft encoder, d) sampling soil water from suction lysimeters post irrigation and e) Class A evaporation pan.

Piezometer installation and soil sample collection

Piezometers were installed at each site. Holes were drilled with hollow augers mounted on an Investigator rig. A split tube wire line recovery technique was used to collect core samples for water content, particle size and pore water chloride analyses. All holes were completed with 50 mm class 12 PVC piezometers screened in the Padthaway Formation, just below the water table at depths ranging from 3 m to 10 m. Gravel was packed around the screened interval, and overlaid with a bentonite seal, before being cemented to the surface. A continuous groundwater level transducer was installed in each piezometer, and is connected directly to telemetry units. Groundwater samples were pumped from the piezometers at all sites and analysed for chloride and δ^2H and $\delta^{18}O$ after irrigation application.

Precipitation measurements

Agrilink Automatic rain gauges were installed across all sites. In addition six rain capturing devices were installed across the region (near the study sites – see Chapter 3 for locations) and were sampled monthly for δ^2H and $\delta^{18}O$ and chloride (Plate 2b). To prevent evaporation, 200 ml of paraffin wax was added to the capturing container after each time a sample was collected.

Irrigation application measurements

Shaft encoders to measure actual flows onto the flood irrigation bays were installed at NAP4 and NAP5. At both sites, a concrete base and small “flow straightening” walls were constructed immediately upstream and downstream of the sluice gate (Plate 2c). The water level was measured via a float well and shaft encoder with data being fed into the telemetry network. At MTM and PG depth loggers were used to measure water level. Field gauging was undertaken to establish a relationship between the water level and the corresponding discharge.

Groundwater abstraction

To measure groundwater abstraction, flow meters were installed on the irrigation bores at all sites (Plate 2c).

Soil moisture measurements - capacitance probes

Capacitance probes (Agrilink C - probes) were installed vertically within 75 mm diameter cored RC holes. They measure the dielectric constant of a soil and

hence its water content by the capacitance method. The instruments were not calibrated, however, they were able to produce a soil moisture profile at depth and therefore were useful to determine lag times and the extent that soil moisture moves down the profile after irrigation and rainfall events. Two C -probes were installed at NAP 4 and NAP 5, and one C - probe at each of PG and MTM sites. Based on the soil profile and root system, sensors were set at nominal depths of 10, 20, 30, 50, 100, 150, 200, 250 and 300 cm. The C - probe utilises the telemetry system to log and transmit data.

Salinity and isotope drainage measurements

To quantify a salt flux to the water table, suction lysimeters were installed vertically, to measure soil moisture salinity (chloride) and isotopic composition within the vadose zone. At each of the irrigation sites, three to four 100 mm diameter holes were drilled within the unsaturated zone at nominal depths of about 0.5, 1.0, 2.0 and 3.0 m and equipped with suction lysimeters (see Table 2 for installation depths). The shallow sensor was position within the top soil (above the calcrete later), within the bulk root system. The lysimeters were constructed by attaching a 15 cm porous ceramic cup to the end of 16 mm diameter PVC conduit. These were placed in the hole, with the ceramic cup surrounded by diatomaceous earth to provide a good contact with the surrounding soil. A bentonite seal was placed above the diatomaceous earth and the hole was cemented to the surface. Two groups of four lysimeters were installed at each of the two flood (NAP 4 and 5) irrigation sites to achieve average readings across the bay (Figure 3 and Figure 4).

Table 2 Suction lysimeter sites and depth

Site	Depth Below Ground level (m)			
	SL 1	SL 2	SL 3	SL 4
NAP4 (West)	0.35	1.06	2.03	3.05
NAP4 (East)	0.30	1.13	2.01	2.92
NAP5 (North)	0.35	1.04	2.01	2.51
NAP5 (South)	0.35	0.97	2.02	2.52
MTM	-	1.00	2.00	3.00
PG	0.45	0.80	1.45	3.00

The suction lysimeters were sampled post irrigation. Sampling was carried out by applying a constant negative pressure to the ceramic cup, using a vacuum pump (Plate 2d). This draws pore water through the porous cup and pore water

samples are brought to the surface through a 5 mm tube using a syringe. Samples were analysed for stable isotopes $\delta^{2}H$ and $\delta^{18}O$, electrical conductivity (EC) and chloride following irrigation.

References

Allen, G., Pereira, L.S., Raes, D., Martin, S., 1998. FAO Irrigation and Drainage Paper No. 56 Crop Evapotranspiration Guidelines for computing crop water requirements.

Dincer., 1968. The use of oxygen-18 and deuterium concentrations in the water balance of lakes. Water Resources Research 4, 1289 -1305.

Froehlich, K.F.O., Gonfiantini, R., Rozanski, K., 2005. Isotopes in lake studies: a historical perspective. In: Aggarwal, P.K., Gat, J.R., Froehlich, K.F.O. (Eds.), Isotopes in the Water Cycle, Past, Present and Future of a Developing Science. IAEA, Springer, Vienna, The Netherlands, 381pp.

Gat, J.R., 1981. Lakes Stable Isotope Hydrology- Deuterium and Oxygen-18 in the Water Cycle. In: J.R. Gat, R. Gonfiantini (Eds.). IAEA Technical Report Series No. 210, Vienna, pp. 203 - 221.

Gat, J.R., Bowser, C.J., 1991. Heavy isotope enrichment in coupled evaporative systems. In: H.P. Taylor, J.R. O'Neil, I.R. Kaplan (Eds.), Stable Isotope Geochemistry: A Tribute to Samuel Epstein, Special Publication No. 3, The Geochemical Society, San Antonio, Texas, pp. 159 - 168.

Gonfiantini, R., 1986. Environmental isotopes in lake studies. In: Fritz, P., Fontes, J.Ch. (Eds.). Handbook of Environmental Isotope Geochemistry, 3. Elsevier, New York, pp. 113 -168.

Harrington, N., van den Akker, J., Brown, K. and Mackenzie, G., 2004. Padthaway Salt Accession Study. Volume One: Methodology, site description and instrumentation. South Australia. Department of Water, Land and Biodiversity Conservation. DWLBC Report 2004/61.

Simpson, H. J., Hamza, M. S., White, J. W. C, Nada, A. and Awad, M. A., 1987. Evaporative enrichment of deuterium and $\delta^{18}O$ in arid zone irrigation. In: Isotope. Techniques In Water Resources Development. IAEA-SM-299/125, 241 - 256.

van den Akker, J. and Mackenzie, G., 2004. South East groundwater monitoring status report and assessment of current trends 2003–2004, DWLBC Report 2004/26, Government of South Australia, through Department of Water, Land and Biodiversity Conservation, Adelaide.

van den Akker, J., 2005. Padthaway Salt Accession Study Volume Two: Results, DWLBC Report 2005/15, Government of South Australia, through Department of Water, Land and Biodiversity Conservation, Adelaide.

van den Akker, J., Simmons, C.T. and Hutson, J., 2011a. The use of stable isotopes deuterium and oxygen-18 to derive evaporation from flood irrigation on the basis of pan evaporation techniques. Journal of Irrigation and Drainage Engineering, ASCE. (Posted ahead of print March, 4, 2011).

van den Akker, J., Simmons, C.T. and Hutson, J., 2011b. Salinity impacts from evaporation and transpiration under flood irrigation. Journal of Irrigation and Drainage Engineering, ASCE. (Posted ahead of print March, 31, 2011).

Wohling, D., 2007. Minimising Salt Accession to the South East of South Australia. The Border Designated Area and Hundred of Stirling Salt Accession Projects. Volume 2 - Analytical Techniques, Results and Management Implications, DWLBC Report 2007, Government of South Australia, through Department of Water, Land and Biodiversity Conservation, Adelaide.

CHAPTER 3

The use of stable isotopes, deuterium and oxygen - 18 to derive evaporation from flood irrigation on the basis of pan evaporation techniques

Abstract

The loss of water to the atmosphere during flood irrigation occurs through evaporation and transpiration. Whilst transpiration can be estimated via the FAO56 methodology, actual evaporation is difficult to quantify in water balance studies. In this study we applied two analytical models, previously developed to quantify evaporation from lakes on the basis of stable isotopes, to determine evaporation losses from four flood irrigation sites of varied characteristics. Evaporation losses were determined by empirical relationships derived between heavy isotope enrichment and percent water loss in evaporation pan experiments. Validation of the two isotopic models in this setting was achieved by comparison with conventional non-isotopic methods, carried out in parallel. Results showed that heavy isotope enrichment of applied irrigation waters varied between each of the study sites. Isotope enrichment was notably different between irrigation bays that drained rapidly (+0.05 ‰ to +0.18 ‰ for $\delta^{18}O$ and +1.7 ‰ to +2 ‰ for $\delta^{2}H$) to those where ponding occurred for up to 18 h post application (+1 ‰ to +2 ‰ for $\delta^{18}O$ and +2 ‰ to 7.5 ‰ for $\delta^{2}H$). When compared to local pan enrichment, these isotope enrichments corresponded to evaporation losses of 0.2 % to 2.7 % (0.5 mm to 4 mm) and 2 % to 5 % (4.5 mm to 7 mm) respectively. This study demonstrated that the use of stable isotope data for irrigation waters provided valuable new insights into evaporation losses across different flood irrigation systems. The use of these techniques may be useful in suggesting which management strategies are most effective in improving water use efficiency and water quality.

Introduction

The monitoring of stable isotopes δ^2H and δ^{18}O in water can provide a sensitive indicator of water loss by evaporation, exclusive of transpiration. Isotopic techniques for measuring evaporation from lakes is theoretically sound (Dincer, 1968; Gonfiantini, 1986; Gat and Bowser,1991, and Gat and Matsui, 1991; Simpson et al., 1987; and Froechlich et al., 2005) but few applications to irrigation waters are reported. The aim of this study was to apply a new approach via the use of stable isotopes δ^2H and δ^{18}O to quantify evaporation losses from flood irrigation water, across four irrigation sites, which differ in soil type, irrigation application rate, crop type and bay architecture.

In this study, evaporation losses were estimated using the analytical models developed by Gonfiantini 1986 and Simpson et al. (1987), where relationships were derived between heavy isotope enrichment and fractional water loss from evaporation pan experiments. Previously, these analytical techniques were applied to estimate evaporation losses from lakes and river systems. However, as the principles (water balance and isotopic processes) are much the same, this study examines the validity of the analytical models to estimate evaporation rates from a flood irrigation setting, by comparison with (non-isotopic) conventional weather station methods (Penman - Monteith), described by Allen, et al 1998 and in more recent times, adopted by Debarro, 2006 in this setting.

In the irrigation districts of Padthaway and the Hundred of Stirling in the South East of South Australia, pasture and lucerne is generally flood irrigated. The greatest loss of water to the atmosphere occurs through two pathways: (i) transpiration through crop plants; and (ii) evaporation from delivery channels, surface distribution systems and moist soil. Transpiration and evaporation are often integrated and called evapotranspiration. Both processes concentrate salts in irrigation water and soil, however evaporation can be managed and is the undesirable component of water loss from any irrigation practice. In principle, the higher the proportion of water loss by transpiration through crop plants relative to evaporation, the higher the efficiency of water use.

The importance of quantifying evaporation from flood irrigation is essential to determine the salinity impacts and overall efficiency of the irrigation network.

Whilst the total evapo-transpiration by a crop can be estimated using the standard FAO56 Pan evaporation methodology (Equation 1, Allen et al., 1998), the evaporation of surface water and shallow soil water at different points in a flood irrigation network is much more difficult to quantify and is often neglected.

$$ET = K_c.K_p.E_{pan} \quad (1)$$

Where ET is the crop evapotranspiration (mm day^{-1}), K_c is the Crop coefficient, K_p is the Pan coefficient, and E_{pan} is Pan Evaporation (mm day^{-1}).

Traditionally, evaporation from flood irrigation has been measured and described in several ways. Actual evapotranspiration (ET) is the actual water lost through transpiration, soil evaporation and evaporation of surface water. It can measured by sophisticated and expensive climate stations or flux towers via the eddy covariance technique (Mauder et al., 2007), lysimeters (Lewis, 1875) and water balance and soil water depletion methods (Jensen et al., 1990). Potential evaporation (E_p) is the theoretical upper limit to evaporation. There are many ways of defining potential evaporation. The general definition is that E_p is the maximum evaporation rate that can be sustained from a moist surface and is given by the FAO Penman equation (Penman, 1948 and Allen et al., 1998).

$$E_p = \frac{[\Delta(R_n - G)] / (\lambda + \gamma E_a)}{(\Delta + \gamma)} \quad (2)$$

Where E_p is the potential evaporation of open water (kg/m^2s), R_n is the net radiation (MJ m^{-2} day^{-1}), G is the soil heat flux (MJ$m^{-2}day^{-1}$), Δ is the slope of saturation vapor pressure curve (kPa $°C^{-1}$), γ is the psychrometric constant (kPa $°C^{-1}$), E_p is the potential evaporation (mm day^{-1}), λ is the latent heat of vaporization (MJ kg^{-1}), and E_a is the isothermal evaporation rate (kg/m^2s).

Pan evaporation is the daily evaporation rate as measured by a Class A evaporation pan. The pan evaporation rate (E_{pan}) is related to potential evaporation (E_p) by a pan coefficient (K_p):

$$E_p = K_p.E_{pan} \quad (3)$$

which in turn can be related to evapotranspiration by a crop coefficient via Equation 1

Debarro (2006) quantified actual evaporation from flood irrigation waters at two common research sites. In his study he used a weather station to compute E_p and calculated volume of actual evaporation (E) as follows:

$$E = A.E_p.t \quad (4)$$

Where, A is the surface area (m^2) of the inundated bay or saturated soil surface, E_p is potential evaporation (mm h^{-1}) measured on site via an automatic weather station, and t is the period (h) the bay was inundated/irrigated or soil was at saturation after standing water had drained from the surface. Debarro (2006) assumed that dense lucerne cover was a strong inhibitor of evaporation and hence bay evaporation was calculated only for the irrigations when there was no crop canopy. According to the FAO, for evaporation measurements made in pans surrounded by tall crops, the C_p will need to be increased by 30 % for dry wind climates (Allen et al., 1998).

Better quantification of the surface water evaporation (E) component of the water balance during different stages of irrigation is needed to improve our understanding of the salinity impacts of flood irrigation. In particular, identifying at when and how much surface water evaporation occurs, may assist in developing benchmark irrigation practices for flood irrigation.

Measurement of changes in stable isotopic composition of water is one technique which has been used successfully in the quantification of evaporation from lakes and rivers (Gat, 1981; Simpson et al., 1992; and Gonfiantini, 1986). The principal is that when water evaporates, the ratio of the concentrations of $^1H^{16}O$ and $^2H^{18}O$ to that of $^2H^{16}O$ changes due to small differences in the physical properties of the isotopes (Zimmermann et al., 1967). During evaporation, molecules containing lighter isotopes ($\delta^{16}O$ and δ^1H) leave the liquid surface more easily than heavier ones ($\delta^{18}O$ and δ^2H), with the result that isotopic fractionation occurs and the remaining liquid is enriched in heavy isotopes (Zimmermann et al., 1967; White and Gedzelman, 1984). Since transpiration and evaporation affect residual water isotopic compositions differently, the relative contribution of these two water loss

fluxes may theoretically be resolved from observed changes in residual irrigation water isotopic compositions (Dincer et al., 1978).

The theory behind the two analytical models trialled by this study is described as follows.

Analytical Model 1 – Simpson et al. (1987)

To allow a comparison between each flood irrigation site, our study expanded the approach of Simpson et al. (1987) and adopted an approach, which uses pan evaporation experiments to calculate the percentage of evaporation loss from ponded irrigation water. As local humidity, temperature and wind shear effects are similar to both, the results obtained from drying pan experiments should be comparable to local irrigation waters via the following relationship:

$$E = \frac{\delta_s - \delta_i}{E_f} \quad (5)$$

where E is the percentage of water loss by evaporation, δ_i is the average isotopic composition of the irrigation source (‰), δ_s is the isotopic composition of surface water (‰) at any stage during irrigation (i.e. during irrigation or ponding periods), and E_f is the amount of isotopic enrichment (‰) per 1 % of water loss from an evaporation pan at the study site.

Analytical Model 2 – Gonfiantini (1986)

Water loss by evaporation from flood irrigation was evaluated by using the equation given by Gonfiantini (1986) who estimated the water loss from a lake via the following expression:

$$E = \frac{(\delta_s - \delta_i)(1-h+\Delta\epsilon)}{(\delta_s+1)(\Delta\epsilon+ \epsilon/ \epsilon^*)+h(\delta_A-\delta_s)} \quad (6)$$

where E is the calculated percentage of water loss by evaporation (actual evaporation), δ_s is the mean isotopic values of the lake (‰) (in this case δ_s is the ponded irrigation water), δ_i is the mean isotopic value of the input to the lake (‰)

(flood bay), δ_A is the mean isotopic composition of atmospheric water vapour (‰), h is the mean relative humidity (%), ϵ* is the equilibrium fractionation factor and is well-known for both oxygen and hydrogen as a function of temperature (1.0093 and 1.08 for $\delta^{18}O$ and $\delta^{2}H$ respectively at 25 ^{0}C, see Gonfiantini, 1986), and $\Delta\epsilon$ is the kinetic enrichment factor, evaluated here as $\Delta\epsilon\ \delta^{18}O = 14.2\ (1 - h)$, and $\Delta\epsilon\ \delta^{2}H = 12.5\ (1 - h)$, as most frequently encountered conditions in nature (Gonfiantini, 1986) and $\epsilon = \epsilon^{*}-1$.

Of these parameters, several can be measured or calculated routinely, however the isotopic composition of atmospheric moisture δ_A has proven more difficult to assess in natural situations. This is due to the logistical complications associated with the collection of vapour in suitable volumes for mass spectrometric analysis, and spatial and temporal weighting of data for mass balance calculations, given the transient nature of atmospheric processes (Gibson et al., 1999). An alternate method for estimating δ_A was proposed by Gibson et al. (1999); where lakes are large enough in volume and have sufficient isotopic inertia to minimise shorter fluctuations in atmospheric parameters it may be sufficient to assume δ_A is in isotopic equilibrium with local precipitation (i.e. $\delta_A = \delta_p - \epsilon^{*}$), where δ_p is the weighted mean isotopic composition of precipitation and ϵ* is approximated using mean air temperature records. This technique has been applied to study lakes using isotopic models (e.g. Zuber, 1983; Gibson et al., 1993). In general, precipitation equilibrium is not a valid assumption for isotopic balance studies on times scales of the order of weeks to months (Gibson et al., 1999). Hence this approach is not applicable for the estimation of δ_A over short duration irrigation events.

Isotopic mass balance of evaporation pans has been used in several studies to derive δ_A at time scales ranging from days to months (e.g. Gibson et al., 1999). Various methodologies are summarised in Gibson et al 1999 according to various derivations (Gat, 1970; Welhan and Fritz., 1977; Allison et al., 1979; Barnes and Allison, 1982; Allison and Leaney, 1982 and Simpson and Herczeg, 1992) showed that isotopic mass balance of a constant volume pan can be a reliable method for characterising temporal changes in δ_A. Results of the above study suggest that standard Class A pans are also appropriate for this purpose and also that Class A pans, if allowed to partially dry, can be used in a similar

fashion providing that drying is limited to less than about 50% of the original volume (Gibson et al., 1999). Simpson et al., 1992, used a constant feed pan that was 70 mm deep (buffered with inflow) and showed that there may be some uncertainty in the estimation of isotopic exchange parameters by using Class A pans. For the simple case of a drying pan with no inflow or outflow, the volume V and isotopic changes in the pan water are controlled only by evaporation E.

This study used drying pan experiments conducted during irrigation, to first estimate δ_A (with known E, h, δ_i, δ_s, ϵ^* and $\Delta\epsilon$ values) from Class A pan waters, which will then allow the subsequent determination of E from irrigation waters (with known δ_A, h, δ_i, δ_s, ϵ^* and $\Delta\epsilon$ values). Both δ_A and E were calculated using Equation 6.

Irrigation efficiency

Stable isotope abundance changes in irrigation water was used to provide a direct indication of evaporation and can thus provide a new tool to monitor key parameters (soil type, irrigation application rate, bay architecture etc) relevant to water use efficiency.

The overall efficiency (I_E) of the irrigation network in terms of the actual evaporation losses in respect to potential evaporation (equation 7), and total irrigation volume can be assessed via the following equation:

$$I_E = 100.(E / E_p) \quad (7)$$

where E_p is the potential evaporation measured from Class A evaporation pan (mm) and E actual evaporation calculated from irrigation waters (mm), by isotopic methods.

By monitoring the changes in isotopic composition and chloride (salinity) concentration of irrigation water at different stages during the irrigation delivery (as several locations across the bay during irrigation application and ponding), we were able to quantify the amount of irrigation water lost via evaporation at various stages, which was then used to evaluate the efficiency of the irrigation network. It is intended that the findings will also improve our understanding of

factors that contribute to excessive surface water evaporation from flood irrigation and will therefore be used to develop efficient flood irrigation practices.

Methods

Site description

The four irrigation study sites selected for this study lay within the inter-dunal flats of Padthaway and Tatiara PWA's in the Upper South East of South Australia (Figure 1). Pasture, clover and lucerne crops are flood irrigated at these sites. The climate within the study areas can be characterised by warm to hot dry summers and cool wet winters. The average annual maximum temperature is 22 ^{o}C, with February being the hottest month at 29.8 ^{o}C and July being the coldest month, at 5.5 ^{o}C. A rainfall gradient exists across the study area, with average annual rainfall being slightly higher in Padthaway at 509 mm/y to 490 mm/y in Keith. 40 % of the annual rainfall occurs during the months of June to August. Annual potential evaporation is 1600 mm/y and 1700 mm/y for Padthaway and Keith respectively.

The soil texture under each field site varies from loam in the northern portion of the Padthaway PWA to sand in the Hundred of Stirling Management Area. The partial size distribution of top soil (0 - 0.50m) at each flood irrigation site was determined previously (Harrington et al. 2004) and Wohling, 2007). At Padthaway the top soil is 70 % sand, 7 % silt, 21 % clay (sandy loam), compared to soil at the Hundred of Stirling which is 87 % sand 2.4 % silt, 9.8 % clay (sand). The topsoil is mostly shallow < 0.50 m and overlies a shallow calcrete topped limestone known as the Padthaway Formation. The overlying calcrete is a hard 2 - 5 cm thick layer and in some cases has been ripped to allow drainage. The Padthaway Formation is one of the main unconfined aquifer systems in the region. Due to the secondary porosity of the limestone, bore yields are highly variable and can range from 0.2 L/s to 300 L/s (Harrington et al., 2004). Depths to water in bores below the inter-dunal flats range between 3 to 7m, and groundwater salinity ranges from 1000 to 3000 mg/L in Padthaway and from 2000 to 8000 mg/L within the Hundred of Stirling irrigation district.

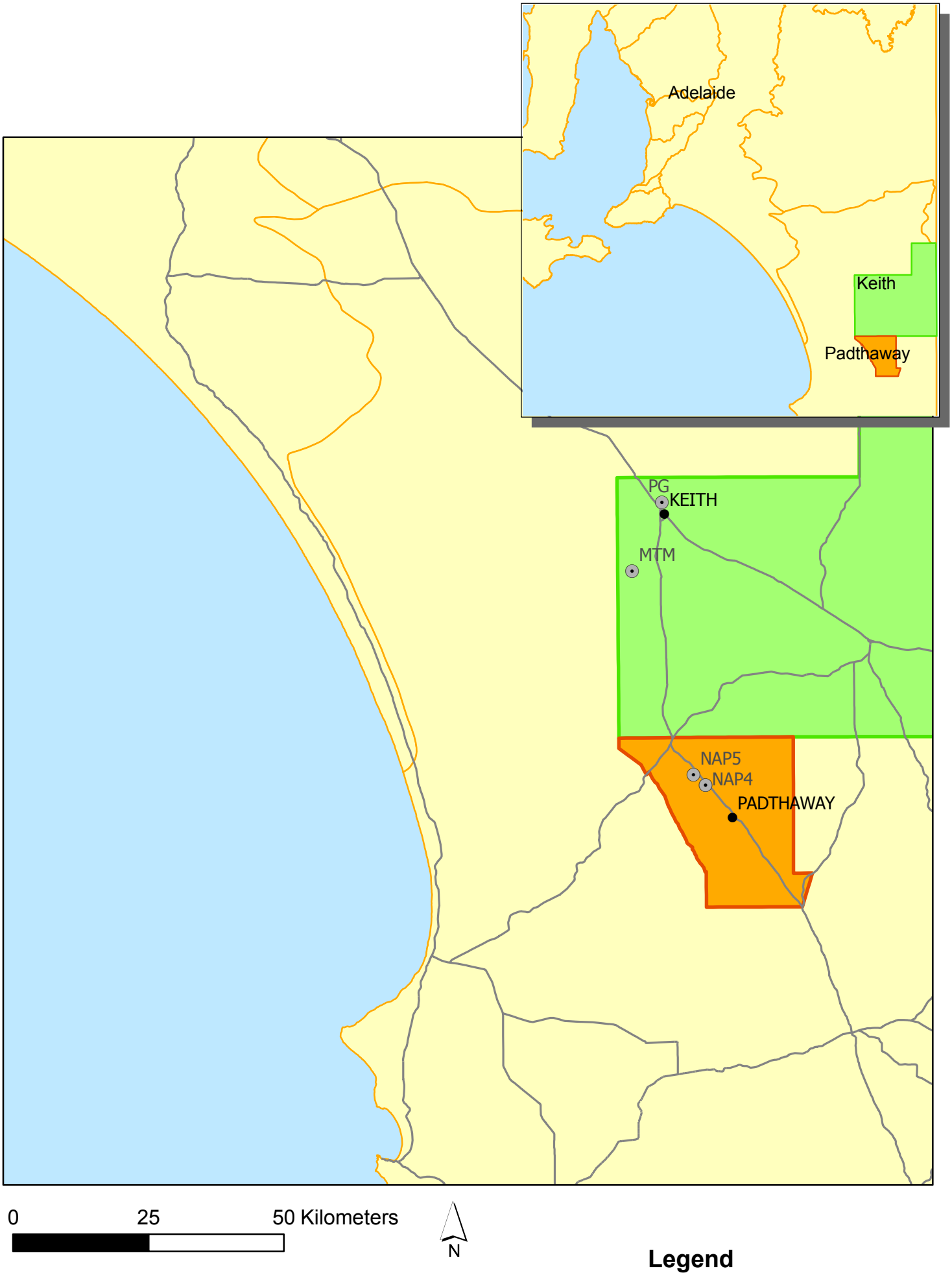

Figure 1 Site Location

Study site selection

Field measurements outlined below were made at four flood irrigation sites (Figure 1). Each field site differs in terms of soil type; thickness of top soil; irrigation delivery (i.e. pumping rate, length and head of delivery channel); area of irrigation bay; and crop type. The characteristics of the four flood irrigation sites are summarised in Table 1.

A schematic diagram of the sampling locations and instrumentation set up for a typical irrigation bay is shown in Figure 2.

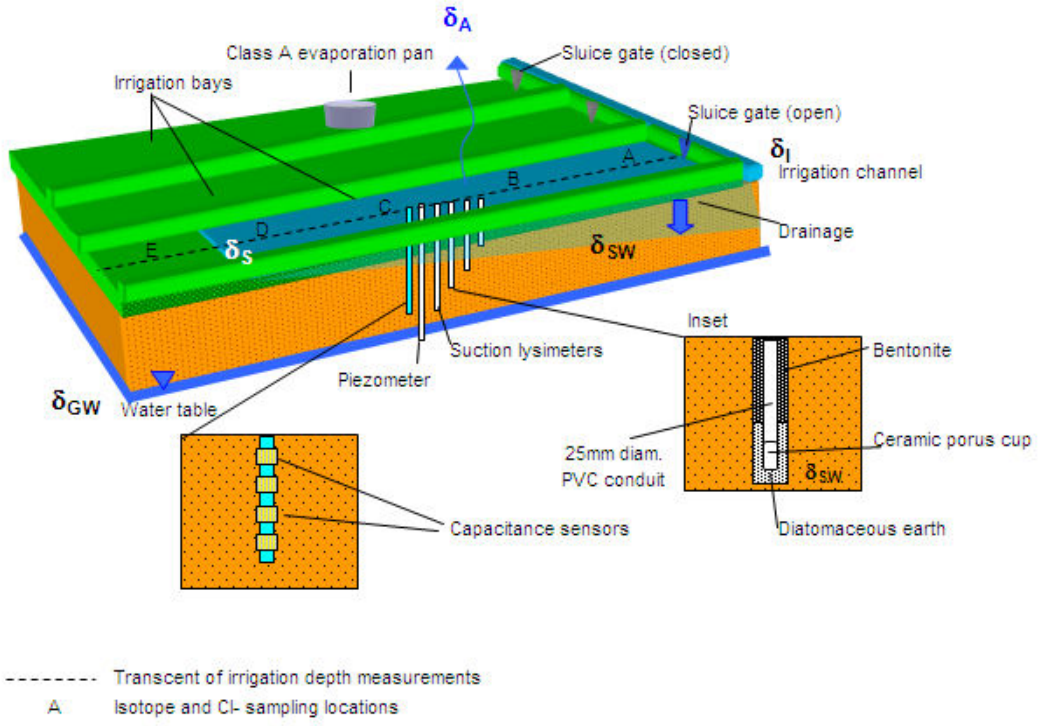

Figure 2. Schematic diagram of a typical flood irrigation site, showing instrumentation and sampled water balance components of a flood irrigation system.

Table 1: Characteristics of the four flood study sites

Site	Soil and crop type			Irrigation application			Dimensions of irrigation bay				Irrigation Channel		
	Top soil	Soil thickness (m)	Crop Type	Application duration (hrs)	Volume (Ml/ha)	Ponding duration (hrs)	Width (m)	Length (m)	Area (ha)	Laser leveled	length (m from bore)	head at sluice gate (m) Start of irrigation	head at sluice gate (m) End
NAP4	Loam	0.35-0.5	Pasture	10	1.10	24 - 28	125	200	2.50	N	180	0.244	0.22
NAP5	Loam	0.1	Clover	8	1.47	18 - 22	50	500	2.50	Y	620	0.175	0.175
MTM	Sand	<0.30	Lucerne	2.5	2.00	6 - 15	20	300	0.60	Y	500	0.27	0.23
PG	Sand	<0.30	Lucerne	6	1.55	8	50	425	2.13	Y	105	0.8	0.2

Sampling and surface water monitoring

Water samples for δ^2H, $\delta^{18}O$, Cl^- and EC were collected during two irrigation events from each irrigation bay during the 2005/06 irrigation season. Water samples were collected in 50 ml glass McCartney bottles from; i) the irrigation bore; ii) along the irrigation channel; and iii) at five evenly distributed locations (labelled A to E) across the flood irrigation bay (Figure 2). Water samples were collected at 2 - 4 h intervals during the irrigation and ponding periods.

Approximately 24 hours after irrigation, soil water samples were extracted via a vacuum pump from suction lysimeters buried within the vadose zone at nominal depths (0.30, 0.5, 1.0, 2.0 and 3.0 m). As drainage can continue to occur at depth a number of days after irrigation, the changes in the isotopic signature of the wetting front as it moves through the vadose zone was monitored over time during the second round of sampling. Using the capacitance response as a guide, the suction lysimeters at NAP4 and NAP5 were subsequently sampled every 2 to 3 days after irrigation

Groundwater abstraction from irrigation bores was measured by flow meters (Mace Agriflow), which recorded flow rate (L/s) pumped from the irrigation well. Inflow to the bay was measured using either Dataflow Systems 392 (Plate 1c) or shaft encoders (Plate 2a) that record the depth of water flowing through the irrigation gate to the irrigation bay and the timing of an irrigation event. The depth of ponded water was measured manually along the bay at various time intervals during and after irrigation application to assess application uniformity, flow, distribution and infiltration dynamics.

Evaporation pan experiments (Class A drying pans)

A series of evaporation pan experiments were conducted next to each irrigation bay during each irrigation event. Class A pans (272 L) having a diameter of 125.7 cm were used at each site. The pans were positioned close to the irrigation bay and filled with source water (from the irrigation bore) at the commencement of each irrigation event. No water was added after the initial filling of the pan. Water loss and evolution of chloride, EC, δ^2H and $\delta^{18}O$ composition was measured in residual pan water at time intervals ranging from 2 - 4 h (in parallel with field sampling above), throughout irrigation application and ponding periods.

From this data, an enrichment factor was calculated which represents the enrichment of δ^2H or $\delta^{18}O$ in residual pan water per 1% of water loss from the pan. From this relationship, the percentage of ponded irrigation water lost by evaporation was estimated via Equation 5.

Pan evaporation (E_{pan}) measured from the Class A pan was converted to potential evaporation (E_p) via a pan coefficient (K_p) using equation 3. K_p was sourced from local Bureau of Meteorology (BoM) stations and typically ranged from 0.7 to 0.9. E from flood irrigation waters was calculated according to the methodology of Debarro (2006), (Equation 4).

Where possible, E_p was validated with daily ET (FAO56) measurements obtained from the BoM stations located at Padthaway (station No. 26089) and Keith (station No. 25507), which are < 5 km from each site. In addition, local air temperature (T) and relative humidity (h) readings were also obtained from local BoM weather stations.

Determination of δ_A and E from Class A evaporation pan experiments

δ_A was determined from drying pan experiments by rearranging Equation 6 to solve for δ_A. Where E_{pan} is the measured percentage water loss by evaporation from the pan at end of the experiment (at time t_1), δ_s becomes the isotopic values of pan water (t_1), δ_i becomes the isotopic value of the input to the pan at time t_0, h is the mean relative vapour pressure, obtained from local BoM weather stations, ϵ^* is the equilibrium fractionation factor at 25 ^{0}C (1.0093 and 1.08 for $\delta^{18}O$ and δ^2H respectively), $\Delta\epsilon$ is the kinetic enrichment factor, evaluated here as $\Delta\epsilon\ \delta^{18}O = 14.2\ (1 - h)$, and $\Delta\epsilon\ \delta^2H = 12.5\ (1 - h)$, as most frequently encountered conditions in nature (Gonfiantini, 1986) and $\epsilon = \epsilon^* - 1$.

Once δ_A was determined, Equation 6 was subsequently used to calculate the percentage water loss by actual evaporation E, where values for δ_s and δ_i were substituted with isotopic values for irrigation water (at different time intervals) and the mean isotopic value of the input to the flood bay, respectively.

Isotope analysis

Groundwater samples for δ^2H and $\delta^{18}O$ were analysed by the CSIRO isotopic laboratory in Adelaide, using a Europa Scientific Ltd. GEO 20-20 dual inlet gas ratio mass spectrometer. Water samples for $\delta^{18}O$ analysis were first equilibrated with CO_2 of a known isotopic composition and $\delta^{18}O$ was determined by mass spectrometry of the equilibrated CO_2 gas with a precision of ± 0.1 ‰. Results are expressed as $\delta^{18}O$ ($^{18}O/^{16}O$) in per mil (‰) as a deviation from the V–SMOW (Vienna Standard Mean Ocean Water), where:

$$\delta_{sample} = 1000((R_{sample}/R_{V\text{-}SMOW})-1)$$

and therefore:

$$\delta^{18}O‰ = \frac{(^{18}O/^{16}O)_{sample} - (^{18}O/^{16}O)V\text{-}SMOW \times 1000}{(^{18}O/^{16}O)V\text{-}SMOW} \quad (8)$$

For analysis of δ^2H, 20 µL of sample was reduced to hydrogen by circulating it as vapour across hot uranium at 810°C. This was then introduced into the mass spectrometer. Results are expressed as δ^2H ($^2H/^1H$) in per mil (‰) relative to V-SMOW, where:

$$\delta^2H‰ = \frac{(^2H/H)_{sample} - (^2H/H)V\text{-}SMOW \times 1000}{(^2H/H)V\text{-}SMOW} \quad (9)$$

Including errors induced by the azeotropic distillation, the overall precision of the $\delta^{18}O$ and δ^2H analysis are ± 0.1 ‰ and ± 1 ‰ respectively.

Results

Pan evaporation experiments

Pan evaporation measured on site was corrected to potential evaporation using the pan coefficient, which ranged from 0.67 to 0.92. K_p was calculated from weather data obtained from nearby BoM stations and averaged over a daily time step. Potential evaporation measured onsite during the sampling (irrigation) periods ranged from 3 mm to 7 mm, resulting in a 1.3 to 3.5 % reduction of the pan water volume (Figure 3). Evaporation of flood waters, measured during the period the bays were inundated, as per the method of Debarro (2006) (Equation 4) revealed lower evaporation rates (0.5 mm to 6 mm).

Potential evaporation measurements recorded here were similar to those measured at local BoM stations. Comparisons with the BoM stations could only be made for sites where evaporation was measured over a full 24 h, i.e. measurements made at 9 am each morning.

The potential daily evaporation was similar for all sampled irrigations and ranged from 4.7 mm to 6.2 mm per day. However, at NAP4 the potential evaporation was lower during the first sampling event, when irrigation took place during the night (Figure 3). At NAP5 the daily potential evaporation was 2.2 mm higher during the ponding period during second (later) sampling period.

Determination of the enrichment factor

The enrichment trends for $\delta^{18}O$ and $\delta^{2}H$ as a function of the percentage of evaporation (water loss from the pan) for each pan experiment is illustrated in Figure 4. A linear relationship between the stable isotopes and the percentage of initial volume can be seen (r^2 = 0.92 to 0.99).

From all pan experiments conducted during the irrigation season, it was determined that for every 1% of water evaporated from the pan, leads to an enrichment of 0.19 ‰ to 0.38 ‰ for $\delta^{18}O$ (0.7 ‰ to 0.9 ‰ for $\delta^{2}H$), Figure 4. These values are consistent with pan experiments conducted in previous studies by Simpson et al. (1987); Aly et al. (1993) and El-Bakri et al. (1996) (0.19 for $\delta^{18}O$ and 0.7 for $\delta^{2}H$), where up to 70 % of the pan water had evaporated. The slight variations calculated for each site may be attributed to differences in pan

water salinity which ranged from 1400 to 6500 mg/L for irrigation sites at Padthaway and Hundred of Stirling respectively. This is supported by Gonfiantini (1965) and Lloyd (1966), who showed that the isotopic enrichment of pan water was reduced at higher salinities.

Pan water enrichment trends are also shown in $\delta^{18}O$ versus $\delta^{2}H$ plots in relation to the Local Meteoric Water Line (LMWL) developed for the region (Figure 4). Evaporation lines for each pan experiment are characterised by slightly lower slopes (3 - 4) which fits within the range given by Gat (1980), Payne (1983) and Gibson et al (1999), in comparison to the LMWL (7.65).

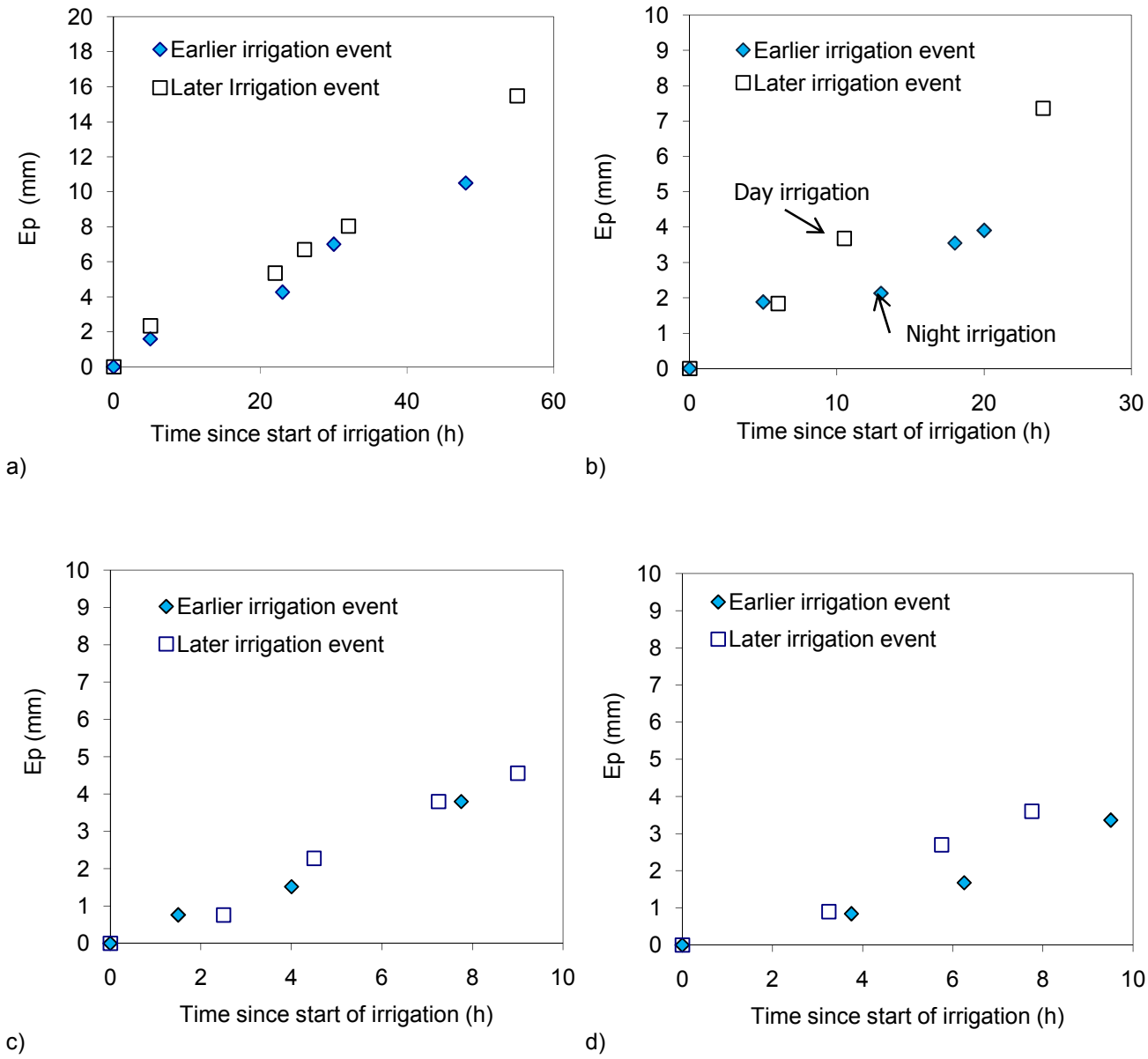

Figure 3 Potential (E_p) evaporation corrected from Class A evaporation pan experiments conducted during each irrigation at a) NAP5, b) NAP4, c) MTM; and d) PG.

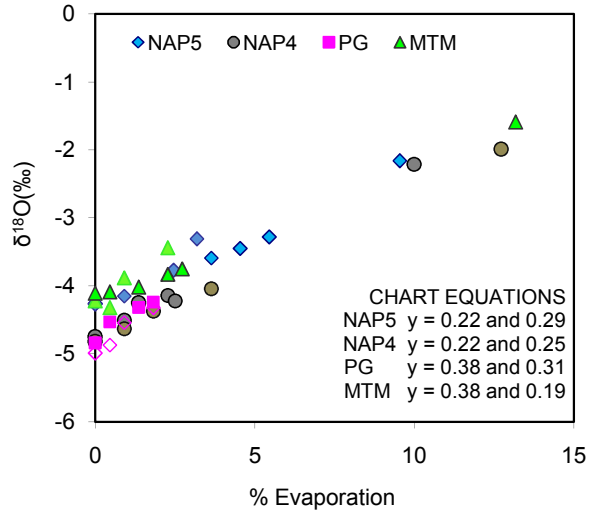

a)

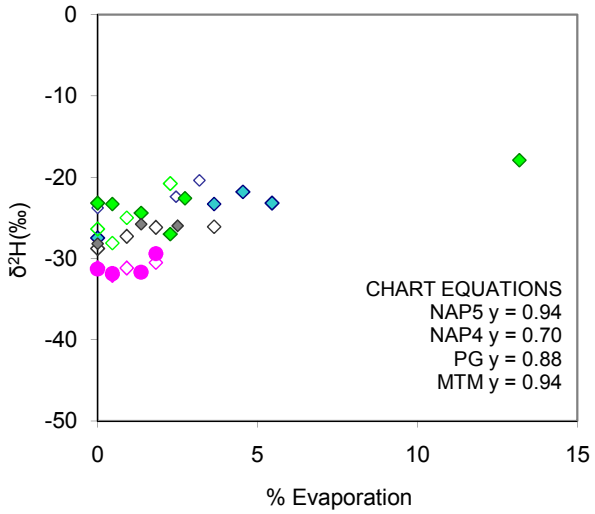

b)

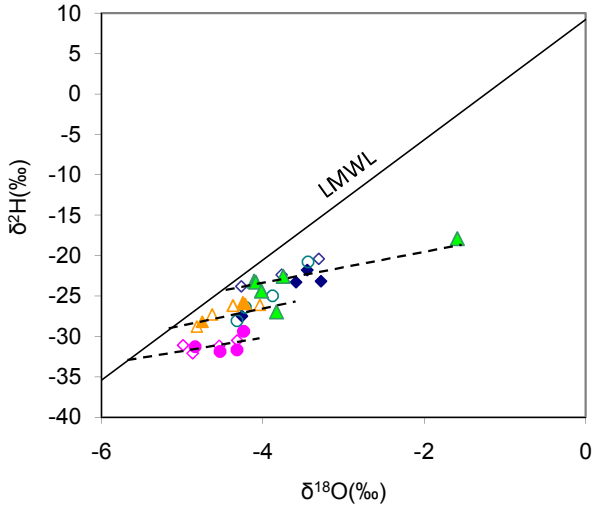

c)

Figure 4 Relationship between isotopic composition and percentange water loss from Class A evaporation pans for a) $\delta^{18}O$ and b) $\delta^{2}H$. C) is the relationship of $\delta^{2}H$ and $\delta^{18}O$ of evaporating pan waters for each site

Determination of δ_A from Class A evaporation pan experiments

From Equation 3 it is evident that δ_A of atmospheric vapor can be derived from isotopic changes in pan water (δ_s), provided that E_{pan}, h, δ_i, ϵ^* and $\Delta\epsilon$ values are known. E of pan water was calculated in MSExcel allowing $\delta^{18}O_A$ values of atmospheric vapor to be adjusted until a close calibration between the measured E_{pan} (measured from Class A pan) and calculated E was obtained. Figure 5 shows good correlation r^2 = 0.92 to 0.99 between the calculated E and measured E_{pan} across all sites on the basis of pan data ($\delta^{18}O_s$) alone. Isotopic values adjusted to achieve this strong correlation ranged from 19 to 25 ‰ for $\delta^{18}O_A$, and 120 to 170 ‰ for δ^2H, and have been plotted in relation to δ_p and Local Meteoric Water Line (LMWL), developed for the area (Figure 6). δ_A values are less enriched than δ_p and plot along the LMWL. Pan derived estimates of δ_A under lower humid conditions were less enriched than δ_A estimates under more humid conditions.

Irrigation observations

The volume of irrigation applied to each irrigation bay ranged from 105 mm to 260 mm (Table 2). At PG the initial head in the irrigation channel prior to irrigation was 0.8 m (see Plate 1c – d) which was significantly higher than the measured heads at the other irrigation sites, most notably NAP4 (see Plate 2a and 2e), where the elevation of the channel floor is slightly lower than the elevation of the bay. The higher head at PG and slightly higher pump capacity resulted in faster irrigation application (covering an area of 0.35 ha/h) compared to the other irrigation sites (0.25 ha/h). Irrigations at NAP4 and MTM were sampled under different conditions. At NAP4 the first sampling event was carried out when irrigation was applied between the hours of 12:00 to 22:00 and left to pond during the night. During the second sampling event in March, irrigation was applied between the hours of 22:00 to 8:00 and left to pond during the day. At MTM the first sampled irrigation was conducted just after the lucerne was cut for hay (see Plate 1a). The second sampled irrigation was carried out a time when lucerne cover had reached ~ 90 % (see Plate 1b). The second irrigation application was 1 h longer as a result of the denser crop. The two irrigations sampled at PG and NAP5 were carried out under similar conditions (i.e. time, crop cover and meteorological conditions).

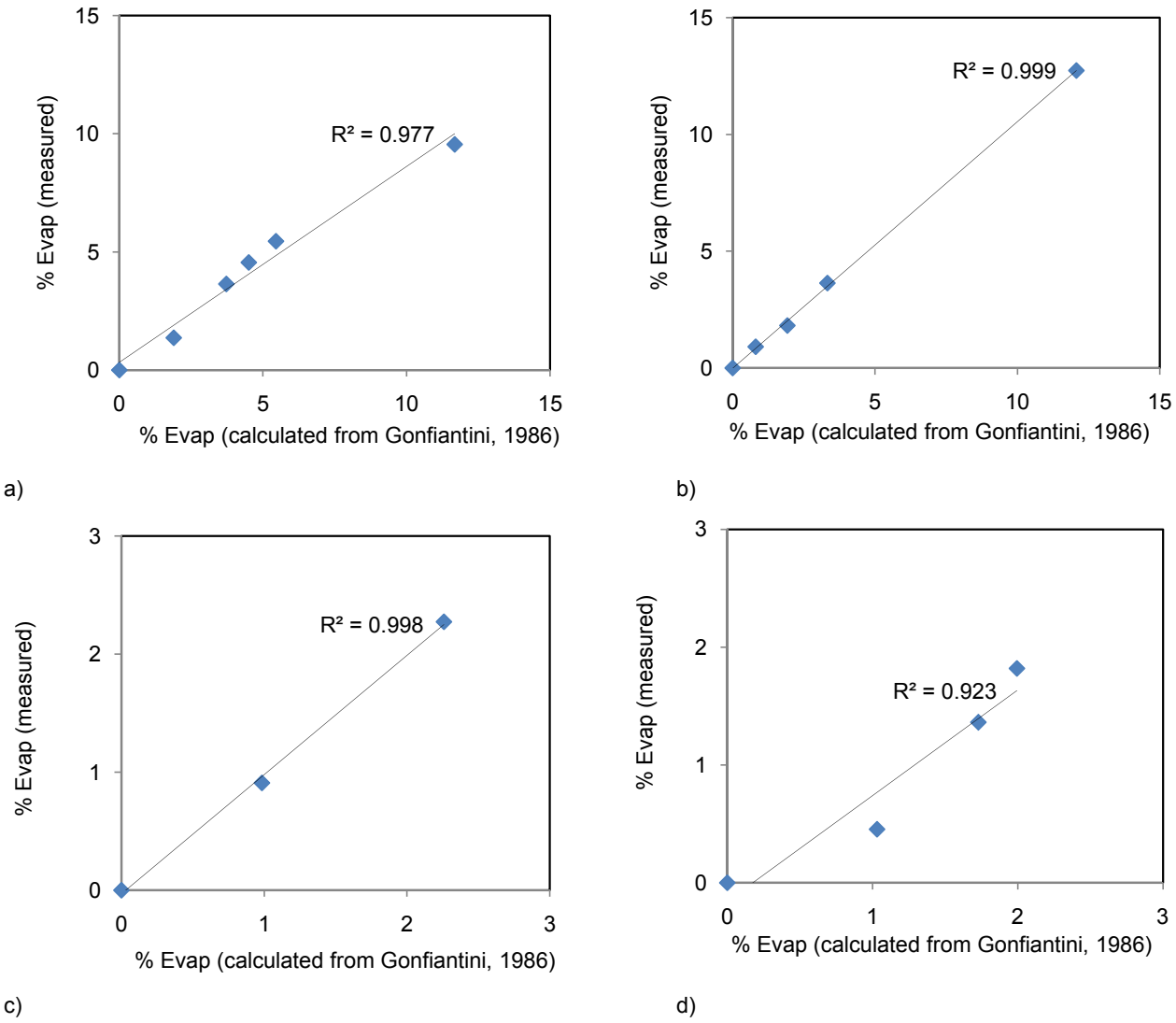

Figure 5 Measured pan evaporation loss vs. calculated evaporation loss for a) NAP5; b) NAP4; c) MTM; and d) PG

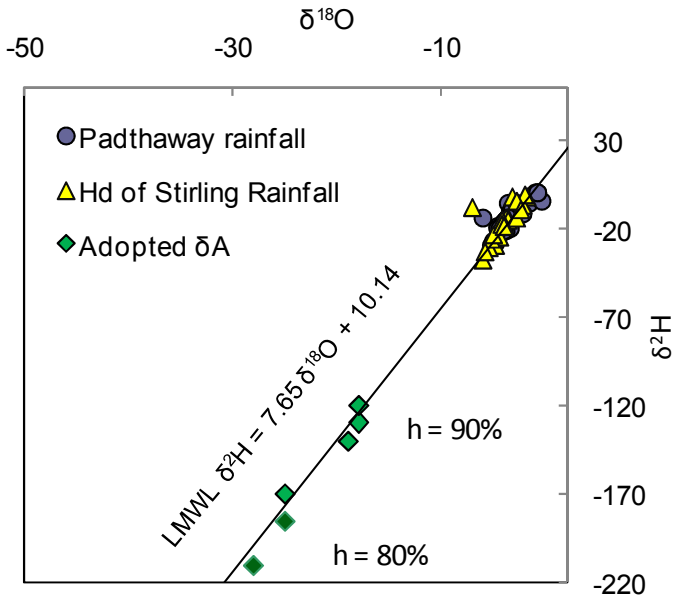

Figure 6. Plots of calculated $\delta^{18}O_A$ versus $\delta^{2}H_A$ from pan evaporation experiments. Also shown are $\delta^{18}O$ and $\delta^{2}H$ of local precipitation collected from 6 sites over 2003 to 2006, with a LMWL for reference.

Table 2. Irrigation Observations

Study Site	Irrigation Application					Volume Applied		Head at sluice gate (m)		Ponding duration (h)	No. Irrigations per season	Salinity (mg/l)	Observations
	Start time	Finish time	Duration (h)	Pump Rate (ML/d)	Application Rate (ha/h)	ML/ha	Total (ML)	Start	End				
NAP5	9:30	17:30	8	11.13	0.31	1.48	3.71	0.175	0.175	24 - 28	9	1889	Day irrigation, mature clover
	9:30	17:30	8	9.73	0.31	1.30	3.24					2144	Day irrigation, mature clover
NAP4	12:00	22:00	10	12.59*	0.25	1.05	2.62	0.244	0.22	18 - 22	16	1434	Day irrigation, mature pasture
	22:00	8:00	10	12.6*	0.25	1.05	2.63					1384	Night irrigation, mature pasture
MTM	10:30	12:50	2.3	12.28	0.24	1.84	1.1	0.27	0.23	6 - 15	5	4874	Day irrigation, min lucerne cover
	12:15	15:30	3.25	12.28	0.24	2.60	1.56					4565	Day irrigation, mature lucerne
PG	11:00	17:00	6	13.2	0.35	1.55	3.3	0.8	0.2	>8	5	6498	Day irrigation, mature lucerne
	9:30	15:30	6	13.2	0.35	1.55	3.3					6458	Day irrigation, mature lucerne

*Two bays irrigated simultaneously

Field measurements of surface water flow across the irrigation bay

Figure 7 shows depth measurements of the irrigation water as it flows across the bay for each site during irrigation and for various time intervals during and after irrigation, which is referred to as the ponding period.

During irrigation, the head of water was higher at the sluice gate and lower at the end of the wetting front (Plate 2a – b). As soon as the irrigation application had ceased, the water at sites NAP4, MTM and PG continued to flow down gradient towards the end of each bay, where the heads reversed, becoming higher at the end of the bay (down gradient) and lower at the start of the bay (up gradient). This was attributed to the bays being laser levelled at these sites. Due to the shallow nature of top soil (loam) at NAP5, the irrigation bays were not laser levelled, causing the irrigation water to pond within the two low-lying areas located at each end of the bay (Plate 2c – d) .While most of the irrigation water drained through the soil profile over night (within approx 14 h post irrigation), 2 to 4 cm of ponded water was still evident 22 h post irrigation, at each end of the bay (Figure 7). At NAP4, where the soil consists of loam, ponding water covered a larger percentage of the bay (70 % to 80 %) for up to 17 h after irrigation. In contrast, sites MTM and PG exhibited higher drainage rates, as most of the surface water had drained within 5 h and 8 h respectively, post irrigation application. This was attributed to a higher sand composition of the topsoil at these sites (Table 1).

Estimation of irrigation water loss by evaporation

The enrichment of $\delta^{18}O$ and salt concentration of irrigation water along the flow path at each irrigation bay is shown in Figure 8**.** Water samples collected at 5 places are arranged to be consistent with water movement in the irrigation bay (denoted by locations A to E) and collection time (denoted by A1, A2 and A3). The isotopic and salt concentration of drainage water taken from suction lysimeters at different depths following irrigation is also shown for comparison (denoted as SL).

The isotopic enrichment of irrigation water measured at the sampled locations ranged from 0.05 to 2 ‰ for $\delta^{18}O$ (1.7 to 7.5 ‰ for $\delta^{2}H$), and was accompanied by an increase in chloride concentration (30 to 130 mg/l). The isotopic and chloride signatures of drainage waters show low fractionating water loss (minor

fractionation) and large increases in salinity, in comparison to the irrigation waters during the application period. This suggests that water loss from transpiration is more dominant than evaporation.

The corresponding evaporation rates, calculated for each flood irrigation site on the basis of Simpson et al. (1987) and Gonfiantini (1986) are shown on Figure 9 for each sample locations (A to E). The volume of water applied and the ponding time, recorded at the time each sample was collected, are also shown for reference.

The actual evaporation rates derived from both isotopic models are in close agreement. These have been compared to conventional pan techniques in Table 3. Evaporation calculated via the two methods ranged from 0.5 mm to 5.6 mm, which were slightly lower than potential evaporation (1.5 to 8 mm) measured from Class A evaporation pans, over the same time period (Figure 9, Table 3).

Similar evaporation rates were obtained between isotopic and traditional methods from irrigation bays characterised by open bodies of water (NAP4, NAP5, MTM-earlier irrigation). However, during irrigations at PG and MTM-later irrigation (carried out under dense crop cover), isotopic methods revealed lower evaporation rates (up to 0.5 mm) than traditional methods (up to 2 mm), and thus confirm that dense crop cover is a strong inhibitor of evaporation. Under these conditions a 30 % adjustment was made to the K_p, to account for dense crop cover, as recommended by the FAO56, for the correction of pan evaporation measurements near dense vegetation.

Potential evaporation during each irrigation event varied from 1.5 to 8.0 mm. To further explore this variable and allow a comparison of efficiency between each irrigation, the percentage of actual evaporation (calculated from ponded waters) relative to the total potential evaporation (measured from respective Class A evaporation pans) was determined (E_a / E_p .100), Table 3. Here, E represents the average evaporation losses obtained from measurements made from all sampled locations, during the irrigation and ponding periods. The percentage of actual evaporation losses from flood irrigation relative to potential evaporation generally ranged from 10 % in the Hundred of Stirling to 60 % in Padthaway, with

differences being attributed to controlling factors such as duration of irrigation application/ponding, crop cover and timing of irrigation.

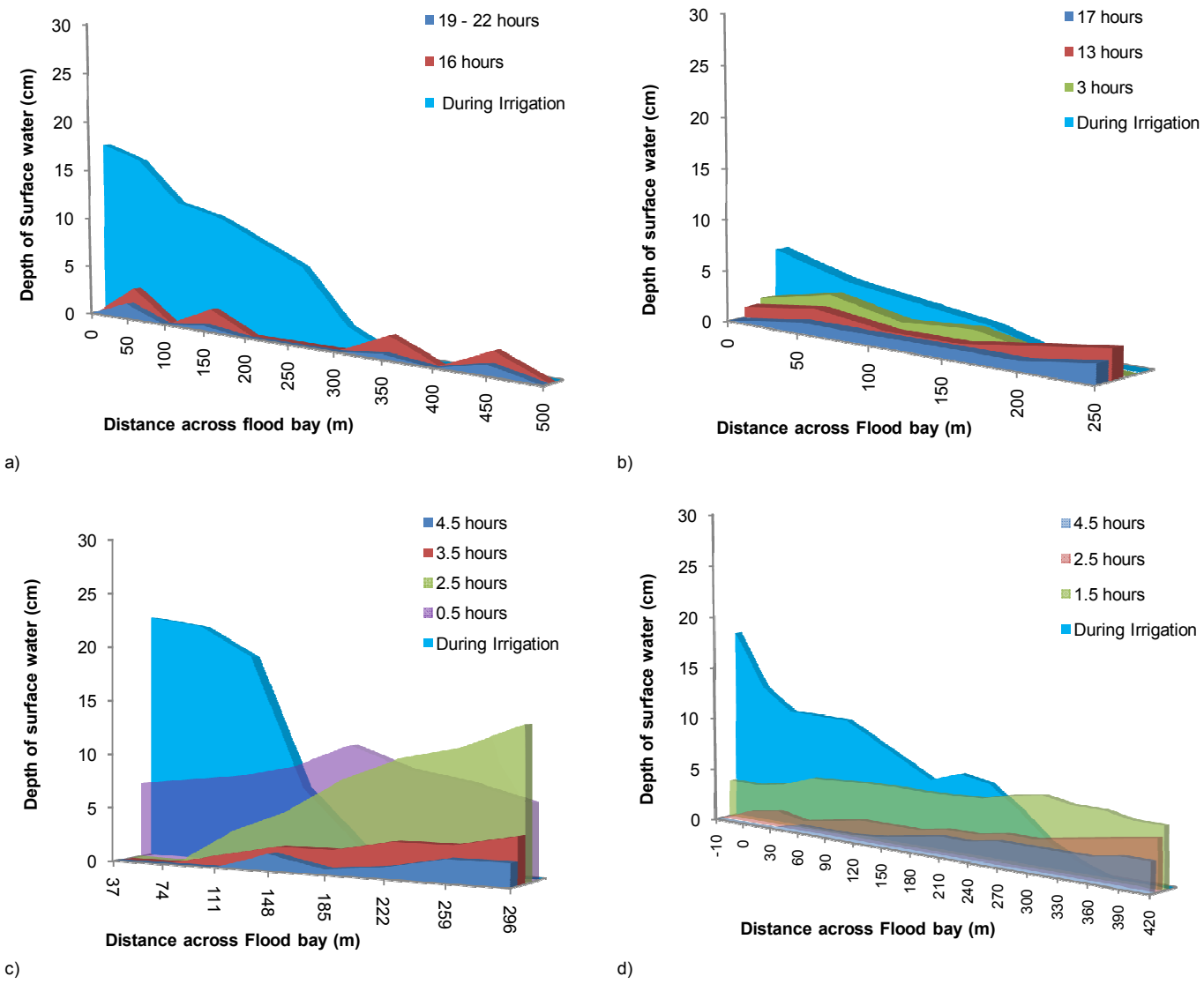

Figure 7 Depth of irrigation water with distance along the irrigation bay at various times during irrigation at sites a) NAP5, b) NAP4, c) MTM and d) PG

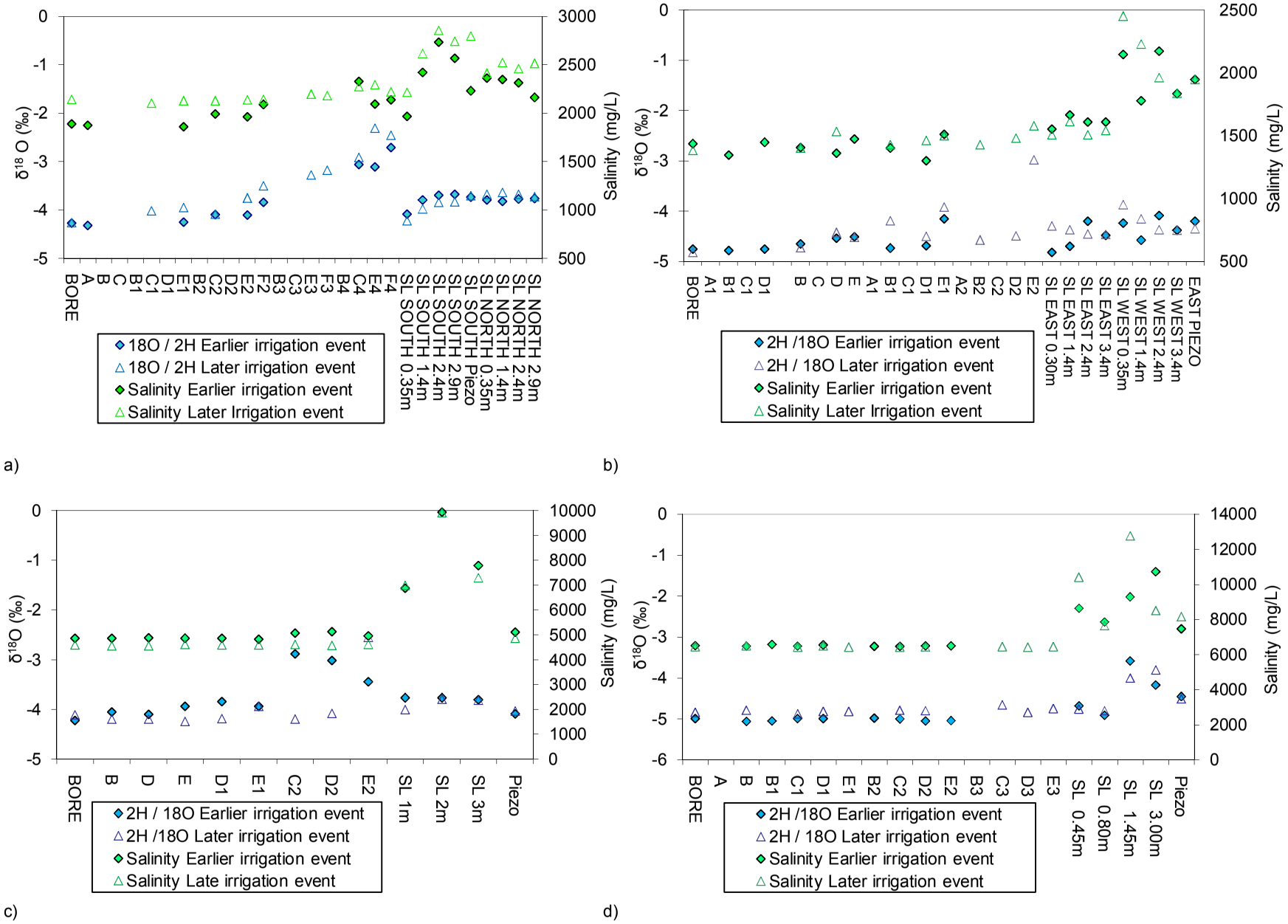

Figure 8 Evolution of $\delta^{18}O$ enrichment and salinity of irrigation water along the flow path at irrigation sites a) NAP5, b) NAP4, c) MTM and d) PG A1, A2, A3, represent measurements taken from location A at 3 different time intervals (see Figure 2 for locations) and SL = Suction Lysimeter water

Table 3 Evaporation and efficiency estimates from flood irrigation

Irrigation Site		Irrigation Duration	Volume applied	Potential evaporation from Class A pan (mm / irrigation)			Average actual evaporation from flood irrigation				Efficiency indicator	Variable at time of irrigation
							Isotopic (Gonfiantini, 1986 and Simpson et al., 1987)		Conventional (Debarro, 2006)			
		(hrs)^	(mm)	Pan (mm)*	Pan.Kp (mm)	%	%	mm	%	mm	E/E_p (%)	
NAP5	Earlier Irrigation	30	148	8.8	7	4	3.1	4.6	3.09	4.57	34	Day irrigation, mature clover
	Later Irrigation	32	130	12	8.04	5.45	4.8	6	4.35	5.65	25	Day irrigation, mature clover
NAP4	Earlier Irrigation	18	105	5	3.55	2.27	1.1	1.2	2.82	2.96	66	Day irrigation, mature pasture
	Later Irrigation	24	105	8	7.36	3.64	3.2	4.7	3.4	3.2	50	Night irrigation, mature pasture
PG	Earlier Irrigation	9.5	155	4	3.36	1.82	0.18	0.4	0.46	0.70 (0.30)$^+$	88	100% lucerne crop cover
	Later Irrigation	7.75	155	4	3.6	1.82	0.35	0.51	1.35	2.10 (0.62)$^+$	86	100% lucerne crop cover
MTM	Earlier Irrigation	4	184	2	1.52	0.91	2.35	4.4	0.93	1.71	0	0% lucerne crop cover
	Later Irrigation	9	260	6	4.56	2.73	1.5	1.23	0.49	1.27 (0.37)$^+$	73	100% lucerne crop cover

^ Irrigation duration represents the period since the start of irrigation to the time when the last sample was collected

* Total evaporation measured at the time when the last irrigation sample was collected

^+K_p adjusted by 0.30 to compensate for crop cover

~ Average percentage evaporation loss calculated on the basis of Gonfiantini (1986) and Simpson et al. (1987)

The percentage water loss by evaporation, relative to the total volume of irrigation water applied is also shown on Table 3. Flood irrigation site NAP5, NAP4 revealed the greatest percentage water loss (3 - 4.5%) compared to PG and NAP (0.2 to 0.8%). MTM reported a higher percentage loss (2.8%) when irrigation water was applied to a young crop.

Across all sites, there was no change in δ^2H and $\delta^{18}O$ composition of irrigation water as it flowed from the bore to the irrigation bay, suggesting minimal evaporation losses from the irrigation channels (Figure 8). This was expected as the residence time of irrigation water within the channel was estimated to be <1 h, making changes in isotopic composition very hard to detect within this small time frame.

During both sampled irrigation events at sites NAP5, MTM and PG, minimal effects of evaporation were detected within the $\delta^{18}O$, δ^2H signatures and salinity concentration of the irrigation water as it flowed across the bay. This minor depletion observed (<0.2 ‰ for $\delta^{18}O$ and <0.8 ‰ for δ^2H), equated to an average evaporation loss of <0.3 %. Data obtained from NAP4 during March 2006 showed some effects of evaporation during irrigation application, where δ^2H increased by 5 ‰, which can be attributed to the longer duration of application during the day (Figure 8).

Isotopic and salinity signatures of the ponded water collected from three locations along the bay at PG remained relatively unchanged during the day, where only minor evaporation losses (<1 mm) during these sampling intervals were calculated. In contrast to PG, isotopic enrichment and hence evaporation was noted at MTM, NAP5 and NAP4 during the ponding period, which varied across each site.

The December 2005 irrigation and sampling event at MTM was conducted at a time when there was no lucerne crop cover, shortly after the lucerne was cut for hay (Plate 1a). Following the commencement of irrigation, the δ^2H concentration of the ponded water increased significantly from -26 ‰ to a maximum of -21 ‰ (Figure 8). When compared to the local pan experiments, this enrichment corresponded to an average evaporation loss of 4 mm (Figure 9). A slight increase in salinity of 248 mg/L (from 2722 mg/l to 2970 mg/l) was also observed

at the sampling sites during this period. During the March 2006 irrigation and sampling event, which was conducted at a time when the crop cover had increased to 95 %. The isotopic signatures and salinity concentration of the irrigation water remained steady during the application and ponding period, signifying a much lower evaporation loss of < 1.5 mm. This data confirmed that crop cover was a strong regulator of evaporation loss and hence concentration of salt as evaporation was superior (up to 3 mm higher) with a young crop as determined using isotopes and EC. E_p calculated from the pan experiments between the two sample events of (i) earlier irrigation / young crop and (ii) later irrigation / mature crop indicate higher evaporation potential during the later irrigation (dense crop cover), thereby indicating that that crop cover was the primary factor for the differences observed (Figure 8, Table 3).

Water samples collected from the ponded water at NAP5, which ponded at the southern and northern ends of the bay the following morning (day 2) indicated only minor enrichment 0.4 ‰ for $\delta^{18}O$ (2.7 ‰ for $\delta^{2}H$) signifying that only a small amount of evaporation loss (corresponding to 1 mm) had occurred over night (Plate 2c –d). The greater effects of evaporation were most evident towards the evening (day 2) when the compositions of $\delta^{18}O$ increased by 1 ‰ to 1.9 ‰ (5 to 7 ‰ for $\delta^{2}H$) at sample times of 0 h, and 22.5 h respectively (Figure 8 and Figure 9). An increase in salinity from 160 to 300 mg/L coupled the above observed enrichment in isotopes. When compared to local pan experiments, the enrichment of both $\delta^{18}O$ and $\delta^{2}H$ represents an average evaporation loss of 6 - 9 mm from these pools. The greater evaporation losses calculated at NAP5 are attributed to the greater duration of ponding and lower crop cover (pasture versus lucerne) which occurred here in contrast to the rapid draining sites at MTM and PG.

The January 2006 irrigation at NAP4 occurred during the day and was left to pond during the night (Plate 2e – f). The isotopic and salinity signatures of water samples collected from ponded water the following morning (11 hours post irrigation application) was only slightly more enriched in comparison to that of the source water at time 0; equating to minor evaporation losses (1 mm) during the night, when the majority of ponding had taken place (Figure 9). During the later irrigation, isotopic signatures remained stable when water was applied to the bay during the night, but had later increased (by 0.9 to 1.84 ‰ for $\delta^{18}O$ and 2.3 to 5.9

‰ for δ^2H) once the water was left to pond for 11 consecutive hours the following day. As predicted, evaporation losses at this time were shown to be much higher (2 - 12 mm, average of 4 mm) in comparison to the earlier irrigation event. These results confirmed the benefit of irrigating at night (Figure 8).

A qualitative comparison of evaporation rates from each irrigation bay can be seen by plotting δ^2H versus $\delta^{18}O$ values relative to the LMWL (Figure 10). The slope of the regression lines (3.6 to 4) deviated from the value (7.65) given by the LMWL. The slopes varied according to the intensity of evaporation and are consistent with slopes given by Gat (1980) for evaporation from open water bodies and more importantly slopes derived from the drying pan experiments (3 to 4).

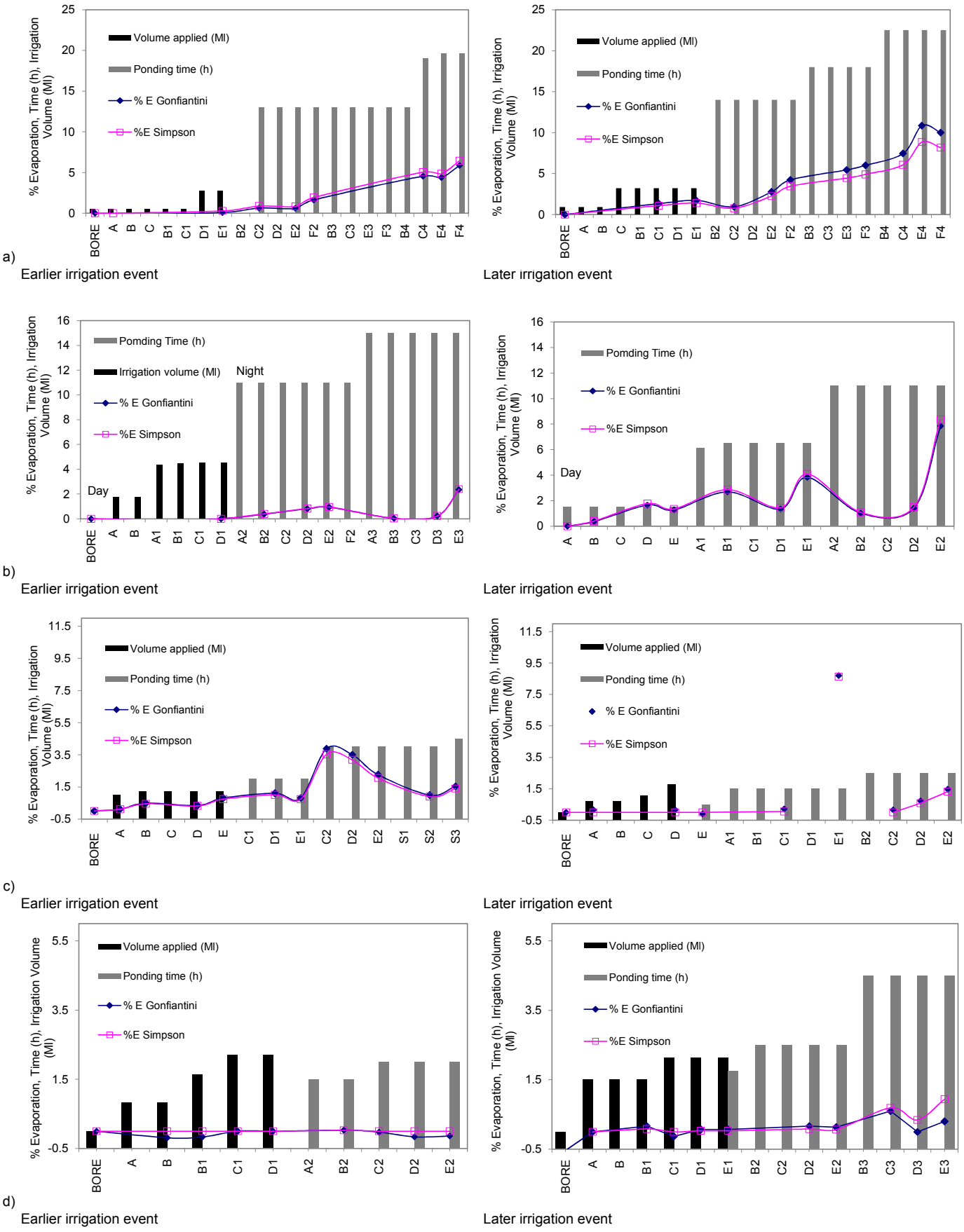

Figure 9 Percentage evaporation losses from flood irrigation, calculated using equations of Simpson 1987 and Gonfiantini 1986 at sampled location (denoted A to E) for flood irrigation sites a) NAP5, b) NAP4, c) MTM and d) PG. A1, A2 and A3, represent measurements taken from

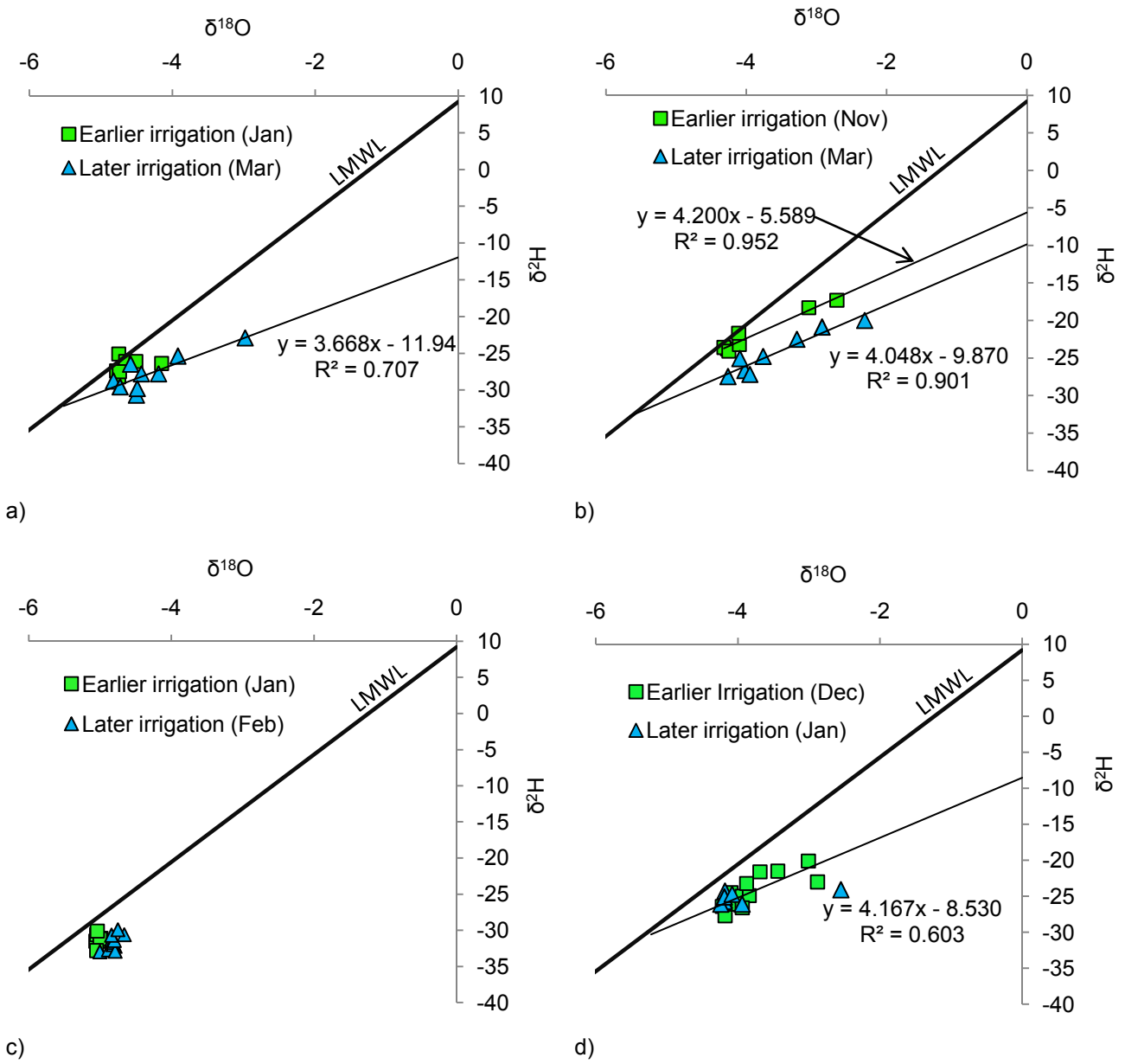

Figure 10 δ^2H and $\delta^{18}O$ plots of irrigation water potted against the LMWL a) NAP4 b)NAP5 c)PG and d)MTM

Discussion

Pan experiments

This study has shown that the enrichment of heavy isotopes δ^2H and $\delta^{18}O$ in residual waters as a result of evaporation can provide a sensitive indicator of water loss from flood irrigation systems. These losses were estimated by relationships between heavy isotope enrichment and percent water loss in evaporation pan experiments, according to analytical models of Simpson et al. (1987) and Gonfiantini (1986), which until now, were previously applied for the determination of evaporation from lakes. When applied to irrigation, a close agreement of percentage water loss E_c was obtained when applying the two equations, however, the method of Gonfiantini (1986) requires the δ_A of atmosphere to be known. It should be emphasis that the estimates of the percentage of water lost to evaporation are sensitive to the choices δ_A. As E_{pan}, h, δ_i, ϵ^* and $\Delta\epsilon$ values are known, values of δ_A were calculated on the basis of drying pan experiments, which yielded values of -18 ‰ for $\delta^{18}O_A$ (-140 ‰ for δ^2H_A). It must be noted there may be some uncertainty with the estimation of isotopic exchange parameters by using drying Class A pan, as the pan waters were not buffered to the temperature of the irrigation water. Although these values lie within a realistic range for this climate, the calculation of evaporation from flood irrigation, via Gonfiantini (1986) equation relies on accurate characterisation of δ_A. Such accuracies can only be verified by comparisons with independent methods (e.g. vapor sampling traps or constant feed evaporation pans).

Comparison of evaporation estimates to non isotopic techniques

The average evaporation losses calculated from isotopic techniques compared well to traditional methods conducted in parallel at sites where open water bodies were allowed to evaporate. However, during irrigations of dense crop cover, evaporation rates derived from isotopic techniques revealed lower evaporation rates compared to traditional methods, suggesting that crop cover is a strong regulator of evaporation (by 23 % to 28 %). The close agreement in evaporation rates from open water bodies gives high confidence in the validity of applying the two isotopic methods to this irrigation setting.

Comparison of water loss by evaporation (efficiency) across each site

The mean evaporation loss calculated for all sites ranged from 0.2 % to 5.0 % (0.4 to 6 mm). Although the overall percentage of water loss by evaporation is appears small, when multiplied by the total volume of water applied to an irrigation bay over an irrigation season (i.e. 5 - 16 irrigations multiply by 1.1 Ml/ha - 2.6 Ml/ha per irrigation), the total evaporation loss can amount to 0.1 - 0.5 Ml/ha/y.

The differences in evaporation losses calculated here are believed to be attributed to variable factors such as (i) soil type (ponding duration), (ii) crop canopy cover, (iii) time of irrigation and (iv) rate at which the water was applied. Hence a new comparative measure of irrigation efficiency across each site was achieved by comparing the ratio of water evaporated from the flood bay to the potential evaporation measured (via Class A evaporation pans) on site. Flood bays characterised by rapid draining soils and dense crop canopy cover showed lower evaporation ratios (higher efficiency 73 % - 88 %) than sites which were characterised by poorer draining soils and minimal crop canopy cover (25 % - 49 %).

The duration of irrigation application varied across each site, ranging between 3 to 10 h, however with the exception of NAP4, undetectable (or minor) changes in isotopic composition of irrigation water measured at all sites was noted, highlighting minimal evaporation during irrigation delivery (from the channel and as water flows across the bay). Evaporation was only detected during the ponding period, which varied from 6 to 28 h across each site and is considered to be the primary factor resulting in excess evaporation losses.

During conditions when irrigation is applied to bare soils, (such as the MTM earlier irrigation), evaporation from wet soil surfaces can be high as from ponded water. However as most of drainage was rapid and occurred during the night, no evaporation from the soil was detected.

In general, sites PG and MTM located in the Hundred of Stirling irrigation district both reflect lower average evaporation losses of 0 to 5 mm (higher efficiency 73 % to 88 %), when compared to Padthaway sites NAP4 and NAP5, which

recorded average evaporation losses of 4.5 mm to 12 mm (lower efficiency of 25 % to 49 %). The higher evaporation losses (and lower efficiency) calculated at both sites in Padthaway are reflected by the duration of ponding which was ~10 to 15 h longer, than observed at the sandier sites in the Hundred of Stirling. Here, sandier soils facilitated quicker drainage rates and therefore resulted in a lower evaporation potential.

The high percentage of evaporation calculated at NAP5 (6 mm to 10 mm), was only detected in pools, which ponded for extended periods of time (20 - 22 h) at each end of the bay (Plate 2c – d) and therefore does not reflect the average evaporation loss across the bay which was much lower (4 mm). The highest evaporation loss (up to 8 %) of residual water was detected at site NAP4 (March 2006 sample event), where water was applied over night and to left to pond for 11 h the following day (efficiency of 49 %). During the January sampling event, when water was left to pond during the night, the evaporation losses of residual water were much lower 1 mm to 3 mm (efficiency = 66 %).

This study confirmed that a higher density of lucerne cover at MTM and PG also contributed to a reduction in evaporation (Plate 1a – b). This was demonstrated at MTM where there was a maximum difference of 27 % (3 mm) in evaporation between an open water body (efficiency of 0 %) and ~95 % crop cover (efficiency of 73 %).

Conclusion

In this study, we have shown that actual evaporation from flood irrigation can be determined using the analytical isotopic methods described by Gonfiantini (1986) and Simpson et al. (1987) for evaporation from lakes. Evaporation rates determined by these techniques were calibrated against Class A drying pan experiments which were used to derive relationships between isotopic enrichment and water loss from the pan.

This study has shown that the isotopic techniques used here to determine E, compared well with traditional techniques described by Penman (1948) and later adopted by Debarro (2006) in this setting - especially for open water bodies, which gave high confidence in the calculations of evaporation rates from flood irrigation and to the validity of these models to this setting.

Under dense crop cover, evaporation rates derived by isotopic methods were 23 % to 28 % lower than traditional methods, indicating that crop canopy cover is a strong inhibitor of evaporation. This observation is confirmed by FAO56, which has shown that under these conditions pan coefficients need some adjustment (by 30 %).

The use of stable isotopes allowed us to quantify evaporation rates at different stages of irrigation for different irrigation sites of varied characteristics (i.e soil type, bay architecture, application rate). Average evaporation during ponding from flood irrigation ranged from 0.5 to 6 mm per irrigation, with greatest evaporation losses occurring during the ponding period.

By comparing actual evaporation to potential evaporation measured via Class A evaporation pans, we were able to examine the efficiency of different flood irrigation configurations. We found that evaporation was strongly reduced at sites where irrigation application and soil infiltration rates were higher (i.e less ponding time).

a) 

b) 

c) 

d) 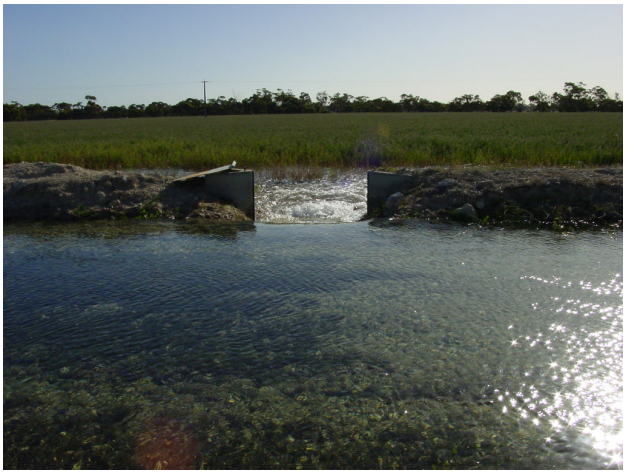

Plate 1 a) MTM bay, recently cut for lucerne prior to first irrigation in December 2005, b) MTM irrigation bay during January 2006 irrigation, showing luceren crop cover at >95%, c) depth logger next to sluice gate at PG, shortly before irrigation and d) sluice gate open at PG, during irrigation. Note the change in head of water in the delivery channel c) prior and d) during irrigation at PG. The higher head observed here results in a much quicker application rate compared to the other irrigation sites.

a) 

b) 

c) 

d) 

e) 

f) 

Plate 2 a) Irrigation application at NAP5, looking North from shaft encoder during November 2005 irrigation, b) Irrigation application at NAP5, looking north during March 2006 irrigation, c) and d) ponds at the southern and northern ends of the bay at NAP5 respectively, 18 h post irrigation, e) ponding at NAP4, looking west, 1.5h post irrigation application during March 2006 and f) ponding at NAP4 1.5h post irrigation application during March 2006, looking east.

References

Allen, R.G., Pereira, L.S., Raes, D., Smith, M., 1998. Crop Evapotranspiration: Guidelines for Computing Crop Water Requirements. United Nations Food and Agriculture Organization, Irrigation and Drainage Paper 56. Rome, Italy, 300 pp.

Allison, G.B., Brown, R.M., Fritz, P., 1979. Estimation of the isotopic composition of lake evaporate. J. Hydrol. 42, 109–127.

Allison, G.B., Leaney, F.W., 1982. Estimation of isotopic exchange parameters using constant-feed pans. J. Hydrol. 55, 151–161.

Aly, A. I. M., Froehlich, K., Nada, A., Awad, M. A., Hamza, M. and Salem, W. M., 1993. Study of environmental isotope distribution in the Aswan High Dam Lake Egypt, for estimation of evaporation of lake water and its recharge to adjacent groundwater. Environ, Geochem. & Health. 15(1), 1-9.

Barnes, C.J. and Allison, G.B., 1982. Interpretation of stable isotope profiles in arid zone dunes. Hydrol. Water Resour. Symp., IEA, Melbourne, pp. 9~101.

Debarro, J. 2006. Dividing the droplet: A water balance study for lucerne seed production resourced by an underground aquifer. A Report for the Rural Industries Research and Development Corporation. Project No. DEB-3A.

Dincer,1968. The use of oxygen-18 and deuterium concentrations in the water balance of lakes. Water Resources Research 4, 1289-1305.

Dincer, T., Hutton, L.G, Kupee, B. J., 1978. Study using stable isotopes, of flow distribution , surface /groundwater relations and evapotranspiration in the Okarango Swamp, Botswana Isotope Hydrology 1978, IAEA, Vienna. Vol. 1, pp. 3-26. 1979.

El-Bakrim, A., Tantawi, MS., Hamza, S. and Awad, M.A. 1996. Estimation of groundwater inflow to irrigation drains in Minia, Upper Egypt, based on a deuterium and oxygen-18 evaporation pan technique. Hydmlogical Sciences - Journal- des Sciences Hydrologiques, 41(1) February 1996.

Froehlich, K.F.O., Gonfiantini, R., Rozanski, K., 2005. Isotopes in lake studies: a historical perspective. In: Aggarwal, P.K., Gat, J.R., Froehlich, K.F.O. (Eds.), Isotopes in the Water Cycle, Past, Present and Future of a Developing Science. IAEA, Springer, Vienna, The Netherlands, 381pp.

Gat, J.R., 1970. Environmental isotope balance of Lake Tiberias. Isotopes in Hydrology, 1970. IAEA, Vienna, pp. 151–162.

Gat, J.R., 1980. The isotopes of oxygen and hydrogen in precipitation. In: Fritz, P., Fontes, J.Ch. (Eds.). Handbook of Environmental Isotope Geochemistry, 1. Elsevier, New York, pp. 27– 47.

Gat, J.R., 1981. Lakes. Stable Isotope Hydrology- Deuterium and Oxygen-18 in the Water Cycle. In: J.R. Gat, R. Gonfiantini (Eds.). IAEA Technical Report Series No. 210, Vienna, pp. 203–221.

Gat, J.R., Bowser, C.J., 1991. Heavy isotope enrichment in coupled evaporative systems. In: H.P. Taylor, J.R. O'Neil, I.R. Kaplan (Eds.), Stable Isotope Geochemistry: A Tribute to Samuel Epstein, Special Publication No. 3, The Geochemical Society, San Antonio, Texas, pp. 159–168.

Gat, J.R., Matsui, E., 1991. Atmospheric water balance in the Amazon Basin: an isotopic evapotranspiration model. J. Geophys. Res. 96, 13 179–13 188.

Gibson, J.J., Edwards, T.W.D., Bursey, G.G., Prowse, T.D., 1993. Estimating evaporation using stable isotopes: quantitative results and sensitivity analysis for two catchments in northern Canada. Nordic Hydrol. 24, 79–94.

Gibson, J.J., Edwards, T.W.D., Prowse, T.D., 1999. Pan-derived isotopic composition of atmospheric water vapour and its variability in northern Canada. Journal of Hydrology 217, 55–74.

Gonfiantini, R., 1986. Environmental isotopes in lake studies. In: Fritz, P., Fontes, J.Ch. (Eds.). Handbook of Environmental Isotope Geochemistry, 3. Elsevier, New York, pp. 113–168.

Harrington, N., van den Akker, J., Brown, K. and Mackenzie, G., 2004. Padthaway Salt Accession Study. Volume One: Methodology, site description

and instrumentation. South Australia. Department of Water, Land and Biodiversity Conservation. DWLBC Report 2004/61.

Jensen, M.E., Burman, R.D., and Allen, R.G. 1990. Evapotranspiration and Irrigation Water Requirements. ASCE Manuals and Reports on Engineering Practice No. 70. 332p.

Lewis, E., 1875. Sturtevant E. Lewis (Edward Lewis), Sturtevant's Notes on Edible Plants (BiblioBazaar, LLC, 2009).

Lloyd, R. M., 1966. Oxygen isotope enrichment of sea water by evaporation. Geochem. Cosmochim, Acta, 130, 801 - 814.

Mauder, M., Foken, T., Clement, R., Elbers, J.A., Eugster A., Grunwald, T., Heusinkveld, B., and O., Kolle 2007. Quality control of CarboEurope flux data – Part II: Inter-comparison of eddy-covariance software, Biogeosciences Discuss., 4, 4067 - 4099.

Payne, B.R., 1983. Introduction. In: Guidebook on Nuclear Techniques in Hydrology. Technical Reports Series No. 91, IAEA, Vienna.

Penman, H. L. 1948. Natural evaporation from open water, bare soil and grass. Proc. Roy. Soc. London, A193, 120 - 146.

Simpson, H. J., Hamza, M. S., White, J. W. C , Nada, A. & Awad, M. A., 1987. Evaporative enrichment of deuterium and 1S0 in arid zone irrigation. In: Isotope Techniques In Water Resources Development. IAEA-SM-299/125,241-256.

Simpson H.J, Herczeg AL, Meyer WS.,1992. Stable isotope ratios in irrigation water can estimate rice crop evaporation. Geophys. Res. Lett. 19:377-380.

Welhan, J.A., Fritz, P., 1977. Evaporation pan isotopic behavior as an index of isotopic evaporation conditions. Geochim. Cosmochim. Acta 41, 682–686.

White, J. W. C. & Gedzelman, S. D., 1984. The isotopic composition of atmospheric water vapour and concurrent meteorological conditions. / Geophys. Res. 89, 4937-4939.

Wohling, D., 2007. Minimising Salt Accession to the South East of South Australia. The Border Designated Area and Hundred of Stirling Salt Accession

Projects. Volume 2 – Analytical Techniques, Results and Management Implications, DWLBC Report 2007, Government of South Australia, through Department of Water, Land and Biodiversity Conservation, Adelaide.

Zimmermann, U., Ehhalt, D. and Miinnich, K.O., 1967. Soil water movement and evapotranspiration: changes in the isotopic composition of the water. Proc. Syrup. on Isotopes in Hydrology, Vienna, 1966, Int. At. Energy Agency (I.A.E.A.), Vienna, pp. 567--584.

Zuber, A., 1983. On the environmental isotope method for determining the water balance of some lakes. J. Hydrol. 61, 409–427.

CHAPTER 4

Salinity impacts from evaporation and transpiration under flood irrigation

Abstract

Transpiration and evaporation rates from irrigated pastures can be adequately assessed by conventional methods and in more recent times, by the use of stable isotopes δ^2H and $\delta^{18}O$. However, the salinity impacts transpiration and evaporation have on infiltrating irrigation waters and residual soil waters have not been independently assessed in a flood irrigation setting. In this study, oxygen-18, deuterium and chloride concentrations of irrigation water, soil water and groundwater were monitored along with soil water content over time, to independently assess the salinisation impacts of evaporation and transpiration. This study was carried out across four flood irrigation sites which overlay a heterogeneous loam-sand and limestone vadose zone. Results showed that minor evaporation losses were detected across most flood irrigation sites through the use of stable isotopes δ^2H and $\delta^{18}O$. The associated increase in chloride concentration of irrigation water as a result of evaporation (minor fractionating water loss) was low (0 mg/l to 129 mg/l) compared to the chloride increase as a result of transpiration (150 mg/l to 2,800 mg/l), noted in shallow soil water. Across all sites, the fractionating water loss detected in soil water was minor (<1‰ $\delta^{18}O$ from the source), with isotopic signatures reflecting partially evaporated irrigation waters. The high soil water chloride concentrations, minor fractionating loss and corresponding decrease in soil water content suggests that transpiration is the dominant cause of water loss and therefore the largest contributor to salinity impacts during flood irrigation. Salinity impacts caused by transpiration (0.4 to 2.6 t/ha) were 3 to 50 times greater than the salinity impacts caused by evaporation from irrigation and soil waters (0.01 to 0.3 t/ha).

Introduction

During flood irrigation, water loss to the atmosphere occurs through two pathways: 1) Evaporation (E) from the irrigation water and soil water and 2) Transpiration (T) from the crop. Both fluxes result in the concentration of salts in residual irrigation waters and soil waters, (a process referred to as salinisation), however evaporation can be managed and is the undesirable component of water loss from any irrigation practice. This study offers a new method via the use of stable isotopic and chemical tracers to independently assess the contributions these processes (E and T) have on infiltrating irrigation waters. This technique was applied to four flood irrigation bays, which vary by way of soil type, crop type and irrigation delivery (pump rate and bay architecture).

Salt accumulation in the soil zone over the long term is determined by the salinity of the irrigation water, the volume applied and the amount of drainage water. Whilst transpiration cannot be managed, reducing evaporation losses in terms of only applying the minimum amount to satisfy plant transpiration plus a leaching fraction, leads to the most efficient irrigation.

In water balance studies, evaporation and transpiration rates can be quantified via the widely accepted conventional FA056 Penman-Monteith method (Penman, 1948; Monteith, 1965; Allen et al, 1998), lysimeters (weighing or non-weighing), water balance approach, soil water depletion techniques, and in recent times, via sophisticated climate stations or flux towers, using the eddy covariance technique (Mauder et al., 2007).

A major challenge with these methodologies is determining which flux (E or T) has a greater contribution to salinisation in the soil profile. Quantifying such impacts can only be assessed by the monitoring of soil water and plant interactions post irrigation. The monitoring of environmental isotopes δ^2H and $\delta^{18}O$ in soil water and xylem-leaf water have been used in recent times to independently quantify evaporation rates from soils (Allison and Barnes, 1983, 1984; and Zimmermann et al., 1967) and transpiration rates from a crop (Dawson and Ehleringer, 1998; Ehleringer and Dawson, 1992), however this work has not been expanded to quantify the salinisation impacts of the two processes, during flood irrigation.

Evaporation leads to enrichment in water molecules with heavier isotopes (δ^2H and δ^{18}O) because of preferential loss to the atmosphere of water molecules consisting of lighter isotopes (δ^1H and δ^{16}O), a process referred to as fractionation (Zimmermann et al., 1967; White and Gedzelman, 1984). In contrast, transpiration does not result in any fractionation, allowing the two processes to be separated out in the water balance. Since evaporation and transpiration affect residual water isotopic compositions differently, the relative contribution of these two water loss fluxes may theoretically be resolved from observed changes in residual irrigation soil water isotopic compositions (Dincer et al., 1978).

Enrichment and fractionation of δ^2H and δ^{18}O abundances of soil water owing to evaporation have been used to aid the determination of water origins (Gat and Tzur 1967; Gat, 1971) and to estimate the degree of evaporation (Allison and Barnes, 1983, 1984; and Zimmermann et al., 1967). In their studies, empirical procedures were developed for quantifying evaporation rates from soils, however little is known about the effect that the independent processes of evaporation and transpiration have on infiltrating irrigation waters and residual soil waters, or about their contribution to salinity impact.

The analysis of stable isotopes hydrogen and oxygen bound in plant and soil water offers one of the most powerful tools for addressing plant water uptake (Dawson and Ehleringer. 1998; Ehleringer and Dawson 1992). Both the evaporation process, as well as irrigation events results in soil water content and isotopic profiles that vary with soil depth (Allison and Hughes, 1983; Ehleringer and Daweson, 1992). As the uptake of water by roots at different depths occurs without fractionation (Thorburn et al., 1993; Walker and Richardson, 1991), the isotopic signature of water in the plant stem is the average of the soil water isotopic values weighted by the proportion of water acquired from each soil layer. Simple linear mixing models have been developed to estimate the relative contributions of numerous water sources to plant uptake.

Few studies have highlighted the potential utility of coupling isotopic techniques to independently assess salinisation from evaporation and transpiration, particularly from flood irrigation. One way of doing this is by using conservative tracers such as chloride concentrations of soil water, which can be used

conjunctively to separate impacts of transpiration and evaporation. For example, Simpson et al., 1987 reported large increases of salinity in shallow groundwaters beneath irrigated regions, compared to River Nile input total dissolved solids concentrations, which were not accompanied by heavy isotope enrichment proportional to the increase in dissolved solids. Dincer et al. (1979) distinguished between the water loss by evaporation and by transpiration of the aquatic plants in the Okavango swamp. Therefore, the combination of chloride and stable isotope data for agricultural drainage waters can provide valuable new insights into the main mechanisms (E or T) responsible for salinisation and suggest which management changes are more likely to improve water use efficiency and water quality of drainage waters most effectively.

In the irrigation districts of the south east of South Australia, the soil zone is shallow (0.5 to 1 m thick) and overlays the Padthaway Formation, a hard calcrete topped limestone. Previous studies undertaken in this region indicated that the presence of this calcrete layer might control drainage and constrain the depth of the evaporation front to within the upper soil horizon only (van den Akker et al., 2006). Due to the presence of the calcrete layer, the approaches developed by other studies (Allison and Barnes 1983; 1984) to investigate evaporation from the soil, may not be applicable in this setting. Therefore this warrants further investigation.

The objective of this study was to quantify the independent impacts of evaporation and transpiration from flood irrigation. In this study we compare the build up (enrichment) of stable isotopes of soil water (by evaporation only) to that of salinity which is increased by the combined evapotranspiration flux (evaporation + transpiration). This was achieved by the monitoring of soil water content, $\delta^{2}H$ and $\delta^{18}O$ and Cl^{-} concentrations in irrigation water, soil water and groundwater over time at four flood irrigation sites in the South East of South Australia.

Methods

Site description

The four irrigation study sites selected for this study lie within the inter-dunal flats of near the townships of Padthaway and Keith in the Upper South East of South Australia (Figure 1). Pasture, clover and lucerne crops are flood irrigated at these sites. The climate within the study areas can be characterised by warm to hot dry summers and cool wet winters. The average annual maximum temperature is 22 ^{o}C, with February being the hottest month at 29.8 ^{o}C and July being the coldest month, at 5.5 ^{o}C. Annual potential evaporation is 1600 mm/y and 1700 mm/y for Padthaway and Keith respectively.

Soil particle size (% sand, silt and clay), bulk density, water content and soil water chloride was previously determined at each site from soil cores (see Harrington et al., 2004 and Wohling, 2006). Soil cores were collected at 50 cm depth increments from either excavation pits or during drilling. Based on the particle size distribution, the soil classification for the top soil ranges from loam at Padthaway to sand in the Hundred of Stirling. Each site exhibits one or more calcrete layers which were encountered at depths of <0.50 m at Padthaway and < 1 m at the hundred of Stirling. The texture of most upper part of the Padthaway Formation resembles a weathered marly-clay.

Field measurements

Field measurements were made in four flood irrigation bays, consisting of pasture, clover and lurcern. Collection of water samples from irrigation water, soil water (suction lysimeters) and groundwater took place during two irrigation irrigation events at each site, which occurred within the 2005/06 irrigation season, spanning from November 2005 to March 2006. The ponded water samples were collected at five evenly distributed places in the flood bay (at stations labelled A to E, Figure 2) to detect isotopic change during surface water movement. Controlled, Class A Pan evaporation experiments were also conducted in parallel to monitor the evolution of chloride and δ^{2}H and δ^{18}O concentrations over time as a result of potential evaporation. Figure 2 shows the sampling locations at a typical instrumentation site, consisting of capacitance probes, suction lysimeters and piezometers.

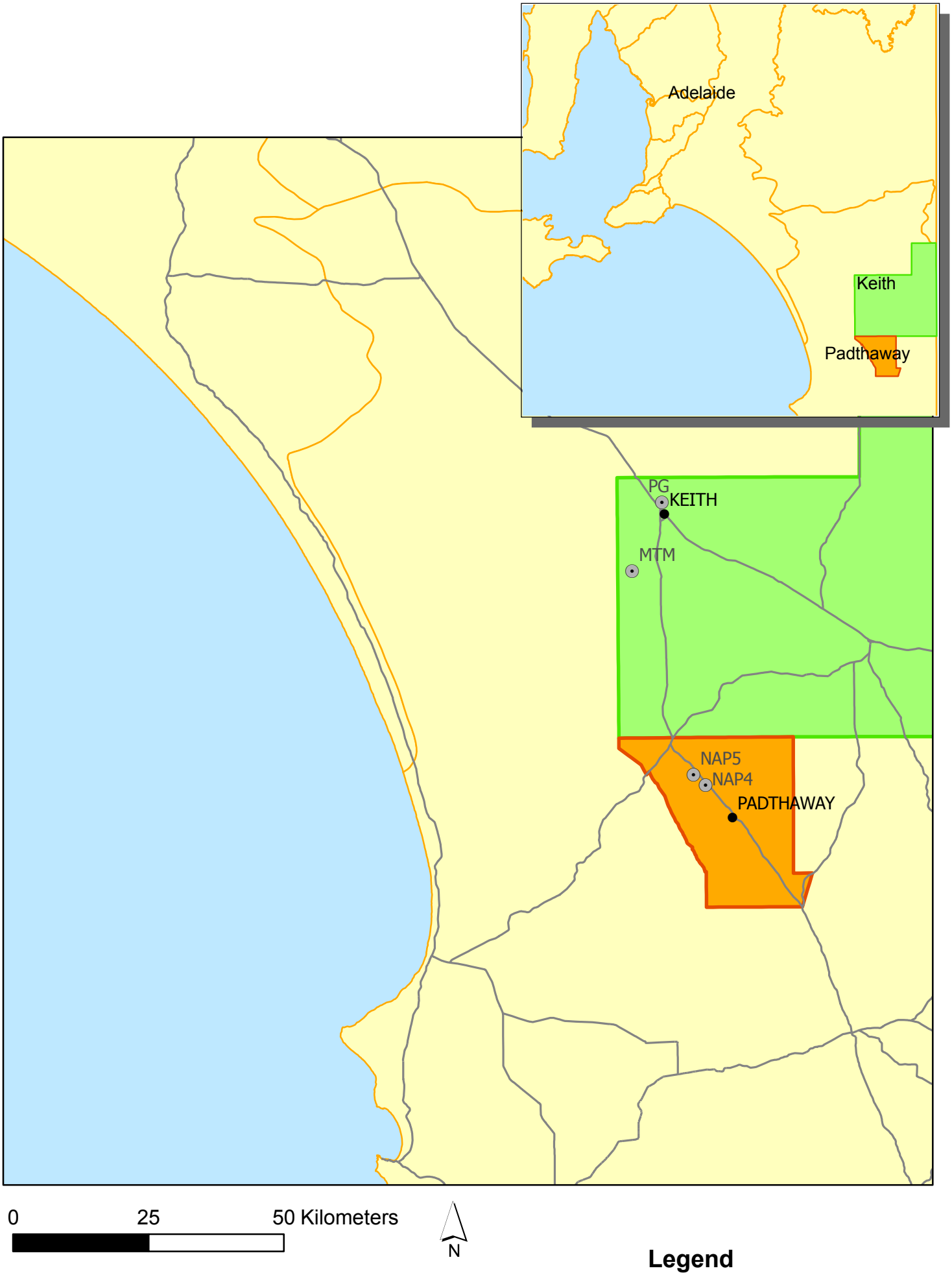

Figure 1 Site Location

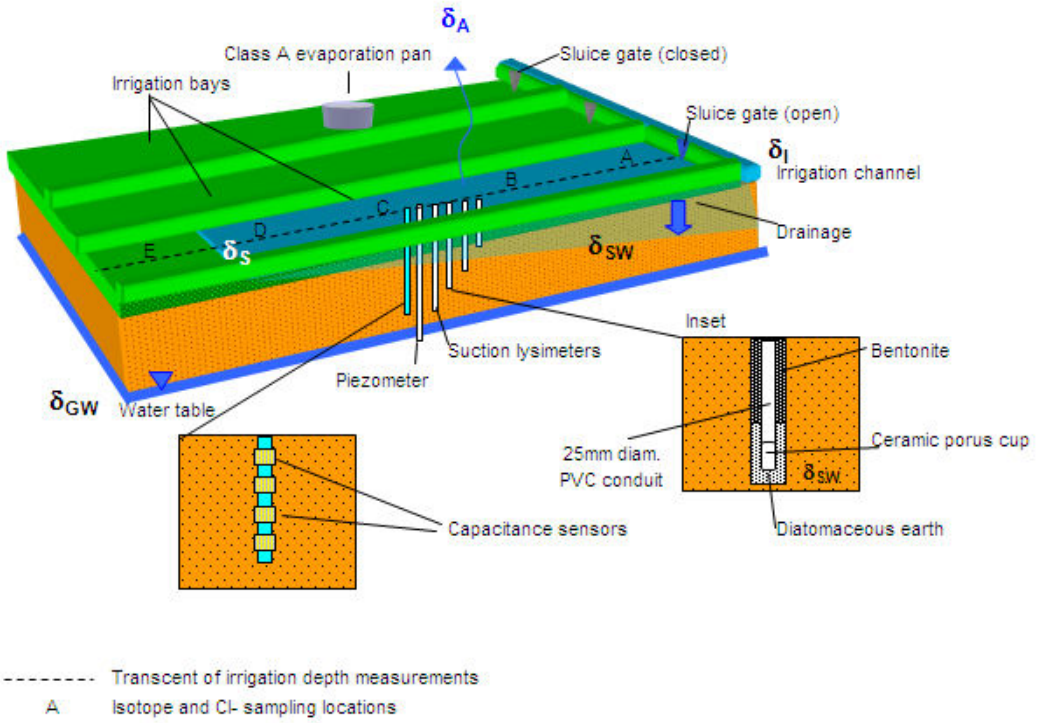

Figure 2. Schematic diagram of a typical flood irrigation site, showing instrumentation and sampled water balance components of a flood irrigation system.

All water samples were analysed for δ^2H and $\delta^{18}O$ concentration, total dissolved solids (TDS, mg/L) and chloride (Cl^- mg/L). A measurement of TDS was used to give an overall assessment of the salinity, while Cl^- helps distinguish between increases in salinity caused by evapotranspiration and soil/water interaction. The measurement of δ^2H and $\delta^{18}O$ allows us to determine evaporation (E only), whilst the build up of Cl^- along with decrease in soil water content will allow us to assess the total evapotranspiration flux (E + T).

Groundwater samples for δ^2H and $\delta^{18}O$ were analysed by the CSIRO isotopic laboratory in Adelaide, using a Europa Scientific Ltd. GEO 20-20 dual inlet gas ratio mass spectrometer. Results are expressed as $\delta^{18}O$ ($^{18}O/^{16}O$) in per mil (‰) as a deviation from the V - SMOW (Vienna Standard Mean Ocean Water). The overall precision of the $\delta^{18}O$ and δ^2H analysis are ± 0.1 ‰ and ± 1 ‰ respectively.

Capacitance Probes

Capacitance probes (Agrilink C - Probes) were installed vertically into the vadose zone to measure the dielectric constant of the soil and hence the water content by the capacitance method. They represent one experimental *in situ* technique that is available for monitoring root activity (plant water use) and soil drainage. Whilst the water content measurements provide an indication of advancing wetting fronts, they cannot resolve the difference between large and small drainage fluxes.

Holes were drilled (50 mm diameter) to depths of 3 m via air hammer techniques to accommodate the C-probe. Soil capacitance is measured via a number of sensors positioned at nominal depths of 10, 20, 30, 50, 100, 150, 200, 250 and 300 cm within the vadose zone. Sensors were located both within the top soil horizon and underlying Padthaway Formation. C - Probes were used to determine lag times and the extent of water movement through the profile after an irrigation event and were used to map and monitor crop water uptake (root activity). The C-probes utilised a telemetry system to log and transmit data every 15 minutes. At the Padthaway irrigation sites, two C-probes were installed within the irrigation bays, and at the Hundred of Stirling irrigation sites one C-probe was installed in the middle of the bay.

Suction Lysimeters

Suction lysimeters were installed to measure soil water salinity (and chloride) and isotopic ratios of hydrogen (δ^2H / δ^1H) and oxygen ($\delta^{18}O$ / $\delta^{16}O$) within the vadose zone over time. The chloride and isotopic concentrations measured from extracted soil water, reflects the chloride and isotopic concentrations of drainage water that would eventually recharge the unconfined aquifer.

At each site, four vertical, 100 mm diameter holes were drilled via air hammer techniques within the unsaturated zone to nominal depths ranging from 0.3 to 4.0 m, (depending upon rooting depth and soil structure) and equipped with suction lysimeters, installed in the bottom 5 cm of the hole. The top lysimeter is located in the top soil and the bottom 3 lysimeters were position within the unsaturated zone of the Padthaway Formation. The lysimeters were constructed by attaching a 15 cm porous ceramic cup to the end of 16 mm diameter PVC conduit. These were placed in the hole, with the ceramic cup surrounded by diatomaceous earth

to provide a good contact with the surrounding soil. A bentonite seal was placed above the diatomaceous earth and the hole was cemented to the surface. Two groups of four lysimeters were installed at each of the of the two flood irrigation sites (NAP4 and NAP5) in Padthaway to achieve average readings across the bay. Soil water samples were extracted via a vacuum pump from suction lysimeters after irrigation at a time when the soil profile appeared to be approaching field capacity, as determined by the capacitance response. As drainage can continue to occur for a number of days after irrigation, the changes in the isotopic signature of the wetting front as it moves through the vadose zone was monitored over time during the second round of sampling. Using the capacitance response as a guide, the suction lysimeters at NAP4 and NAP5 were subsequently sampled every 2 to 3 days after irrigation. Repeat sampling was not possible at sites PG and MTM, as sufficient amounts of soil water required for analysis could not be obtained due to the sandier soil, lower soil water retention, and hence lower water contents after irrigation.

Piezometers

Piezometers were installed 3 to 10 m below the water table in the middle of each bay. All piezometers were constructed from 50 mm diameter Class 12 PVC pipe with slotted screens just below the water table. δ^2H δ^{18}O, EC and chloride concentrations were measured in groundwater, sampled from the piezometers 1 - 2 days after irrigation. A whaler pump was used to pump groundwater until three bore volumes had been purged.

Results and Discussion

Wetting front movement

The capacitance response from sensors located at various depths throughout vadose zone show rapid drainage to the water table following irrigation (Figure 3). The high capacitance responses from the sensor located in the topsoil at NAP4 is indicative of ponded irrigation water, which ponded for up to 24 h after the initial irrigation. The capacitance sensors show evidence of water loss either by root activity or evaporation to depths of 0.20 m and 0.30 m. This depth corresponds to the depth of the topsoil and therefore the extent and bulk of the root zone. This is underlain by a calcrete-topped limestone. A change in the advancement rate of the wetting front was observed below this depth, as water drains through the underlying limestone. Sensors positioned in the limestone indicate that post irrigation, drainage continued to occur for up to 60 h at NAP4 and 16 h at NAP5, which represents a time when the profile approaches field capacity. Due to the heterogeneous nature of the unsaturated zone, preferential flow through cracks and cavities (karstic features) may not be accounted for or detected using the capacitance response. The results confirm that water loss via evaporation and transpiration is likely to be constrained to the top soil (upper 0.3m) above the calcrete layer.

Vertical distribution of soil water Cl^-, δ^2H and $\delta^{18}O$

Vertical distribution of soil water Cl^- measured from suction lysimeters post irrigation, remained uniform with depth, as a result of the high volume of irrigation water applied and high drainage (Figure 4). However, long term soil water Cl^- data collected monthly at these sites over 2003 - 2006 show variations in the upper part of the profile over longer term, which was attributed to evapotranspiration from the top portion of the soil profile.

Evaporation from the soil following irrigation at NAP4 and NAP5, was small and seemed only to affect the soil water isotope values in the top 0.30 m ($\delta^{18}O$ enrichment was 0.25 ‰ to 0.45 ‰ and δ^2H enrichment was < 5 ‰) where as the isotope values below this depth remained steady over time (Figure 4). The lack of isotopic enrichment below this depth, suggest that i) evaporation may be inhibited by a calcrete layer, commonly found at shallow depths (0.3 m) or (ii) rapid infiltration of irrigation water via large cracks, channels, coupled with a large

reservoir of relatively immobile soil water, owing to high marl content of the Padthaway Formation.

When there is no crop cover, such as during December irrigation at MTM, evaporation from saturated soil surfaces can be high as from ponded water (Jensen et al, 1990). However as most of drainage occurred during the night (after 5:30 pm), evaporation from the soil was not apparent in the isotopic signatures of soil water, which were collected the following day. At all other sites, evaporation from the soil was inhibited by dense crop cover and the calcrete layer at shallow depth (0.3 m).

Landon et al. (1999) showed that soil water obtained from suction lysimeters may not be representative of drainage water (mobile/gravity), as differences in the isotopic values of soil water collected using suction lysimeters, wick samplers and core samples were found to occur because these methods collect different fractions of the total soil-water reservoir. They showed that wick samplers collect primarily mobile, gravity drainage water that is in excess of soil field capacity. Suction lysimeters collect a mixture of immobile water that is bound to the soil matrix at a tension of less than about 35 kPa, and mobile water that is present in excess of field capacity at the time when suction is applied.

It can be postulated that due to the large volume of irrigation water applied here, the large amounts of soil water encountered in the suction cup directly after irrigation is comprised mostly of irrigation water. When extracting soil water from the suction lysimeters, only minor suction was required over a short time to obtain sufficient volumes of soil water, suggesting that the soil water extracted was mostly comprised of mobile water (as mobile water is expected to be drawn into the cup before immobile connate water from the soil matrix). This may also be explained by the possibility of a poor seal between the soil and lysimeter tube, thereby creating preferential flow paths. In future, this may be overcome by horizontal installations.

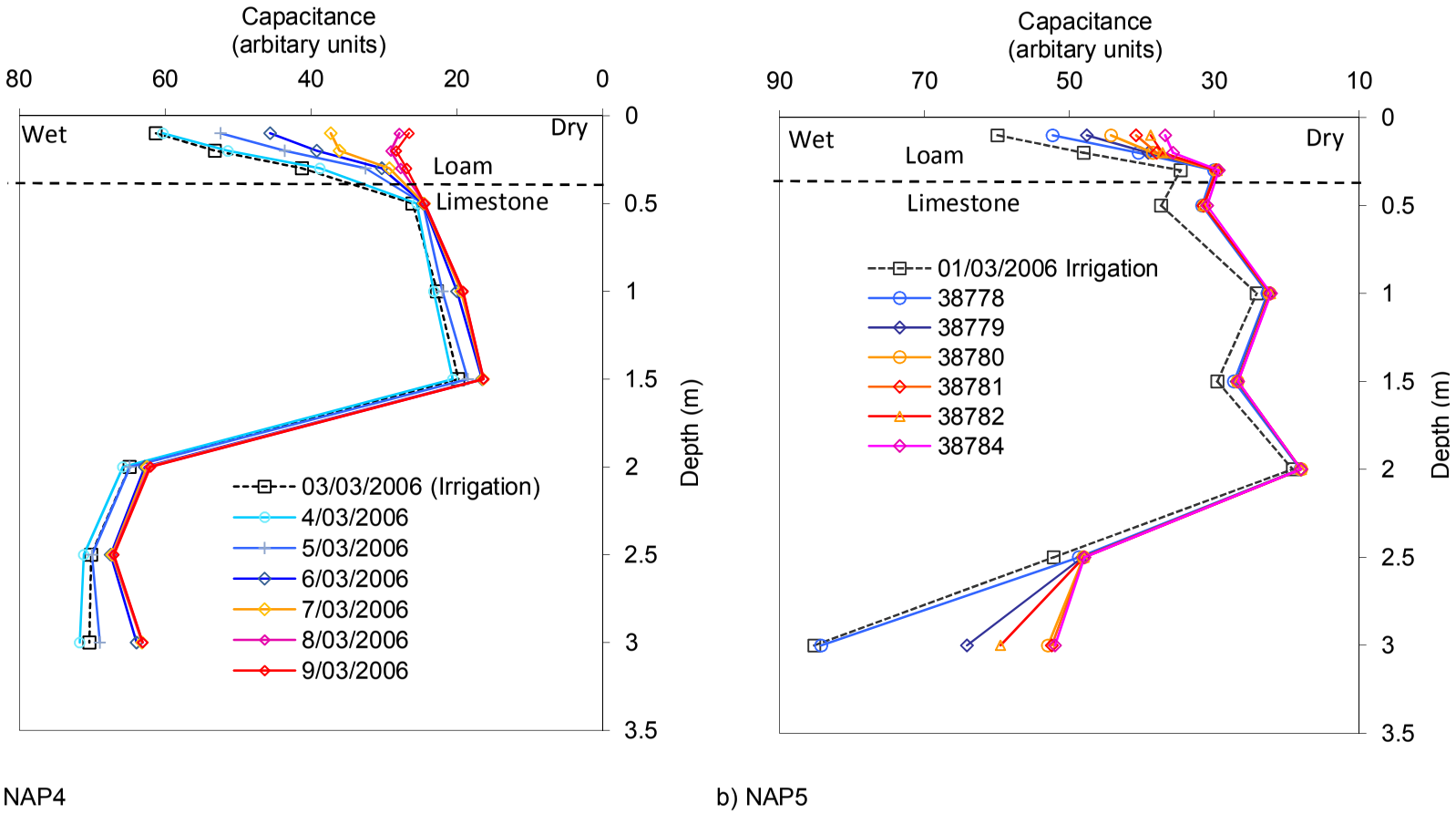

a) NAP4

b) NAP5

Figure 3 Daily average soil water content (as a measure of capacitance) measures during and post irrigation at a)NAP4 and b) NAP5 Note that the greatest change in soil water content is contrained to the top 0.3 to 0.4m of the soil profile, corresponding to the calcrete layer found at these depths

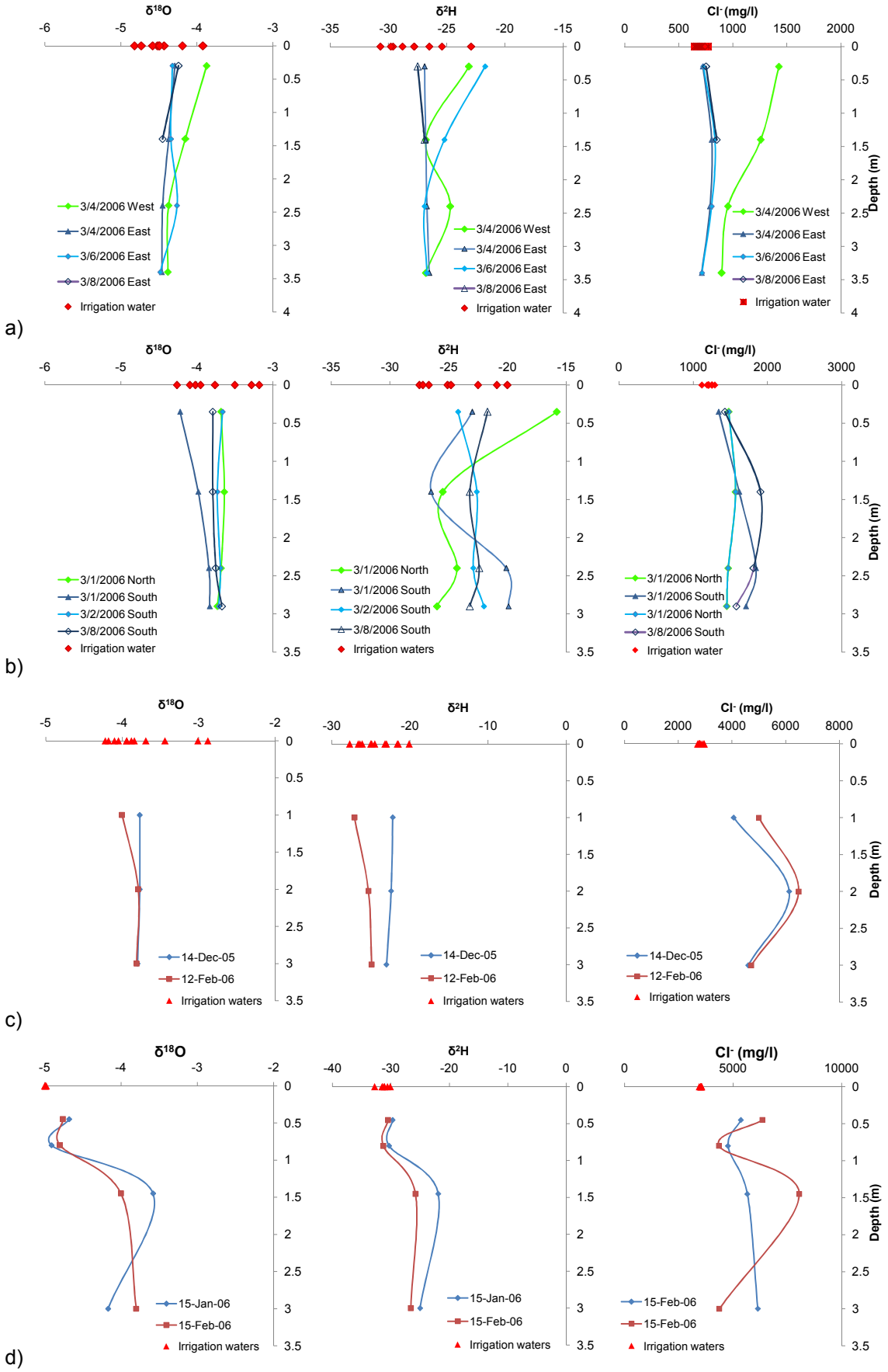

Figure 4 Vertical distribution of soil water $\delta^{18}O$, $\delta^{2}H$ and Cl- extracted from suction lysimeters following flood irrigation at a)NAP4, b)NAP5, c) MTM and d) PG

Isotopic and salinity values of irrigation water, soil water and groundwater

$\delta^{18}O$ versus salinity plots of soil water, irrigation water and groundwater are displayed in Figure 5 for each site. $\delta^{2}H$ versus salinity plots are not shown here but showed a similar trend. Table 1 shows the i) average increase in chloride concentration and enrichment of irrigation water relative to the source (irrigation bore) and ii) the average increase in chloride concentration and enrichment of soil water relative to ponded irrigation waters. Table 1 and Figure 5 show the comparison between the salinity impacts as a result of evaporation (fractionating water loss) and transpiration from both irrigation water and soil water. The percentage increase of chloride concentration as a result of fractionating water loss (evaporation) in irrigation water is small (0 - 5 %) in comparison to the percentage increase of chloride concentration in soil water (23 % - 117 %). The low fractionating water loss detected in soil water and large increase in chloride concentrations suggest transpiration is the dominant process across all sites.

The $\delta^{18}O$ and $\delta^{2}H$ composition of soil water extracted from the suction lysimeters buried at each end of the irrigation bay at NAP4 and NAP5 are similar and they plot close to the irrigation bore water (on the x axis), signifying minor enrichment post irrigation (Figure 5). This minor enrichment suggests that most of the irrigation drainage that recharges the aquifer has undergone a small amount of evaporation. Therefore the isotopic enrichment of these evaporated waters was not reflected in isotopic signatures in soil water.

During irrigation, the increase in chloride concentration of irrigation waters at NAP4 and NAP5 ranged from 30 mg/l to 60 mg/l (4.7 % - 9.5 %) and 9 mg/l to 35 mg/l (0.75 % - 2.5 %), respectively. However, the chloride concentration of soil water extracted 1 to 3 days post irrigation was much higher than that of the irrigation water, showing respective increases of 170 mg/l and 189 mg/l (26.5 % - 29.5 %) and 274 mg/l to 377 mg/l (23 % - 31 %) at NAP4 and NAP5, respectively. In both cases the minor fractionating water loss (< 0.1 ‰ for $\delta^{18}O$) and the higher chloride concentration of soil water suggest that transpiration was the dominant process at these sites.

The greater effect of evaporation on the open irrigation water, sampled during the December 2005 irrigation at MTM is clearly evident by the greater spread of data points (exhibiting greater fractionation), which plot further towards the right

across the x - axis, than observed during the February irrigation, when crop cover was ~95% (Figure 5). The corresponding increase in chloride concentration of irrigation water as a result of evaporation (fractionating water loss) was greater during the December irrigation (129 mg/l, 5 % increase), than the February irrigation (<1 %), where chloride concentrations remained relatively unchanged. Due to the high crop cover in February, irrigation waters were not subjected to the same amount of evaporation to that measured in the evaporation pan over the same period (Figure 5).

As observed across all sites, the isotopic enrichment of soil water collected 1 to 3 days post irrigation at MTM was minor (0.5‰) and reflected partially evaporated irrigation water. The increase in chloride concentration as a result of fractionating water loss was only minor (0 to +129 mg/L, 0 - 5 % increase) compared to the increase in chloride concentration as result of transpiration (+2070 to 3070 mg/L, 79 % to 118 %).

The reduced influence of evaporation owing to dense crop cover was also confirmed by experiments conducted at irrigation site PG. Crop cover was close to maximum cover during both sampled irrigations, during which time, the enrichment in $\delta^{18}O$ (<0.15 ‰) and increase chloride concentrations (0 to +30 mg/l, 0 - 0.82 % increase) of irrigation water, were much lower to the increases measured in evaporating pan water ($\delta^{18}O$ enrichment was 0.66 ‰, Cl^- +44 mg/l to +90 mg/l) over the same time period (Figure 5).

During the January sampling event, there was some minor enrichment detected in the soil water (< 1 ‰ $\delta^{18}O$ and 1 - 3 ‰ $\delta^{2}H$), which was equivalent to the enrichment of pan waters (1 ‰ $\delta^{18}O$). The increase in chloride concentration of soil water (+1968 mg/l to +2100 mg/l, 54 - 58 %), which was subject to both E + T, was much greater than the increase in chloride of pan water (+90 mg/l), which was subject to E only (Figure 5). This suggests that the concentration of salt in the soil water was dominated by transpiration at this site.

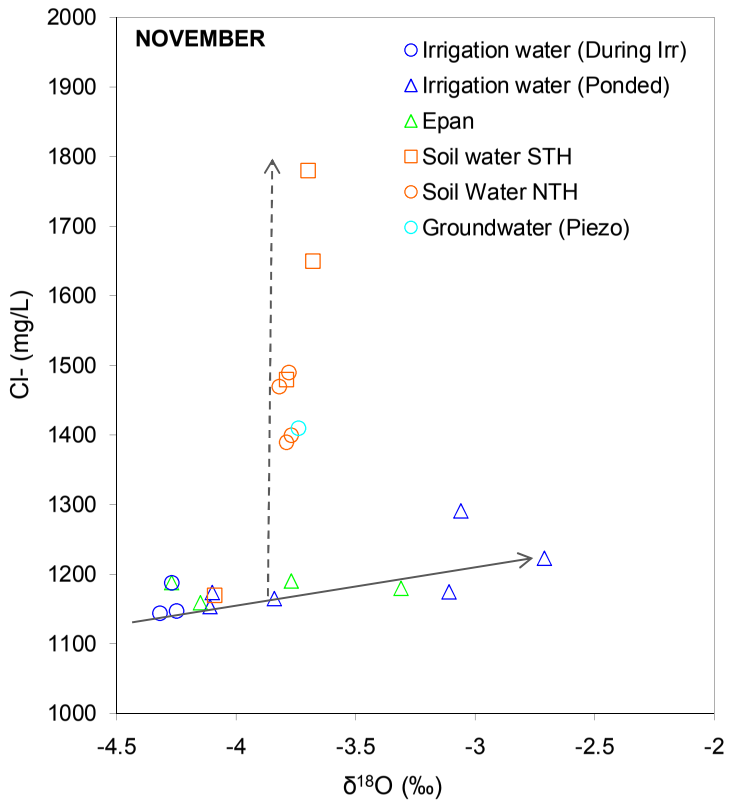

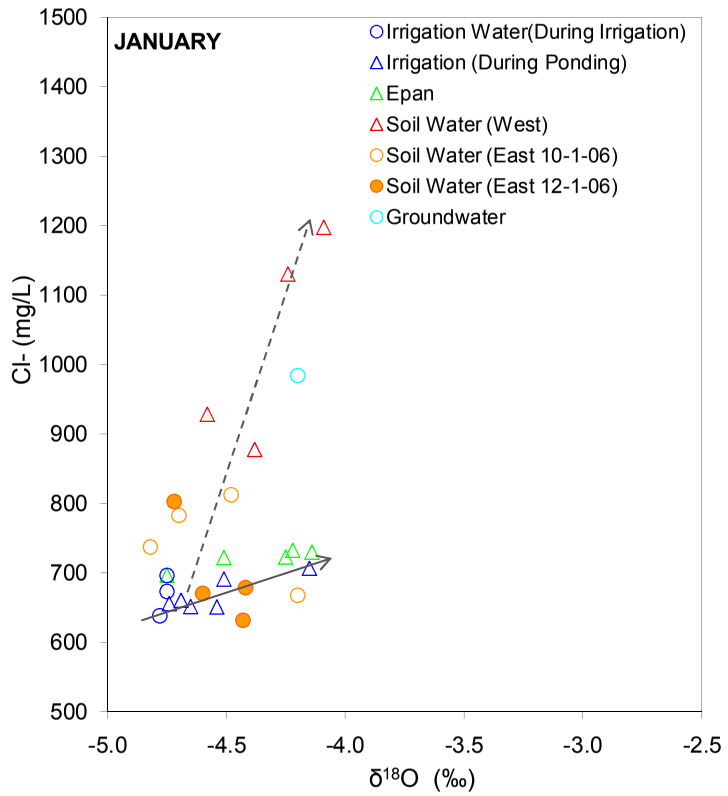

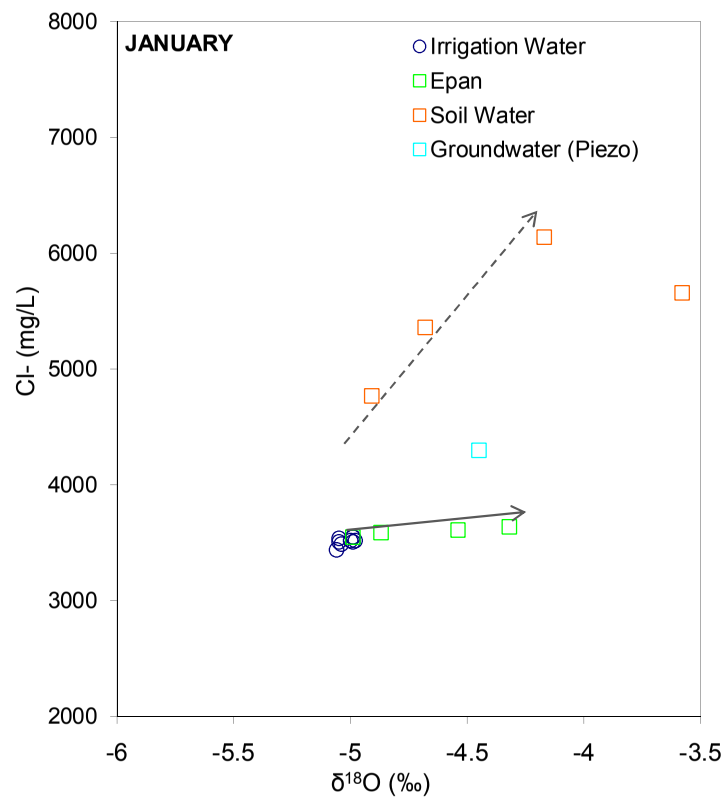

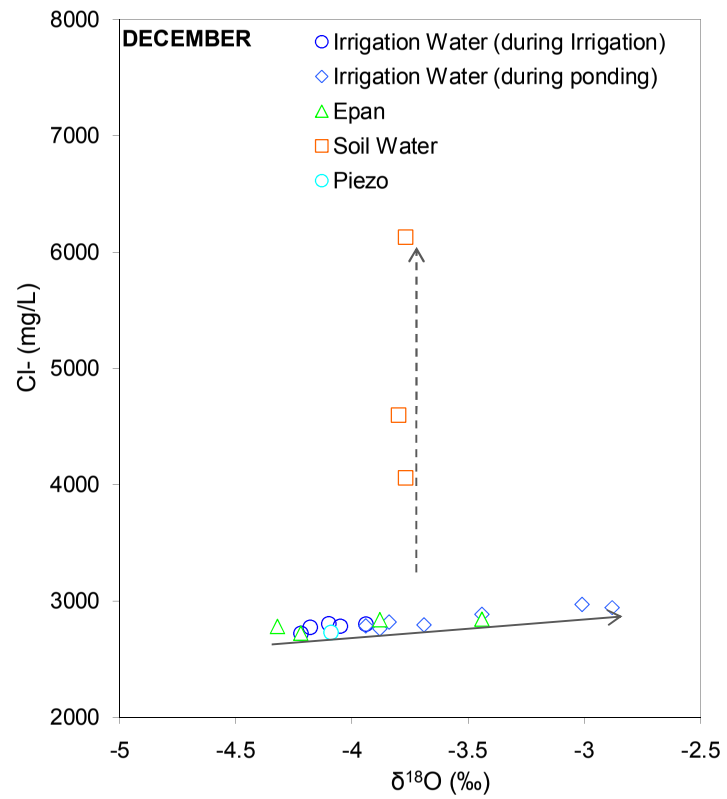

a) b) c) d)

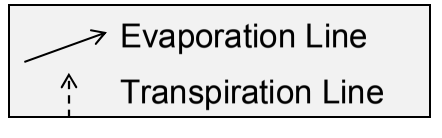

Figure 5 Cl^- v $\delta^{18}O$ plots of irrigation, soil, pan and groundwater collected during and post irrigation application at flood irrigation site a)NAP5, b)NAP4, c)PG and d)MTM

Table 1. Average increase in chloride concentration and enrichment of irrigation water and soil water

Study Site and Irrigation	Crop type	Soil type	Irrigation Water			Soil Water			Variable at time of irrigation
			Increase in $[Cl^-]$ (mg/l)	% ↑ $[Cl^-]$	$\delta^{18}O$ enrichment (‰)	Increase in $[Cl^-]$ (mg/l)	% ↑ $[Cl^-]$	$\delta^{18}O$ enrichment (‰)	
NAP5-NOV	Clover	loam	9	0.76	0.9	274	23.06	0	Day irrigation
NAP5-MAR	Clover		35	2.95	1.07	377	31.73	0	Day irrigation
NAP4-JAN	Pasture	loam	30	4.69	0.2	170	26.56	0.1	Day irrigation
NAP4-MAR	Pasture		61	9.53	0.7	189	29.53	0	Night irrigation
PG-JAN	Lucerne	sand	0	0	0	1968	53.92	1	Day irrigation, min crop cover
PG-FEB	Lucerne		30	0.82	0.09	2102	57.59	0.41	Day irrigation, mature crop
MTM-DEC	Lucerne	sand	129	4.96	0.84	2078	79.92	0	Day irrigation, mature crop
MTM-FEB	Lucerne		<5	<1	0.12	3070	118.08	0.2	Day irrigation, mature crop

Soil water salinity and isotopic signatures monitored over time

Wetting front movement along with soil isotopic and salinity values were measured 2 and 4 days following irrigation application at NAP4 and NAP5. The results are shown as Figure 6a - b: changes in water content versus soil water chloride and Figure 6c - d: soil water content versus soil water δ^2H / $\delta^{18}O$. Figure 6a - b shows that the isotopic composition of soil water remains reasonably steady over time; whilst Figure 6c - d shows an increase in soil water salinity with decreasing soil water content over the same period. Therefore, this decrease in soil water content and increase in soil water salinity can only be explained by transpiration. The increase in soil water chloride was mainly constrained to the top 0.30 m, signifying the extent and effect of evapotranspiration, which may be constrained by root activity and the calcrete layer commonly found at this depth. Below this depth only minor changes in salinity and isotopic composition were detected over time (Figure 4).

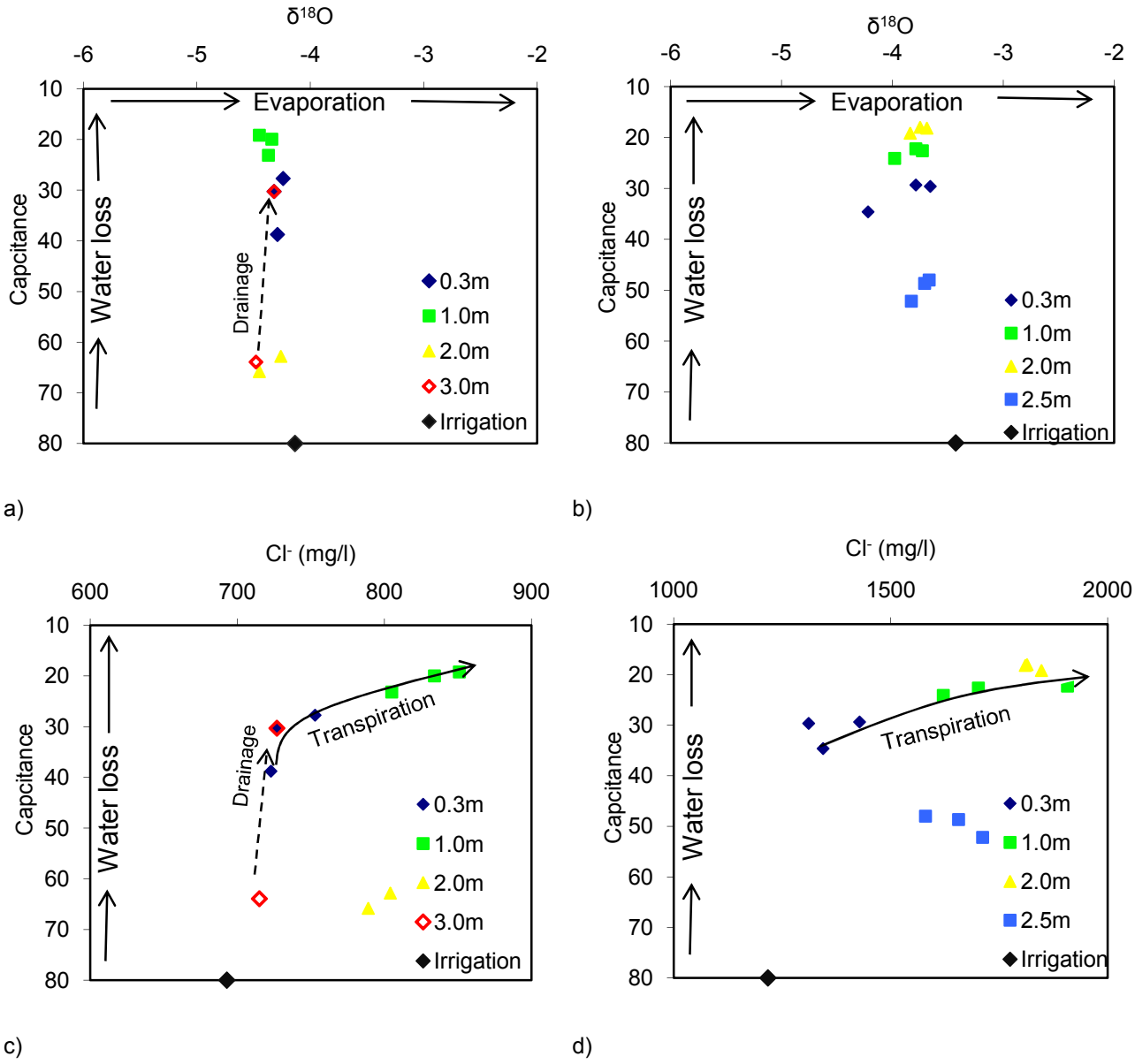

Figure 6. Soil capacitance vs soil water ^{18}O: Plots a) and b) showing minor fractionating loss in respect to the source and a decrease in capacitance with depth, following irrigation at a) NAP4 and b) NAP5. **Capacitance vs soil water Cl^- :** Plots c) and d) showing a decrease in soil water content and corresponding increase in Cl^-, attributed to transpiration, following irrigation at c) NAP4 and d) NAP5. The large decrease in capacitance from 3 m to 1 m at NAP4 is a result of drainage. The decrease in campacitance at 0.3 m is mostly due to transpiration.

Salinity impact

The salinity impact owing to the recycling of irrigation water has been assessed at each flood irrigation site. A net salinity impact to the unconfined aquifer can be calculated using drainage rate and drainage water salinity estimates. Unsaturated zone drainage rates (D, mm/y) were estimated using the water balance approach (Equation 1).

$$D = P + I - ET + \Delta S \qquad 1)$$

where P is the precipitation (mm), I is the volume of irrigation water applied to the bay (mm), D = the drainage below the irrigation bay (mm), ET is the evapotranspiration (mm) and ΔS is the change in soil water content (mm), which due to the large volume of irrigation water applied can be assumed to be negligible.

The salinity of drainage water under flood irrigation is assumed to be equivalent to that of the soil pore water salinity below the root zone which is sampled at the two and three metre suction lysimeters. A salinity increase (Δsal, mg/L^{-1}) due to the use of groundwater for irrigation is calculated as the difference between the estimated salinity of drainage water and the irrigation water that is applied (Harrington, et al 2006).

The net salinity impact to the aquifer (t/ha/y) from the evaporation of irrigation water and evapo-concentration of soil water is then given by:

$$SI_{EVAPORATION} = \Delta sal_{IW} \times I$$
$$SI_{EVAPOTRANSPIRATION} = \Delta sal_{SW} \times D \qquad 2)$$

where I is the volume of irrigation water applied to the bay, D is the drainage below the irrigation bay, Δsal_{sw} represents the net increase of salinity of drainage water (obtained from suction lysimeters below 0.5m) minus salinity of irrigation water and Δsal_{IW} represents the net increase in salinity of irrigation water during the ponding period. The salt balance and net salinity impacts owing to transpiration and evaporation of surface waters for each site are compared in Table 2. Figure 7 compares the water, isotopic ($\delta^{18}O$) and salt balance for each flood irrigation site.

Table 2. Salinity impact from flood irrigation per irrigation

Site	Increase in salt concentration from source (mg/l)				Salt Inputs and Outputs				Net Salinity Impact (t/ha)				Total net salinity impact (t/ha)	
	Increase in [TDS] of irrigation water		Increase in [TDS] of soil water		Input (t/ha)	Output (t/ha)	Input (t/ha)	Output (t/ha)	Via Evaporation		Via Transpiation			
	1st Irrigation	2nd Irrigation	1st Irrigation	2nd Irrigation	1st Irrigation		2nd Irrigation		1st Irrigation	2nd Irrigation	1st Irrigation	2nd Irrigation	1st Irrigation	2nd Irrigation
NAP5	100	80	420	150	2.75	3.3	3.1	3.63	0.12	0.12	0.43	0.4	0.54	0.52
NAP4	10	65	340	285	1.53	1.78	1.5	1.77	0.01	0.07	0.23	0.16	0.24	0.24
PG	10	5	1291	1100	10.15	10.76	10.17	10.57	0.016	0.01	0.6	0.4	0.6	0.4
MTM	150	35	1400	2400	9.6	11.2	9.2	11.77	0.3	0.07	1.3	2.5	1.6	2.57

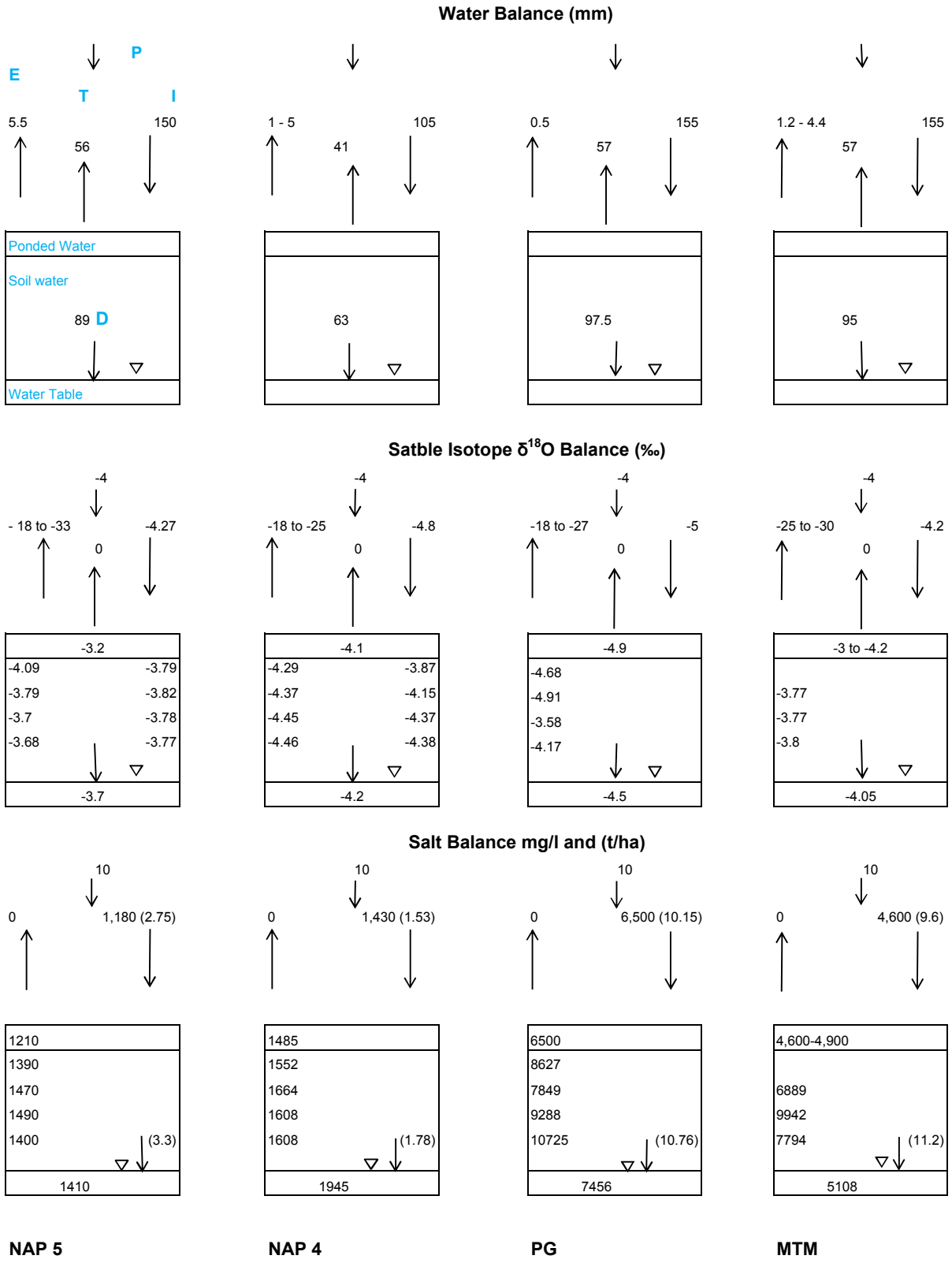

Figure 7 Water, isotopic and salt balance for each flood irrigation site. Where evaporation (E) is water lost from irrigation waters and soil water following irrigation, calculated via the use of stable isotopes, Transpriation (T) was calculated via FAO56 methodology over one irrigation cycle and Drainage (D) calculated via the water balance approach

An estimated 1.53 to 11.3 t/ha of salt per irrigation was applied to flood irrigation bays (Table 2). The high salt loads applied at sites PG and MTM (9.6 – 11.2 t/ha) was attributed to the higher salinity of irrigation water (4,800 to 6,400 mg/L, TDS).

Across all sites, the total salts output was slightly greater than the total salt inputs (Table 2 and Figure 7). This may be due to the flushing (mobilization) of accumulated salt from the soil profile, between irrigations, over the short term. Over the longer term however, it is reasonable to assume that the input of salt to the unsaturated zone, via irrigation equals output, via drainage.

The average salinity impact owing to evaporation of surface waters is minor (15%) in comparison to salinity impact as a result of transpiration (85 %). This is supported by Dincer et al. (1979) who showed that the contribution of transpiration from aquatic plants to water loss was highest (71 %) during summer, and Simpson et al. (1992) who showed that transpiration over a entire rice cropping season accounted for 60 % of total losses to the atmosphere, with evaporation providing the remainder.

At NAP4 and NAP5 where ponding occurred for up to 18 hrs post irrigation the salinity impact as a result of evaporation over the irrigation and ponding period ranged from 4 % to 30 % compared to the salinity impact as a result of transpiration (41 % to 95 %). In contrast, evaporation from rapidly draining soils at PG and MTM contributed only 2 % to 18 % of the impacts, compared to transpiration (81 % to 97 %).

An isotope study undertaken in parallel at the same study sites (van den Akker et al, 2011) showed that evaporation from flood irrigation can amount to 6 mm day, however when the crop was mature, evaporation was strongly limited by the dense canopy cover and can be 30 % lower, and in some cases, negligible (i.e. < 1 mm) when applied to rapid draining soils. This is supported by Figure 5 and that showed that isotopic signatures of soil water collected post irrigation resemble partially evaporated irrigation waters, suggesting that soil water did not undergo significant evaporation following irrigation. Transpiration of lucerne and pasture calculated by conventional methods (FAO56) can range from 4 mm to 6 mm per day (using crop coefficients of 0.8 and 0.9 respectively). Hence, over a

14 day irrigation cycle, water lost via transpiration can amount to > 56 mm between irrigations.

The cumulative water loses due to E and T and the corresponding salinity increase and soil moisture (capacitance) decrease in the top soil (0.2m), measured over a typical 14 day irrigation cycle following irrigation, is shown on Figure 8 for study sites NAP4 and NAP5. The results showed that 88% of water is lost by transpiration over the 14 day irrigation cycle. The water loss via transpiration and corresponding increase of salt concentration in the soil zone between irrigations is an ongoing process (amounting to + 300 mg/l, TDS over a 4 day period post irrigation). The salt water balance at these sites indicates that approximately 0.2 to 0.4 t/ha of salt had accumulated between irrigations, over a 14 day time frame. In contrast the increase in salt concentration via evaporation was much less (amounting to +100 mg/l) as evaporation of irrigation waters occurred over a much shorter duration of 1 to 2 days, during the irrigation and ponding period only.

At NAP5, the salinity impact due to evaporation of irrigation water over the duration of irrigation spanning 1.5 days was 0.12 t/ha or 0.08 t/ha/d, however the salinity impact due to transpiration through concentration of soil water salts over 14 days (between irrigations) was 0.4 t/ha over 14 days or 0.03 t/ha/d (Table 2). At PG the salinity impact due to evaporation of irrigation water over duration of irrigation was 0.032 t/ha/d, and the salinity impact due to transpiration through concentration of soil water salts over 14 days (between irrigations) was 0.4 - 0.5 t/ha over 14 days or about 0.3 t/ha/d (Table 2).

The salinity impacts owing to evaporation at NAP4, was slightly higher during the second irrigation, than observed during the first irrigation. This was a result of irrigating at night during the second irrigation, thereby allowing water to pond and evaporate the following day. Salinity impacts owing to evaporation were also higher at MTM during the first irrigation when there was little crop cover (when was E > T). Likewise, the salinity impact owing to transpiration was 1 t/ha greater during the second irrigation at MTM when the lucerne had reached maximum growth (when T > E), Table 2.

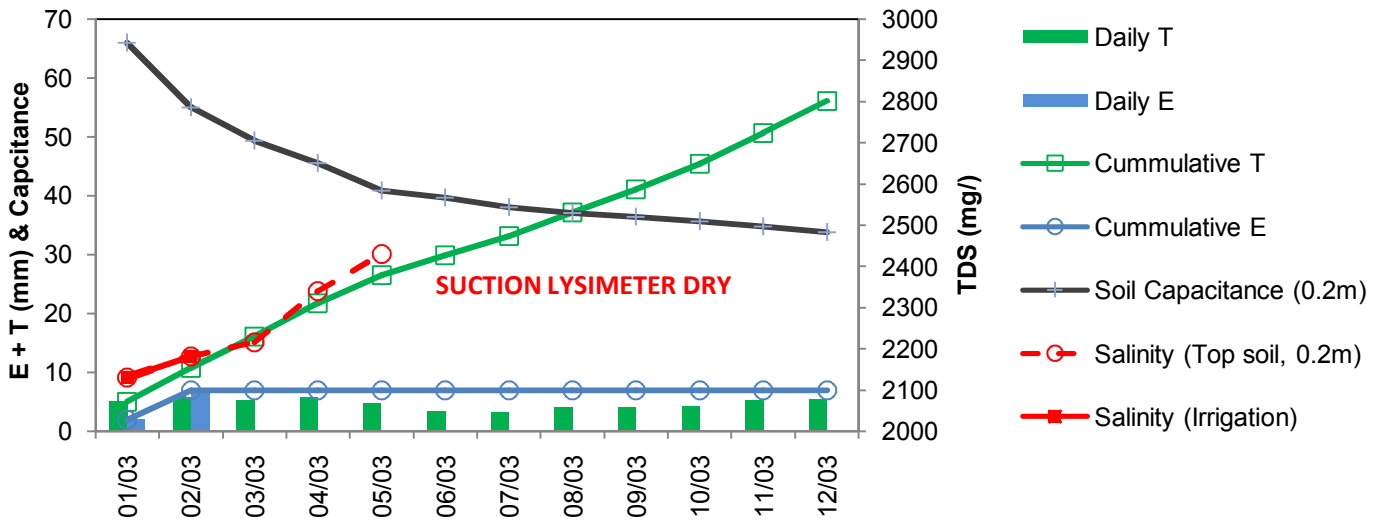

a)

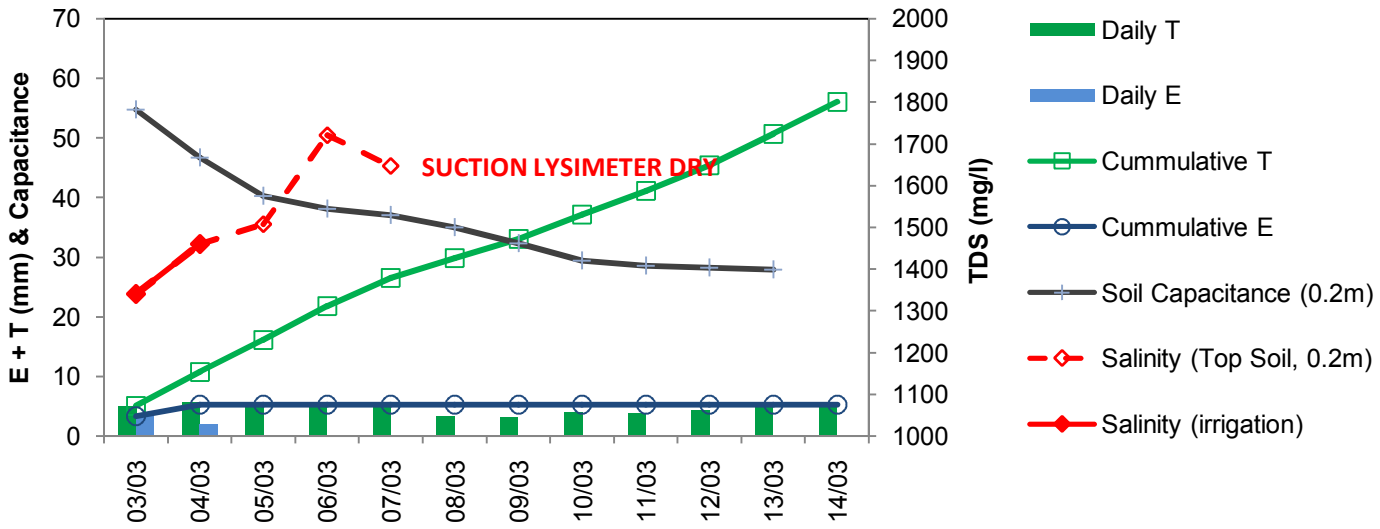

b)

Figure 8 Comparrison of transpiration (calculated via the FAO56 methodology) versus evaporation of irrigation waters (calculated via stable isotopes) during flood irrigation of a mature crop at study sites a) NAP5 and b) NAP4. Also shown is the reduction in soil moisture capacitance and corresponding increase in soil water salinity following irrigation.

Source of salinity

As salinity (TDS) and Cl^- concentration are very strongly correlated $R^2 = 0.987$ (Figure 9), and Cl^- is chemically inert and not involved in chemical reactions in the aquifer, the increase in salinity is not due to mineral–water interactions within the aquifer and can only be explained from concentration though evaporation or transpiration. An increase in total salts (TDS) through water-rock interaction (water-mineral reaction) would result in a non linear Cl^- - TDS relationship. A TDS versus Cl^- plot of evaporated pan water has been included for comparison and showed similar linear Cl^- - TDS relationship as exhibited by soil water.

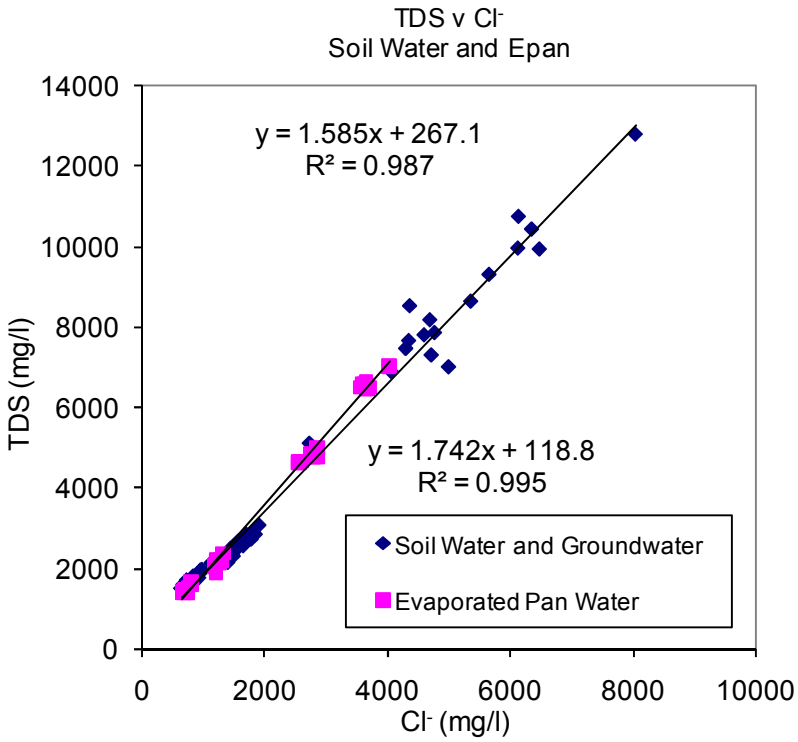

Figure 9 Cl^- versus TDS relationship of soil water beneath flood irrigation and pan evaporation.

Conclusion

By monitoring isotopic (δ^2H / $\delta^{18}O$) and chloride concentrations in irrigation water and soil water, along with soil moisture content, we have been able to show that transpiration was the dominant process by which salts are concentrated during flood irrigation and therefore the major contributor to salinity impact to the water table.

This study showed that the increases in soil water chloride and decrease in soil water content post irrigation was not accompanied by significant enrichment of δ^2H and $\delta^{18}O$ over time, thus suggesting that transpiration was the dominant process by which water was lost to the atmosphere. This was confirmed by experiments described by van den Akker et al. (2011) (Chapter 3), which showed that over a typical irrigation cycle, evaporation from irrigation was much lower (0.5 mm to 6 mm) compared to transpiration, an ongoing process which can amount to 85 mm between irrigations.

The combined monitoring of soil capacitance, stable isotopes and Cl^- of soil water, confirmed that in this setting, evaporation and transpiration was also constrained by crop cover and calcrete layers, often found as shallow as 0.30 m.

Across all sites, the isotopic composition of soil water was similar to that of partially evaporated irrigation water, as observed during the early stages of irrigation, suggesting that no further evaporation of soil water took place following irrigation. This observation was also supported by other studies (Barnes and Allison, 1983; Allison et al., 1983). Zimmermann et al. (1967) reported that isotope profiles beneath grass were relatively less enriched than nearby profiles under bare ground and concluded that in their case the main effect of the grass cover was the reduction in soil evaporation, leading to a less enriched profile beneath the vegetation. In addition drainage was rapid at the tested sites, thereby limiting the degree to which infiltrating water were isotopically enriched by evaporation.

Salt water balances and *in situ* measurements of soil water salinity confirmed that the increase in concentration of salts via transpiration occurs between irrigations, where as the increase in concentration of salt via evaporation

occurred over a much shorter duration, during the irrigation and ponding period, i.e. 1 - 2 days.

The percentage increase in chloride concentration as a result of evaporation (fractionating water loss) during irrigation was low (0 - 5%) compared to the salinity increase measured in soil water, 23 - 118 %, as a result of transpiration. The percentage increase in salt from transpiration, translated to a net salinity impact of 0.16 to 2.5 t/ha per irrigation.

Across all sites, the total salt outputs were slightly greater than the total salt inputs (Table 2). This may be due to the flushing (mobilisation) of salt from the soil profile which accumulated between irrigations. Over the longer term however, it is reasonable to assume that the input of salt to the unsaturated zone, via irrigation equals output, via drainage, and hence irrigation has to be managed to reduce the amount of irrigation water applied, through minimising evaporation.

The efficiency of a flood irrigation network on the above mentioned sites was assessed by van den Akker et al (2011) (Chapter 3) on the basis of evaporation, by comparing the ratio of water evaporated from the flood bay to the potential evaporation measured (via class A evaporation pans) on site. The study confirmed the benefit of flood irrigation on sandy soils, which resulted in lower ponding time and lower evaporation losses.

This study has shown that the increase in Cl^- concentration of irrigation water owing to evaporation was greater during irrigations which had longer ponding periods (22 - 30 %) and lower during irrigations over sandy soils, under dense crop canopy cover (< 2%), confirming that both crop cover and soil type was a strong regulator of salinity impact from evaporation and hence irrigation efficiency.

Whilst flood bays which revealed higher irrigation efficiency resulted in a lower net salinity impacts from evaporation of surface waters, this study has demonstrated that the overall salinity impact as a result of evaporation was mostly insignificant (0.1 - 0.3 t/ha per irrigation) in comparison to the salinity impact from transpiration (0.16 - 2.5 t/ha per irrigation).

This study has shown that transpiration was the dominant mechanism responsible for groundwater salinity increase beneath the flood irrigated areas.

References

Allen, G., Pereira, L.S., Raes, D., Martin, S., 1998. FAO Irrigation and Drainage Paper No. 56 Crop Evapotranspiration Guidelines for computing crop water requirements.

Allison G.B., Bames C.J. and Hughes M.W.,1983. The distribution of deuterium and oxygen-18 in dry soils: II. Experimental. J. Hydrol. 64: 377 - 397.

Allison, G.B. and Barnes, C.J., 1983. Estimation of evaporation from non-vegetated surfaces using natural deuterium. Nature, 301:143 - 145.

Allison, G.B. and Barnes, C.J., 1984. Estimation of evaporation from the normally "dry" Lake Frome in South Australia. J. Hydrol., 78: 229 - 242

Allison, G.B. and Hughes. M.W., 1983. The use of natural tracers as indicators of soil-water movement in a temperate semi-arid region. J. Hydrol., 60:157 - 173.

Barnes C.J. and Allison G.B., 1983. The distribution of deuterium and oxygen-18 in dry soils: 1 Theory, J. Hydrol. 60: 141 - 156.

Dincer, T., Huttion, L. G. & Rupee, B. J., 1978. Study, using stable isotopes of flow distribution, surface groundwater relation and évapotranspiration in the Okavango Swamp, Botswana. In: Isotope Hydrology, (Proc. Symp. Neuherberg, 1978), 3-26. IAEA, Vienna, Austria.

Dincer, T., Zimmermann, U., Baumann, U., Imevbore, A.M.A., Henderson, F., Adeniji, H.A., 1979. Study of mixing patterns of Lake Kainji using stable isotopes. In: Isotopes in Lake Studies. IAEA, Vienna, pp. 219 - 225.

Dawson, T.E., and J.R. Ehleringer., 1998. Plants, isotopes and water use: a catchment-scale perspective, p. 165-202. In C. Kendall and J. McDonnell (eds.), Tracers in Catchment Hydrology. Elsevier, Amsterdam.

Ehleringer and Dawson.m 1992. Water Uptake by plants: perspectives from stable isotope composition. Plant Cell and Environment 15:1073-1082.

Gat, J.R. and Tsur, Y., 1967. Modification of the isotopic composition of rainwater by the processes which occur before groundwater recharge. Proc. Symp. Isotop. Hydrol., IAEA, Vienna. pp. 49 - 60.

Gat, J.R., 1971. Comments on the stable isotope method in regional groundwater investigation. Wat. Resour. Res. 7: 980 - 993.

Harrington, N., van den Akker, J., Brown, K. and Mackenzie, G., 2004. Padthaway Salt Accession Study. Volume One: Methodology, site description and instrumentation. South Australia. Department of Water, Land and Biodiversity Conservation. DWLBC Report 2004/61.

Landon, M.K., G.N. Delin, S.C. Komor, C.P. Regan., 1999. Relation of pathways and transit times of recharge water to nitrate concentrations using stable isotopes, Ground Water. Submitted for publication.

Mauder, M., Foken, T., Clement, R., Elbers, J.A., Eugster A., Grunwald, T., Heusinkveld, B., and O., Kolle 2007. Quality control of CarboEurope flux data – Part II: Inter-comparison of eddy-covariance software, Biogeosciences Discuss., 4, 4067 - 4099.

Monteith, J.L., 1965. Evaporation and environment. pp. 205-234. In G.E. Fogg (ed.) Symposium of the Society for Experimental Biology, The State and Movement of Water in Living Organisms, Vol. 19, Academic Press, Inc., NY.

Penman, H.L., 1948. Natural evaporation from open water, bare soil, and grass. Proc. Roy. Soc. London A193:120 - 146.

Simpson, H,J., Herczeg, A.L, and Meyer, W.S.,1992. Stable isotope ratios in irrigation water can estimate rice crop evaporation.

Thorburn, P.J., Hatton, T.J. and Walker, G.R., 1993. Combining measurements of transpiration and stable isotopes of water to determine groundwater discharge from forests. Jour. Of Hydrol., 150: 563 - 587.

van den Akker, J., Harrington, N., and Brown, K., 2006. Padthaway Salt Accession Study Volume Three: Conceptual Models, DWLBC Report 2005/21, Government of South Australia, through Department of Water, Land and Biodiversity Conservation, Adelaide.

van den Akker, J., Simmons, C.T. and Hutson, J., 2011. The use of stable isotopes deuterium and oxygen-18 to derive evaporation from flood irrigation on the basis of pan evaporation techniques. Journal of Irrigation and Drainage Engineering (Posted ahead of print, March, 4, 2011).

Walker, C.d. and Richardson, S.B., 1991. The use of stable isotopes of water characterizing the sources of water in vegetation. Chem. Geol. (Iso. Geo.Sect). 94: 145 - 158.

White, J. W. C. & Gedzelman, S. D., 1984. The isotopic composition of atmospheric water vapour and concurrent meteorological conditions. /. *Geophys. Res.* 89, 4937 - 4939.

Wohling, D., 2007. Minimising Salt Accession to the South East of South Australia. The Border Designated Area and Hundred of Stirling Salt Accession Projects. Volume 2 - Analytical Techniques, Results and Management Implications, DWLBC Report 2007, Government of South Australia, through Department of Water, Land and Biodiversity Conservation, Adelaide.

Zimmermann, U., Ehhalt, D. and Miinnich, K.O., 1967. Soil water movement and evapotranspiration: changes in the isotopic composition of the water. Proc. Syrup. on Isotopes in Hydrology, Vienna, 1966, Int. At. Energy Agency (I.A.E.A.), Vienna, pp. 567 - 584.

CHAPTER 5

The hydrogen and oxygen isotopic composition of precipitation and evaporated irrigation water in the South East of South Australia

Abstract

Stable isotope ratios of hydrogen and oxygen in shallow groundwater, soil water and irrigation were measured at four flood irrigation sites, to assess the degree of evaporation by plotting δ^2H and $\delta^{18}O$ values relative to the Local Meteoric Water Line (LMWL). The LMWL developed from local monthly rainfall data collected in the South East of South Australia during 2003 - 2006 gave the following regression; $\delta^2H = 7.65\ \delta^{18}O + 10.14$, a slope somewhat consistent to the world MWL ($\delta^2H = 8.0\ \delta^{18}O + 10$) and the LWML developed from the long term station at Adelaide ($\delta^2H = 7.44\ \delta^{18}O + 9.2$). The regression developed here represents the first published LMWL based on direct precipitation for any location in the South East of South Australia. In comparison, the δ^2H and $\delta^{18}O$ compositions of irrigation waters plot to the right of the LMWL, signifying the effects of evaporation. The slope and deviation of δ^2H and $\delta^{18}O$ values from the LMWL varied across each site according to factors such as (i) day or night irrigation, (ii) soil type, (iii) irrigation application rate and (iv) % crop cover (open water vs crop cover) at time of irrigation. The δ^2H and $\delta^{18}O$ of waters undergoing evaporation plot on Local Evaporation Lines defined by variable slopes ranging from 4.2 to 3.64, consistent with slopes generated from evaporation of free water surfaces from Class A evaporation pans. In comparison, slopes (7) closer to that of the LMWL were produced from irrigation waters applied to bays; (i) over rapid draining soils or (ii) under dense crop cover. Linear regressions through the isotopic composition of soil water ($\delta^2H = 6.43\ \delta^{18}O + 0.36$) and groundwater ($\delta\ \delta^2H = 6.49\ \delta^{18}O + 1.65$) collected 1 - 6 days post irrigation also plotted slightly to the right of the LMWL, however exhibited slopes that reveal evaporation of open surface water bodies (5), indicating that soil water was not subject to evaporation post irrigation.

Introduction

Irrigation drainage and evaporation processes can be further understood using the Oxygen 18 ($\delta^{18}O$) and deuterium ($\delta^{2}H$) composition of rainfall, irrigation water, soil water and groundwater through various stages of the irrigation cycle and how that relates to a Local Meteoric Water Line (LMWL).

$\delta^{2}H$ and $\delta^{18}O$ are naturally occurring isotopes that make up the molecular components of water. Values of $\delta^{2}H$ and $\delta^{18}O$ are reported in this paper in 'delta' (δ) notation, where the sample value is expressed relative to the internationally established standard SMOW (Standard Mean Ocean Water). Since all precipitation waters are depleted in their oxygen-18 and deuterium isotopes relative to the standard, the δ-values are negative. The oxygen-18 and deuterium compositions in precipitation waters are directly proportional to the ambient air temperature at the time precipitation is formed. However, they may be modified to a certain extent by the origin and isotopic concentration of the atmospheric water vapour (Gat, 1980). Therefore the isotopic signature of rainfall is characteristic of a particular climatic and geographical area and is a line (relationship) along which all rainfall samples will fall on a $\delta^{2}H$ and $\delta^{18}O$ plot. This is referred to as the Local Meteoric Water Line (LMWL).

The location at which a sample from an individual rainfall event plots along the line depends on factors that vary between rainfall events, such as the amount of rainfall, temperature (season) at which precipitation occurs and storm track. The relationship between $\delta^{2}H$ and $\delta^{18}O$ in precipitation waters can be described by the linear equation

$$d = m^{18}O + b \qquad 1)$$

Where *m* is the slope and *b* is the intercept. Love et al. (1991) report m = 7.44 and b = 9.2 for precipitation of Adelaide. Craig (1961) proposed that the relationship between $\delta^{2}H$ and $\delta^{18}O$ isotopes in rainfall over most of the Earth's surface could be approximated by the equation $\delta^{2}H = 8\delta^{18}O + 10$. The validity of this world meteoric line (WML) is widespread (Gat, 1980; Rozanski et al., 1993) even though there are great variations in climate world-wide.

However it is well known that the precise relationship between the δ^2H and $\delta^{18}O$ of precipitation can vary from geographic region to region, making it advantageous to establish a LMWL for any detailed hydrogeological investigation employing stable isotopes.

Evaporation results in a greater concentration of the heavier isotopes (δ^2H and $\delta^{18}O$) in the remaining liquid owing to fractionation as the lighter isotopes (δ^1H and $\delta^{16}O$) are preferentially evaporated. The effects of evaporation on irrigation/soil water can be demonstrated by plotting delta values in relation to the LMWL, Homanda et al. (2002) and Barnes and Allison (1983). Groundwater, irrigation water and soil water will either plot on or to the right of the LMWL and the isotopic signatures depend on a number of factors. These include processes such as evaporation affecting the isotopic composition of rainfall or irrigation water during its passage through the unsaturated zone. In general, waters that plot to the right of the LMWL are indicative of evaporation, either at the surface (during precipitation or irrigation) or within the soil zone. The further away the samples plot to the right of the LMWL, the greater the influence of evaporation and therefore the lower the recharge. As the waters evaporate, their δ^2H and $\delta^{18}O$ values will increase at different rates resulting in a different δ^2H - $\delta^{18}O$ relationship to that of precipitation waters. Evaporated waters will have smaller values for the slope and the intercept (Gat, 1980). Evaporation from free water surfaces commonly results in *m* values between four and six (Craig et al., 1963; Gat, 1971). For dry soils, in which vapour transport dominates the evaporative process, values for *m* of the soil water may be as low as two or three (Dincer et al., 1974; Allison et al., 1983). In moist soils, where liquid transport at the soil surface dominates the evaporative process, *m* takes on values that approximate those for open water bodies (Barnes and Allison, 1983; Allison et al., 1983). For evaporation where liquid transport dominates, the intersection of the precipitation δ^2H - $\delta^{18}O$ relationship with the evaporation δ^2H - $\delta^{18}O$ relationship is the average isotopic values of the water body before evaporation began.

The aim of this study was to develop a LMWL for the South East of South Australia, based on direct precipitation sampling. Once published this LMWL can be used in future hydrogeological studies in this region. The second objective was to compare the isotopic composition of irrigation water, soil water and groundwater collected during and post irrigation, across four irrigations sites of differing characteristics; soil type, application rate, crop type, bay architecture

(Table 1). It is intended that the results will improve our understanding of factors that contribute to excessive surface water evaporation from flood irrigation, and will therefore be used to develop efficient flood irrigation practises.

Site Description

The six precipitation sites and four irrigation study sites selected for this study lay within the inter-dunal flats of Padthaway and Tatiara PWA's in the South East of South Australia (Figure 1). Pasture, clover and lucerne crops are flood irrigated at these sites. The climate within the study areas can be characterised by warm to hot dry summers and cool wet winters. The average annual maximum temperature is 22 ^{o}C, with February being the hottest month at 29.8 ^{o}C and July being the coldest month, at 5.5 ^{o}C. A rainfall gradient exists across the study area, with average annual rainfall being slightly higher in Padthaway at 509 mm/y to 490 mm/y in Keith. 40 % of the annual rainfall occurs during the months of June to August. Annual potential evaporation is 1600 mm/y and 1700 mm/y for Padthaway and Keith respectively.

Table 1: Characteristics of the four flood study sites

Site	Soil and crop type			Irrigation application			Dimensions of irrigation bay				Irrigation Delivery Channel		
	Top soil	Soil thickness (m)	Crop Type	Application duration (hrs)	Volume (Ml/ha)	Ponding duration (hrs)	Width (m)	Length (m)	Area (ha)	Laser leveled	Length (m from bore)	Head at sluice gate (m) Start	Head at sluice gate (m) End
NAP4	Loam	0.35 - 0.5	Pasture	10	1.10	<24 - 28	125	200	2.50	N	180	0.244	0.22
NAP5	Loam	0.1	Clover	8	1.47	<18 - 22	50	500	2.50	Y	620	0.175	0.175
MTM	Sand	<0.30	Lucerne	2.5	2.00	6 to 15	20	300	0.60	Y	500	0.27	0.23
PG	Sand	<0.30	Lucerne	6	1.55	>8	50	425	2.13	Y	105	0.8	0.2

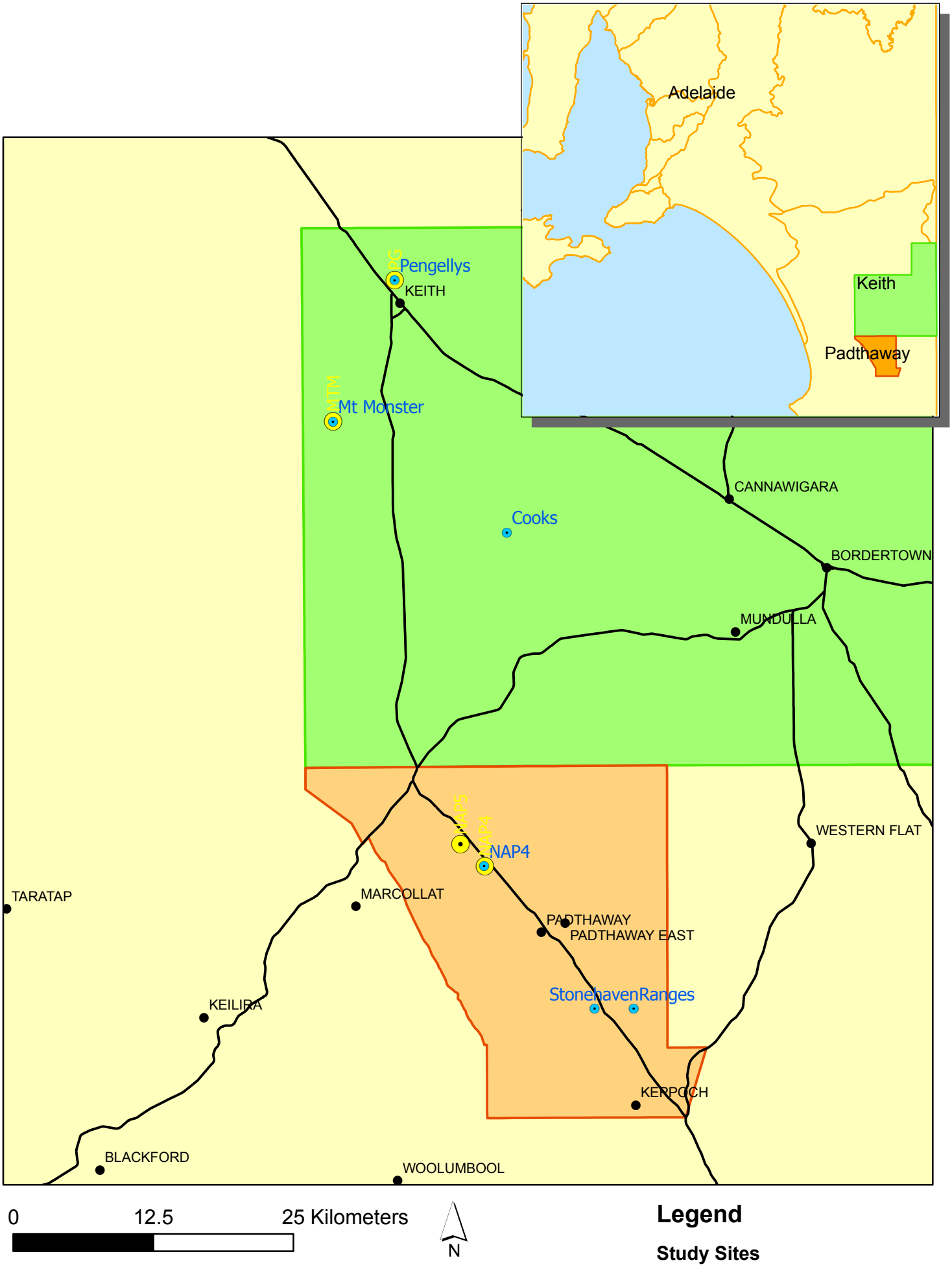

Figure 1 Isotope rainfall collection sites

Methods

Rainfall collection

Precipitation samples were collected monthly during 2003 to 2006 from six rain capturing devices, installed throughout the South East of South Australia (Figure 1). The rain capturing devices consisted of 20 cm diameter plastic funnels which directed water into a 20 L plastic container, via 2 cm diameter PVC conduit, stemmed to the base of the container (see Plate 2 - Chapter 2). To stop evaporation, 200 ml of liquid paraffin wax was added to the capturing container each time a sample is collected (container emptied). The volume of rainwater captured was also noted and a weighted monthly mean was calculated by the following expression:

$$\delta W = \frac{\Sigma\, Pi\, \delta p}{\Sigma\, Pi} \quad [1]$$

where: Pi is the monthly precipitation (mm), and δp is the "δ" values for monthly samples.

Flood irrigation measurements

A full description outlining the sampling methodology can be found in Chapters 3 and 4. Briefly, field measurements were made in four flood irrigation bays, consisting of pasture, clover and lurcern, located in the South East of South Australia (Figure 1, Table 1). The collection of water samples from irrigation water, soil water (suction lysimeters) and groundwater took place during two irrigations at each site, over the 2005/06 irrigation season, spanning from November 2005 to March 2006. The ponded water samples were collected at five places distributed in the flood bay to detect isotopic change during surface water movement. Collection of soil water and shallow groundwater was carried out at time intervals ranging from 1 to 3 days post irrigation. In addition evaporation and evolution of isotopic concentration was measured in a class A evaporation pan, during and following each irrigation.

δ^2H and $\delta^{18}O$ composition of irrigation water, evaporation pan water, soil water and groundwater was plotted against the LMWL to compare slopes and intercepts of regression lines across each site. The monitoring of δ^2H and $\delta^{18}O$ in pan water (during each irrigation), allowed for a direct comparison between slopes and intercepts generated from irrigation waters, to those generated by evaporating pan waters, which were a controlled indicator of potential evaporation from free water surfaces at the time.

Results and Discussion

Climate Data

The two measurement years (2004/05 and 2005/06) differed in total rainfall received and its distribution throughout the year, and in temperature and humidity. Table 2 rainfall, maximum and minimum air temperature) provides a brief overview of the climate. Year 2004/05, was the driest in annual and irrigation season rainfall and in humidity deficit. Reflecting the pattern across much of Australia, air temperatures (mean, maxima and minima) trended warmer from 2003 to 2006. There were more than 10 extremely dry days (maximum VPD > 50 hPa) in the 2004/05 and 2005/06 irrigation seasons. The latter occurred in conjunction with an above-average spring and summer rainfall, so evaporative water losses were expected to be large because of this large atmospheric demand.

The distribution of rainfall varied across the measurement years, with large spring and summer rainfalls making the 2005/06 irrigation season the wettest (Figure 2). The rainfall deficit recorded in the spring and autumn of the 2004/05 overwhelmed the slight above-average rainfall recorded in the preceding winter to yield a very dry irrigation season and year. Autumn rainfalls were below average in both measurement years (Figure 2).

Table 2 Climate summary

Year	Annual Rainfall (mm)		Daily Temperature °C				Vapor Pressure Deficit	No. of Days when VPD Exceeded	
	LTA	BoM	LTA Max	BoM Max	LTA Min	BoM Min	Average	20hpa	40Hpa
2003/04		509.9		20.6		8.1	8.89	86	7
2004/05	506.9	389.1	21.1	21.7	8.4	8.6	9.7	110	12
2005/06		421		22.5		8.4	9.53	94	11

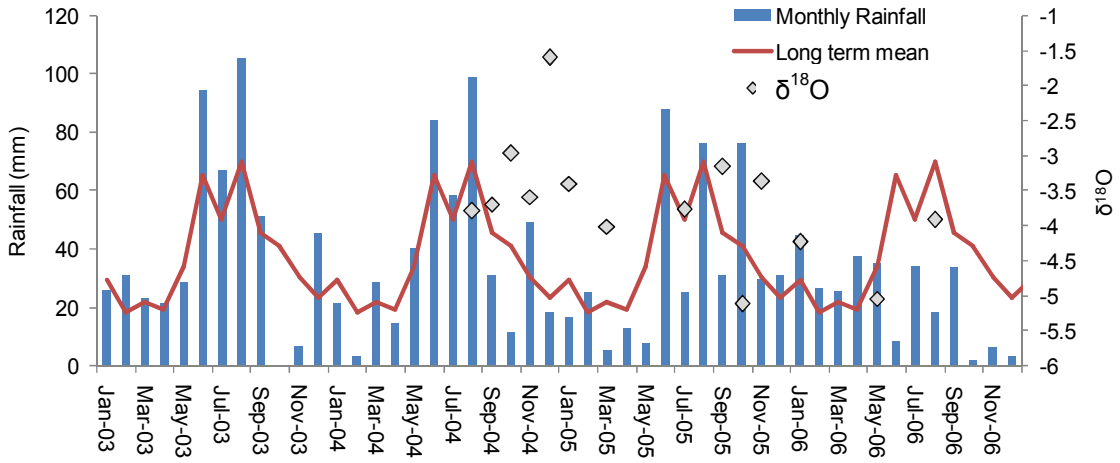

Figure 2 Monthly rainfall and $\delta^{18}O$ composition of rainfall

Precipitation waters

The results of the weighted mean isotope δ^2H and $\delta^{18}O$ compositions of 64 rainfall samples collected on a monthly basis from six rainfall collection stations across the study area from 2004 to 2006, are compiled together with their respective chloride values in Table 3. Monthly isotope values of precipitation range from a low of -7 ‰ for $\delta^{18}O$ (- 37.8 % for δ^2H) to a high of - 0.4 ‰ for $\delta^{18}O$ (- 0.6 % for δ^2H), Figure 3 and Table 3. Isotopic values were slightly more enriched in summer ($\delta^{18}O$ = -2.78 ‰ and δ^2H = -12.8 ‰) and depleted in winter ($\delta^{18}O$ = - 3.94 ‰ and δ^2H = -17 ‰), however, the seasonal isotopic variations captured here are small in comparisons to the longer term data set of Adelaide, which shows greater seasonal variations, averaging from -4.4 ‰ for $\delta^{18}O$ (δ^2H - 24.18 ‰) in winter to - 2.38 ‰ for $\delta^{18}O$ (δ^2H - 9.26 ‰) in summer. The slight depletion in summer is a consequence of warmer air temperatures during precipitation. The monthly data set of $\delta^{18}O$ collected from three rain capturing devises across Padthaway mimic each other with time and demonstrates the range which values can reach (Figure 3). The δ^2H composition of rainfall shows similar trends, but is not shown here. It is known from studies worldwide that the isotopic composition of rainfall tends to change during the passage of weather systems (e.g. Gedzelman and Lawrence, 1982; Nativ and Mazor, 1987) giving rise to isotopic variations across the study area.

Figure 4 shows the combined δ^2H and $\delta^{18}O$ signatures of the rainfall samples collected from the Padthaway and the Hundred of Stirling rain stations, plotted on

a δ^2H vs. $\delta^{18}O$ diagram, with a LMWL for Adelaide shown for reference. The LMWL developed from the weighted mean values of rainfall collected in from 2004 - 2006 are defined by the following regression $\delta^2H = 7.65\ \delta^{18}O + 10.14$ and is consistent with the LWML developed from a long term station in Adelaide which is defined by $\delta^2H = 7.44\ \delta^{18}O + 9.2$, suggesting that this LMWL can be used to represent the long-term signature of rainfall for the study area (Figure 4).

Table 3 Monthly isotopic and chloride concentrations of precipitation

PADTHAWAY	Stonehaven							Naracoorte Ranges							NAP4						
	$\delta^{18}O$	$\delta^{2}H$	d excess	Weighted mean O-18	Weighted mean D	volume ml	Cl^- (mg/l)	$\delta^{18}O$	$\delta^{2}H$	d excess	Weighted mean O-18	Weighted mean D	volume ml	Cl^- (mg/l)	$\delta^{18}O$	$\delta^{2}H$	d excess	Weighted mean O-18	Weighted mean D	volume ml	Cl^- (mg/l)
31-Aug-04	-3.70	-14.50	15.10	-4.51	-24.30	2458	1.0	-3.79	-15.20	15.12	-4.51	-24.30	4400	1.0	-3.4	-9.7	17.5	-4.51	-24.3	1956	4.0
13-Oct-04	-3.75	-16.40	13.60	-4.24	-21.03	1142	5.0	-3.69	-15.10	14.42	-4.17	-20.00	1500	5.0	-3.48	-14.0	13.8	-4.19	-20.1	1212	5.0
17-Nov-04	-2.96	-8.80	14.88	-4.17	-20.41	2200	<1	-2.96	-10.20	13.48	-4.10	-19.32	2740	1.0	-3.24	-9.1	16.8	-4.09	-19.2	2700	3.0
17-Dec-04	-4.50	-18.10	17.90	-3.92	-18.02	1220	4	-3.59	-5.50	23.22	-3.87	-17.47	532	4	-3.84	-21	9.7	-3.87	-16.7	872	5.0
11-Jan-05	-1.37	-4.20	6.76	-3.98	-18.03	550	9	-1.60	-5.80	7.00	-3.86	-17.02	725	4	-0.78	0.1	6.3	-3.87	-17.0	450	14.0
31-Feb-05	-3.49	-19.10	8.82	-3.87	-17.42	900	16.0	-3.40	-19.60	7.60	-3.75	-16.47	1150	<5	-2.1	-11.3	5.5	-3.76	-16.3	1500	<5
31-Mar-05	-3.92	-18.00	13.36	-3.84	-17.53	225	25.0	-4.01	-19.00	13.08	-3.73	-16.70	250	<5	-4.5	-19.3	16.7	-3.57	-15.8	125	10.0
18-May-05	-0.87	0.60	7.56	-3.84	-17.54	550	13	-0.35	-4.60	-1.80	-3.73	-16.73	550	14	-0.64	0.4	5.5	-3.58	-15.8	620	15.0
26-Jul-05	-4.27	-20.90	13.26	-3.73	-16.83			-3.77	-17.00	13.16	-3.62	-16.03			-4.06	-20.3	12.2	-3.45	-15.1		
22-Sep-05	-2.94	-4.90	18.62	-3.85	-17.75	2540	7	-3.16	-8.70	16.58	-3.64	-16.19	3100	7	-2.81	-5.1	17.4	-3.58	-16.2	3100	7.0
26-Oct-05	-4.79	-27.50	10.82	-3.74	-16.18	3050	3	-5.11	-29.50	11.38	-3.58	-15.18	2190	3	-4.05	-21.2	11.2	-3.49	-14.8	3340	4.0
22-Nov-05	-6.01	-14.30	33.78	-3.87	-17.63	2150	5	-3.37	-12.10	14.86	-3.71	-16.42	1050	4	-3.5	-13.6	14.4	-3.57	-15.7	2000	4.0
07-Feb-06	-3.93	-16.00	15.44	-4.05	-17.35	4050	5.4	-4.23	-21.70	12.14	-3.70	-16.25	3100	5.1	-4.38	-19.2	15.8	-3.56	-15.6	4150	8.5
08-May-06	-5.26	-29.90	12.18	-4.03	-17.17	4600		-5.04	-28.00	12.32	-3.75	-12.25	3000		-5.06	-26.6	13.9	-3.67	-16.1	3700	
23-Aug-06	-3.86	-15.40	15.48	-4.20	-18.86			-3.92	-15.70	15.66	-3.87	-13.71			-3.86	-17.6	13.3	-3.82	-17.2		

Table 3 (continued) Monthly isotopic and chloride concentrations of precipitation

Hundred Of Stirling	Pengelly's							Mt Monster							Cooks						
	$\delta^{18}O$	$\delta^{2}H$	d excess	Weighted mean O-18	Weighted mean D	volume ml	Cl^- (mg/l)	$\delta^{18}O$	$\delta^{2}H$	d excess	Weighted mean O-18	Weighted mean D	volume ml	Cl^- (mg/l)	$\delta^{18}O$	$\delta^{2}H$	d excess	Weighted mean O-18	Weighted mean D	volume ml	Cl^- (mg/l)
13-Dec-05	-3.21	-2.1	23.58	-4.51	-24.30	100	24	-1.97	-1.1	14.66	-4.51	-24.30	125	14	-1.68	-1.7	11.74	-4.51	-24.3	150	10
13-Jan-05	-4.77	-29.7	8.46	-4.48	-23.86	225	17	-5.8	-33.4	13	-4.45	-23.72	250	12	-5.94	-37.8	9.72	-4.43	-23.6	200	10
9-Feb-06	-3.55	-13.3	15.1	-4.50	-24.11	1000	5.0	-4.1	-15.1	17.7	-4.51	-24.18	1100	2.2	-3.78	-14.3	15.94	-4.48	-24.2	800	2.3
5-Feb-06	-5.41	-31	12.28	-4.34	-22.37	800	8.6	-4.95	-23.5	16.1	-4.44	-22.62	1350	7.5	-5.14	-25.6	15.52	-4.39	-22.9	1100	8.3
22-May-06	-4.16	-18.5	14.78	-4.47	-23.35	400	14	-4.14	-17.1	16.02	-4.53	-22.77	500	13	-3.65	-14.7	14.5	-4.51	-23.3	350	12
1-Jul-06	-7	-8.2	47.8	-4.45	-23.09	125	20	-2.76	-4.6	17.48	-4.51	-22.43	310	7.3	-2.82	-14.1	8.46	-4.47	-22.9	140	11
17-Aug-06	-4.36	-25	9.88	-4.49	-22.85			-3.9	-18.1	13.1	-4.44	-21.78			-3.96	-17.9	13.78	-4.44	-22.7		
19-Oct-06								-2.44	-8.7	10.82					-2.16	-6.4	10.88				

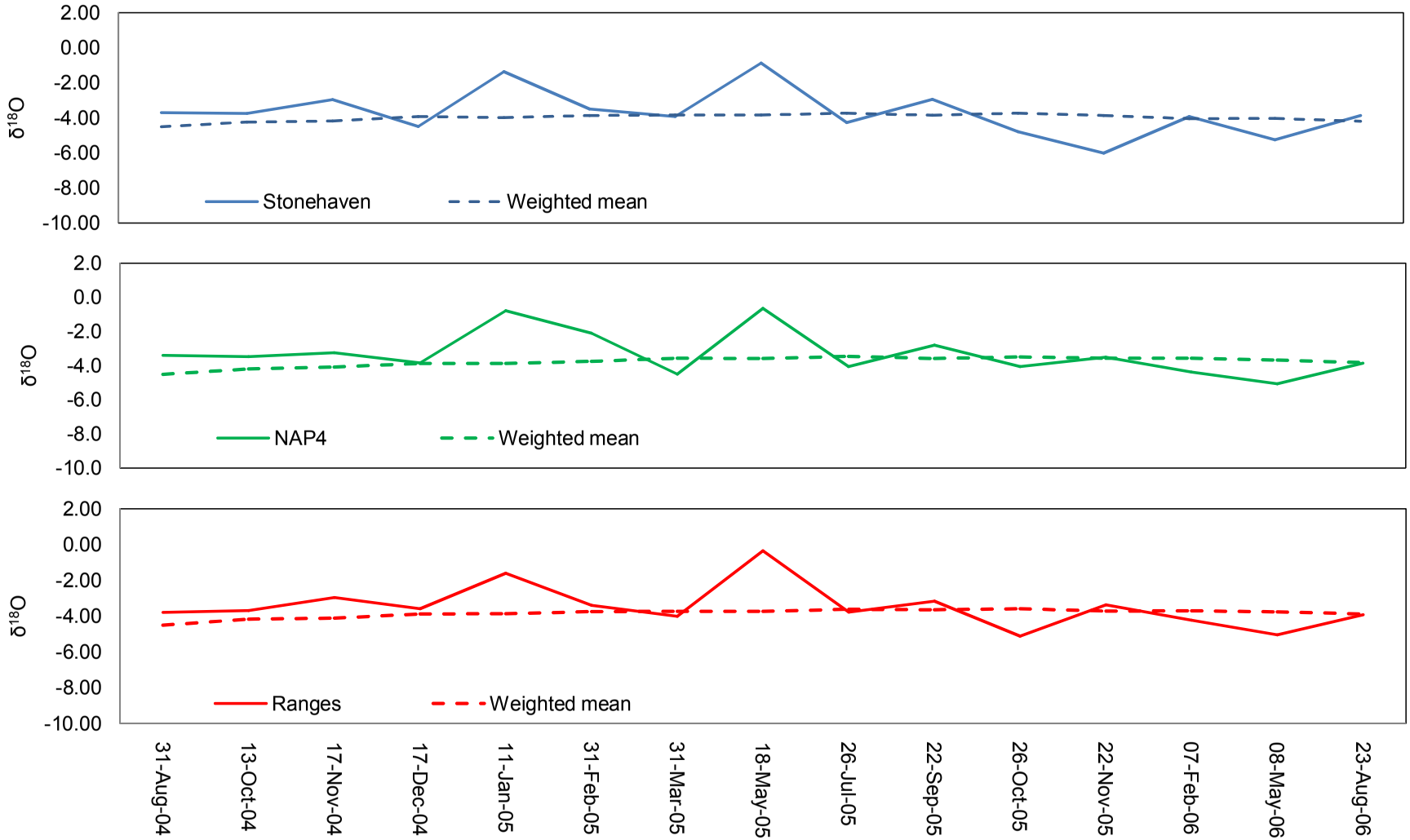

Figure 3 Plot of $\delta^{18}O$ v. Time for monthly rainfall at Stonehaven, NAP4 and Naracoorte Ranges, showing the large variations that can occur on a monthly basis.

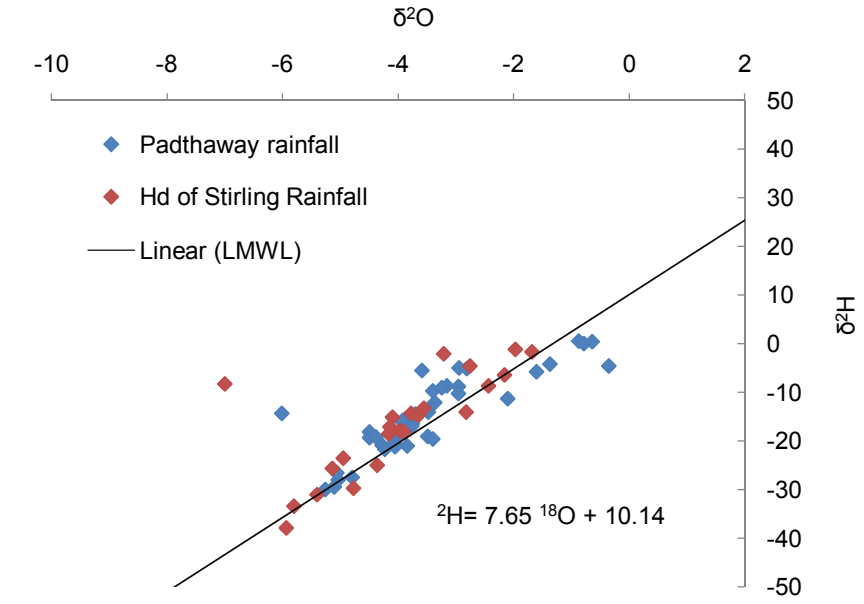

Figure 4. The local meteoric water line for the South East of South Australia, showing precipitation values for δ^2H and $\delta^{18}O$, collected from 6 rainfall stations.

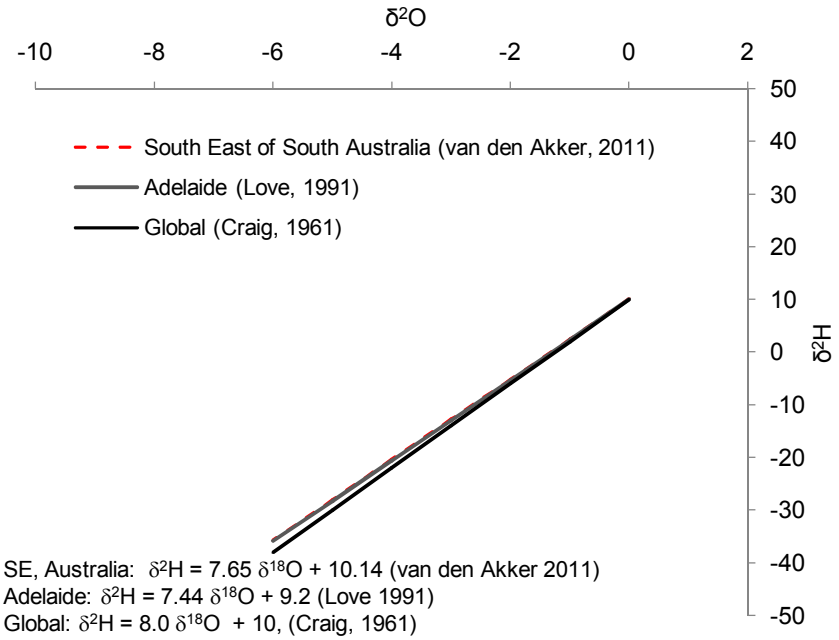

Figure 5 A comparison of the Global LMWL to those developed from long term rainfall stations in Adelaide and more recent short term station in Padthaway and Hundred of Stirling Irrigation areas (South East).

Table 4 also includes the calculated values of the deuterium excess (d) for each precipitation event, calculated by the following equation: $d = \delta^2H - 8\delta^{18}O$ (Dansgaard, 1964). As discussed by previous studies (Merlivat and Jouzel, 1979; Jouzel and Merlivat, 1984; Gat and Matsui, 1991; Gat et al., 1994; Kendall and Coplen, 2001), the d value of a region's precipitation is influenced by the relative humidity and temperature at the moisture source (usually the ocean, but including terrestrial waters when a significant percentage of the moisture comes from re-evaporation of fresh surface water), processes occurring in the upper air column during condensation of ice or rain, and kinetic effects during re evaporation of water as it descends below the cloud base. Precipitation in temperate, continental climates typically has d between 0 ‰ and +20 ‰ (Rozanski et al., 1993; Simpkins, 1995), with a global average of +10 ‰ (i.e., the δ^2H intercept of the global meteoric water line). Values below zero may reflect evaporation after condensation. Such a process can occur during passage of rain or snow from the cloud to the land surface (Harvey, 2001). Deviations to more positive values are most easily explained by addition of evaporated moisture to a continental air mass and are a relatively commonplace phenomenon in South Australia. The d values for precipitation across the study area typically fell in the range +7 ‰ to +17 ‰, with a mean of 14 ‰ (Figure 6).

Deuterium excess values (d) of irrigation water and soil water have also been plotted on Figure 6. By comparison, the d excess of irrigation water and soil water collected from all 4 study sites were lower than precipitation, which suggests evaporation during irrigation.

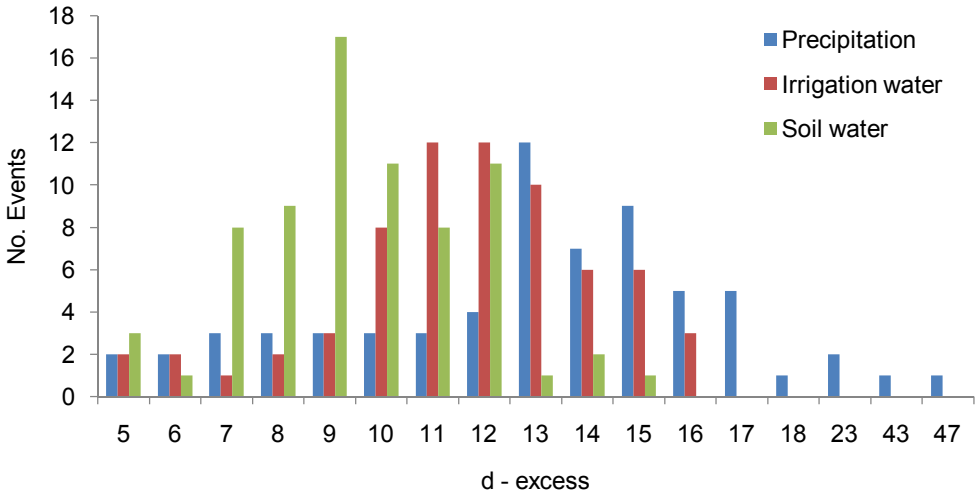

a)

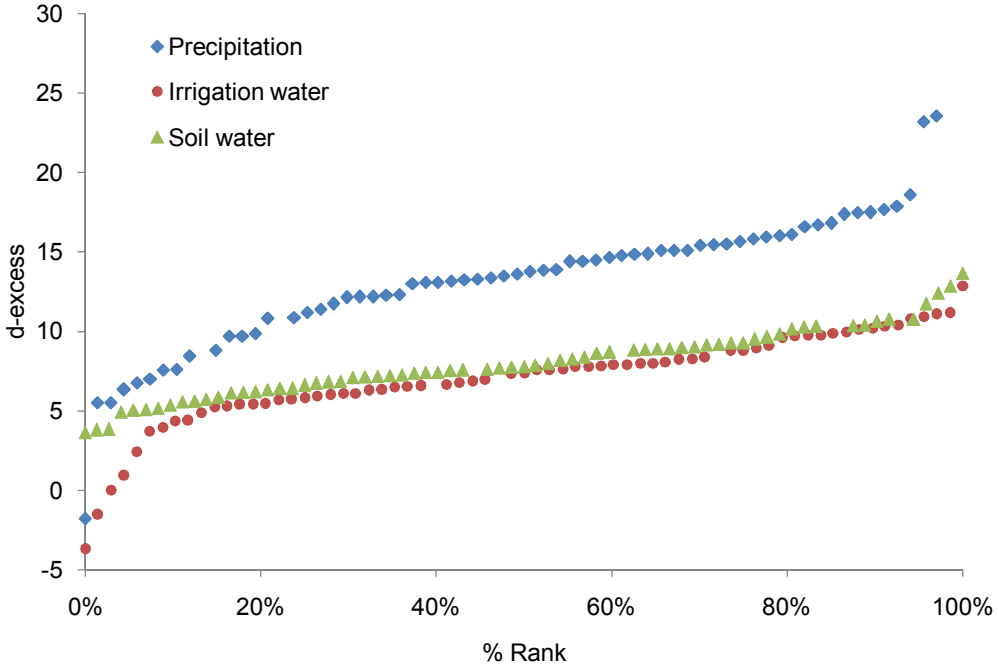

b)

Figure 6. Histogram (a) and percent rank (b) of deuterium excess (d) for precipitation, irrigation water and soil water. As discussed in the text, the absence of d values below zero for precipitation reflect no post-precipitation evaporation, and the lower d-excess of irrigation water and soil water, reflect evaporation during irrigation

Comparison of stable isotopic composition of flood irrigation waters

Figure 7 illustrates the relationship between δ^2H and $\delta^{18}O$ of all irrigation water and soil water, collected from each irrigation bay, compared with the LMWL ($\delta^2H = 7.65\ \delta^{18}O + 10.14$). In most cases, soil water, irrigation water and groundwater are slightly more enriched and plot to the right of the LMWL, indicating that waters have been evaporated during the irrigation process. They plot below the LMWL, on a line which will be referred to as the Local Evaporation Line (LEL). Samples that plot furthest away from the LMWL on a given LEL have had the greatest percentage of water loss to evaporation. The slopes and intercepts produced from linear regressions (LEL's) through the isotopic composition of irrigation water, soil water, pan water and groundwater collected from each site are compared in Table 4. Evaporated waters have smaller values for the slope and the intercept, as illustrated by Figure 8, which shows the correlation (R^2 = 0.823) between percentage evaporated water and slope of the relationship between δ^2H - $\delta^{18}O$ delta values of irrigation water.

Table 4. Regression relationship of δ^2H and $\delta^{18}O$ for precipitation, irrigation water, soil water, groundwater and Class A pan water

Water source	Site	Slope(m)	δ^2H intercept	R^2
Precipitation	SE of South Australia	7.65	10.14	0.99
Groundwater (irrigation bore)	Padthaway	6.39	1.95	0.81
	Hd of Stirling	9.82	0.56	0.89
Groundwater (piezometer)	Padthaway	4.22	-7.71	0.75
	Hd of Stirling	9.82	0.56	0.89
Soil Water	Padthaway	5.21	-3.08	0.45
	Hd of Striling	6.17	-0.43	0.77
Irrigation Water	Padthaway NAP4	---	---	---
	Padthaway NAP4	3.64	-11.89	0.68
	Padthaway NAP5	4.20	-5.58	0.95
	Padthaway NAP5	4.05	-9.87	0.90
	Hd of Stirling MTM	4.17	-8.80	0.70
	Hd of Stirling MTM	---	---	---
	Hd of Stirling PG	7.5	4.56	0.38
	Hd of Stirling PG	---	---	---
Class A evaporation pan	Padthaway NAP4	3.76	-10.22	0.98
	Padthaway NAP5	3.5	-8.84	0.98
	Hd of Stirling MTM	3.11	-12.28	0.65
	Hd of Stirling PG	1.52	-24.17	0.25

---- no slope determined as waters did not deviate from the LMWL, producing low R^2 values

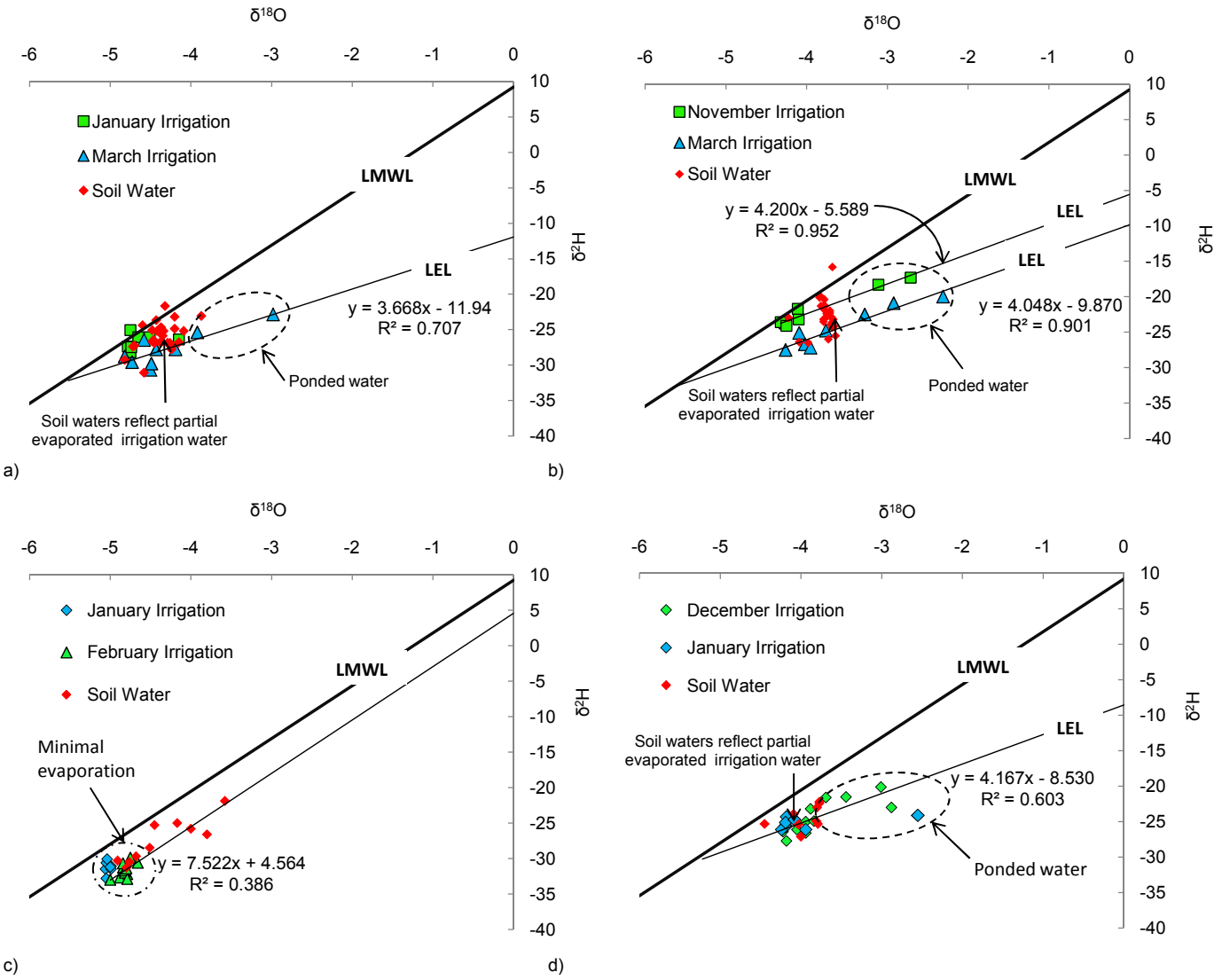

Figure 7 δ^2H and $\delta^{18}O$ plots of soil water and irrigation water potted against the LMWL a) NAP4 b) NAP5 c) PG and d) MTM

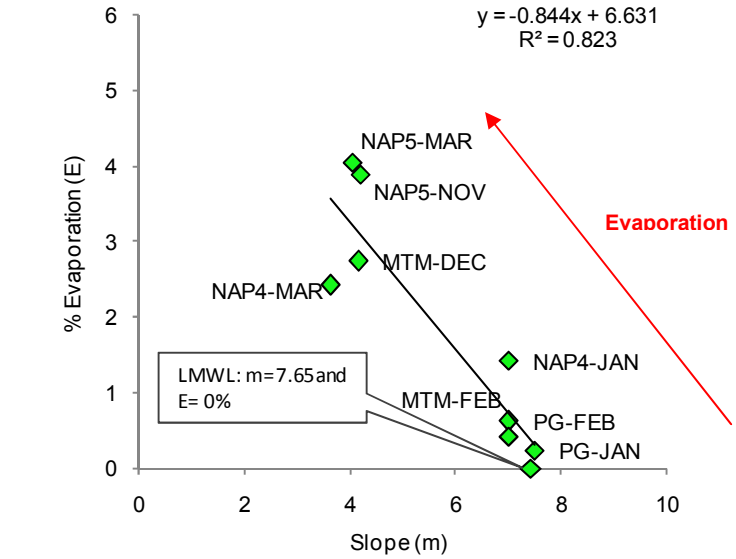

a)

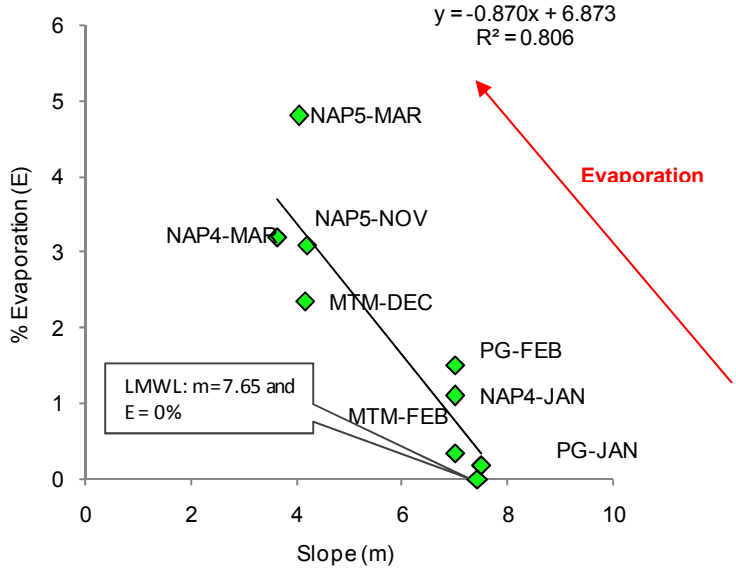

b)

Figure 8. Correlation of percentage evaporation water loss (E) and slope of the relationship between δ^2H - $\delta^{18}O$ delta values of irrigation waters, where E was calculated according to equations of Simpson et al. (1987) and Gonfiantini (1986), outlined in Chapter 3. a) E represents evaporation calculated over ponding period only. b) E represents the average evaporation losses calculated over both irrigation application + ponding periods.

The shift in δ^2H and $\delta^{18}O$ values and difference in the regressions generated by evaporating waters varied according to the intensity of evaporation which took place during irrigation. Therefore variations in evaporation across each site, which are influenced by the time of irrigation, soil type, irrigation application rate and crop cover, control isotopic enrichment (evaporation) leading to variations in slope and intercept.

Irrigation water

The slopes of the LEL regression lines (3 - 4) developed from irrigation waters at NAP4-JAN, NAP5-NOV, NAP5-MAR and MTM-DEC, deviate significantly from the value (8) given by the Adelaide LMWL and more recent vales given in the study for Padthaway LMWL (6.5) and the Hundred of Stirling LMWL (7.4) indicating that irrigation was subject to evaporation (Table 4). The slopes of 3 to 4 encountered here lie in the range expected for evaporation of free water bodies under these conditions (Craig et al., 1963; Gat, 1980; Gat, 1971 and Homanda et al., 2004). In addition, the observed values for the slope of pan water (3.11 to 3.94) undergoing evaporation (measured during irrigation pan experiments outlined in Chapter 3) were slightly lower to those found for the evaporation line of irrigation waters at sites NAP4-JAN, NAP5-NOV, NAP5-MAR and MTM-DEC (Table 4 and Figure 9). Hence (with the exception of PG-JAN, PG-FEB and MTM-FEB) the results of the isotopic enrichment obtained throughout the pan experiment, match to a large extent the isotopic enrichments of irrigation waters.

The δ^2H and $\delta^{18}O$ plots of irrigation water collected from irrigations at MTM-FEB, PG-JAN and PG-FEB produced similar slopes to that of the LMWL and do not deviate to the right of the LMWL, indicating minimal evaporation in comparison to i) their respective pan waters (m = 3) and ii) irrigation waters at other sites (m = 3 to 4). The δ^2H and $\delta^{18}O$ compositions of irrigation water collected during the January irrigation at MTM (during a time when crop cover was 0 %) plots to the right of the LMWL and shares a similar slope (4.7) to the evaporation line produced from pan waters (3.1 to 3.9). In comparison, the δ^2H - $\delta^{18}O$ plot of irrigation waters collected during the February irrigation (during a time when crop cover was close to 100 %) do not deviate to the right of the LMWL, reflecting minimal evaporation losses during this irrigation (Table 4, Figure 9). As the timing of irrigation and meteorological conditions were similar during both irrigations, the

minimal evaporation detected in February is attributed to the increased crop cover and demonstrates the greater effects evaporation has on an open water body. Results from evaporation experiments outlined in Chapter 3 showed that dense crop cover can reduce evaporation rates by 30%.

Similarly, the difference in spread of δ^2H - $\delta^{18}O$ data produced from irrigation waters sampled in January and March at NAP4, was attributed to the difference in evaporation potential as a result of irrigating during the night (m = 3.6) versus the day (m = LMWL), Table 4 and Figure 9. At times, irrigation bays may be irrigated at night, thereby allowing water to pond during the following day. This is commonly the case, when irrigating over soil types which do not facilitate rapid drainage.

These results confirm that combination of rapid draining soils, dense crop cover contribute to a significant reduction in surface water evaporation.

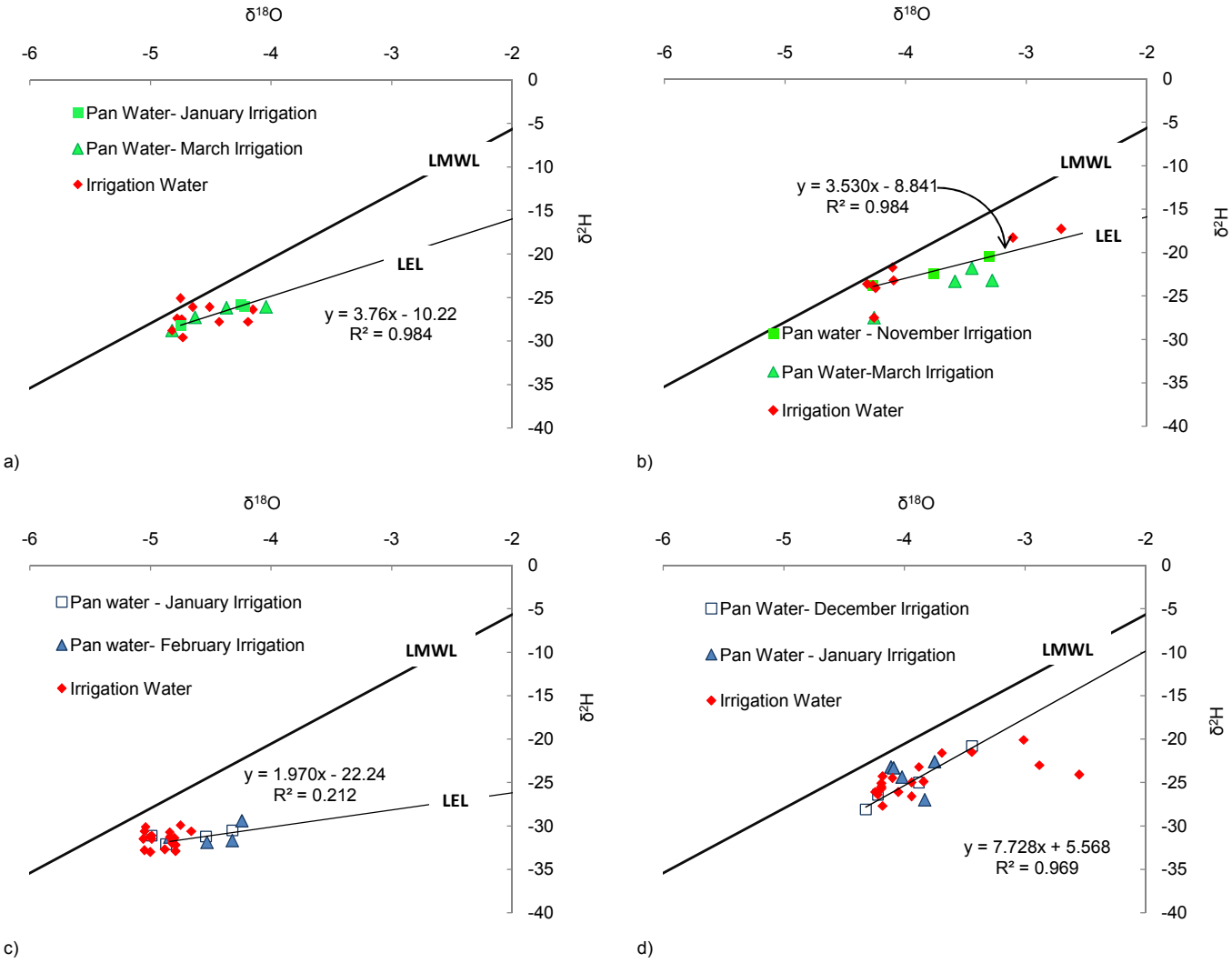

Figure 9 δ^2H and $\delta^{18}O$ plots (LEL) of pan water and irrigation water potted against the LMWL a)NAP4 b)NAP5 c)PG and d)MTM. At PG, the pan waters plot further to the right than irrigation waters, suggesting that the flood bay was not subject to the same degree of evaporation

The δ^2H and $\delta^{18}O$ compositions of irrigation water collected during both irrigations at NAP5 shows a greater spread of data points to the right of the LMWL, in comparison to the other flood irrigation sites (Figure 7 and Figure 9). This is attributed to the longer duration of ponding (up to 22 h) experienced post irrigation. In addition, NAP5 has not been laser levelled, causing water to pool in two low lying areas within the bay for extended periods of time during the day (as discussed in Chapter 3). Water samples taken from these pools showed a greater degree of evaporation, resulting in a greater spread of data along the LEL, to the right of the LMWL, than waters collected from other parts of the bay. The slopes of the LEL regressions produced from irrigation waters (4.05 – 4.2) suggest that irrigation water was subject to the same degree of evaporation as measured in the evaporation pan (3.94).

Soil water and groundwater

The combined δ^2H and $\delta^{18}O$ composition of all soil water collected from suction lysimeters buried at depth intervals ranging from 0.3 to 3 m within the vadose zone post irrigation plot close to LMWL and share a similar isotopic composition to irrigation waters collected during early the stages of irrigation (Figure 7). Therefore, soil water signature reflects partially enriched (evaporated) irrigation water. The slopes generated from δ^2H and $\delta^{18}O$ relationships of soil water, range from 5.2 and 6 for Padthaway and Hundred of Stirling respectively (Figure 10 and Table 3) and take on values that approximate those determined for saturated soils (4 - 6) and also evaporation from open water bodies (4 - 6) (Barnes and Allison, 1983; Allison et al., 1983). This suggests that soil water was not subject to further evaporation post irrigation.

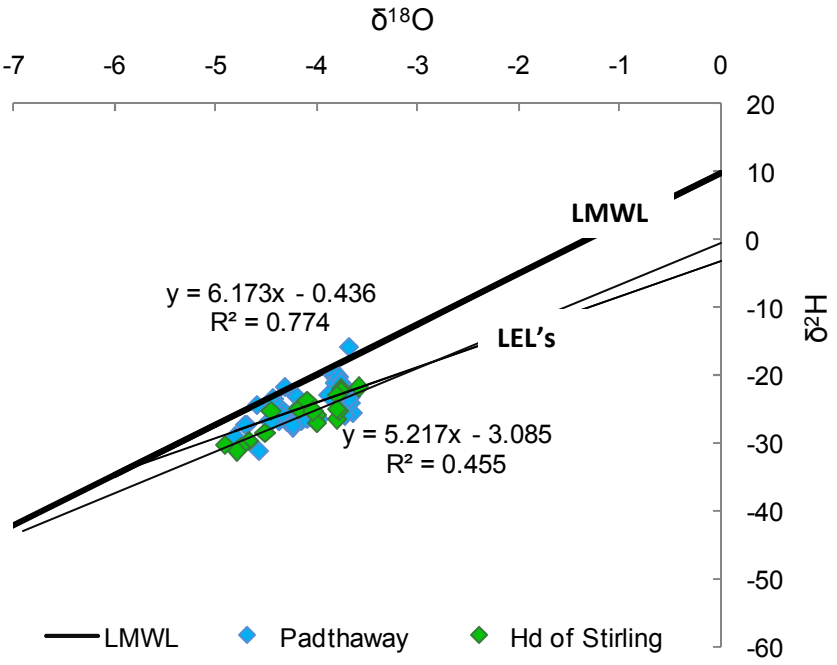

Figure 10 Combined δ^2H - $\delta^{18}O$ regression line for soil water collected post irrigation from flood irrigation sites in Padthaway and Hundred of Stirling

The δ^2H and $\delta^{18}O$ composition of groundwater collected from shallow piezometers (which monitor the Padthaway formation beneath irrigation bays) average - 4.09‰ and - 23.9‰ in Padthaway and - 4.33‰ and - 27.7‰ in the Hundred of Stirling. These values plot slightly to the right of the LMWL for Padthaway and the Hundred of Stirling, indicating a small effect of evaporation (Figure 11). In Padthaway the stable isotopic composition of groundwater's sourced from the shallow piezometers within irrigation bays give a linear regression of: $\delta^2H = 4.2\ \delta^{18}O - 7.1$ a slope somewhat lower to that derived from deeper irrigation bores ($\delta^2H = 6.4\ \delta^{18}O + 1.9$). However, in the hundred of Stirling, groundwater from irrigation bores and piezometers shared a similar linear regression ($\delta^2H = 9.503\ \delta^{18}O + 14.04$) and share a slope which takes on values closer to local rainfall.

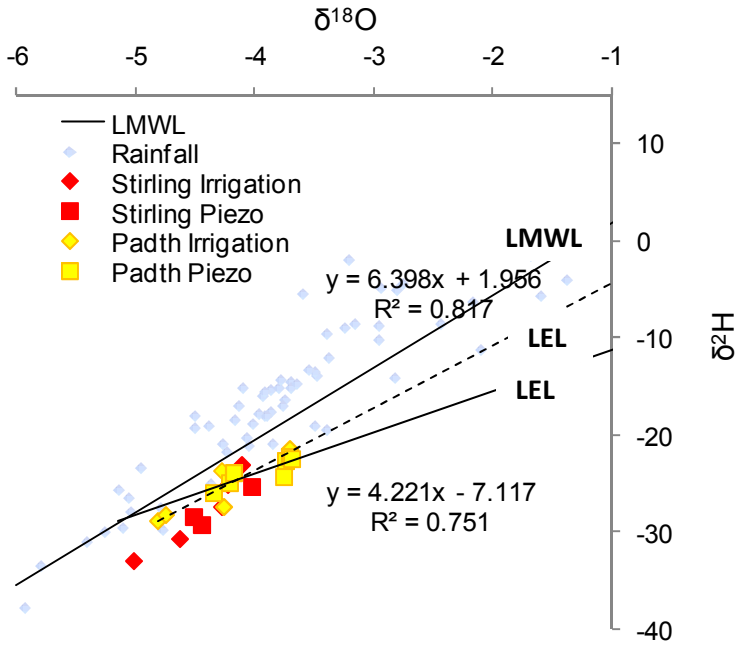

Figure 11 Combined δ^2H - $\delta^{18}O$ regression line for groundwater collected from flood irrigation sites in Padthaway and Hundred of Stirling.

Allison (1982) showed that evaporation from unsaturated zone soil water could have a slope as low as 2, while evaporation from an open body of water will have a slope of around 4 - 6. With a slope of 5.2 to 6.1 given for the isotopic composition of soil water and 5.4 to 9 for groundwater, it does not appear that evaporation has greatly affected drainage water within the soil zone or from an open body of water (e.g. flood irrigation). This is particularly the case in the Hundred of Stirling which produced higher slopes (9) to that of Padthaway (5.2). It can be seen from Chapter 3 that in the Hundred of Stirling water freely and quickly drains through the unsaturated zone, thus not allowing time for significant evaporation to occur when irrigating over these soil types.

Conclusion

The LMWL developed for Padthaway and Hundred of Stirling produced linear regressions of $\delta^2H = 7.65\ \delta^{18}O + 10.14$ which is consistent with regressions developed for the long term station of Adelaide. In contrast, the δ^2H and $\delta^{18}O$ compositions of irrigation waters subject to evaporation produced lower slopes ranging from 3 - 4, which are consistent with the evaporation of free water bodies, and slopes produced by Class A evaporation pan experiments, monitored during irrigation (3.11 - 3.94). Such slopes were found during irrigations at Padthaway where minimal crop cover and longer duration of irrigation/ponding contributed to higher evaporation losses. In comparison, the δ^2H - $\delta^{18}O$ relationship produced from irrigations which occurred over rapid draining soils and during periods of dense crop cover, namely flood irrigation in the Hundred of Stirling, produced slopes somewhat similar to the LMWL, indicating minimal evaporation during irrigation. This study confirms the benefits of flood irrigating under these conditions.

Linear regression of soil waters collected from the irrigation bays 1 to 3 days following irrigation reflect partially evaporated water and exhibited similar slopes to that of the LMWL, suggesting that evaporation from the soil profile was not evident post irrigation. If evaporation from the soil profile was a dominant process, the slopes produced from δ^2H - $\delta^{18}O$ relationships of soil water are expected to be as low as 2. Evaporation from soil profile was inhibited by a combination of dense crop cover and/or calcrete layers commonly found at shallow depths. Furthermore, there was no significant deviation of the shallow groundwater samples from the LMWL and irrigation water, which suggests that drainage has occurred fairly rapidly with minimal isotopic fractionation by evaporative process prior to infiltration.

In the absence of fractionating water loss, the salinity increase measured in the soil water and shallow groundwater waters following irrigation indicates that transpiration is the main mechanism responsible for the groundwater salinity increase beneath the flood irrigated areas.

References

Allison G.B., Bames C.J. and Hughes M.W.,1983. The distribution of deuterium and oxygen-18 in dry soils: II. Experimental. J. Hydrol. 64: 377 - 397.

Barnes C.J. and Allison G.B., 1983. The distribution of deuterium and oxygen-18 in dry soils: 1 Theory, J. Hydrol. 60: 141 - 156.

Craig, H., 1961. Isotopic variations in meteoric waters. Science 133, 1702 - 1703.

Craig, H., Gordon, L.J. and Horibe, Y., 1963. Isotopic exchange effects in the evaporation of water. J. Geophy. Res., 68: 5079 - 5087.

Dansgaard, W., 1964. Stable isotopes in precipitation. Tellus 16, 436 - 468.

Dincer, T., A1-Mugrin, A. and Zimmermann, U., 1974. Study of the infiltration and recharge through the sand dunes in arid zones with special reference to the stable isotopes and thermonuclear tritium. J. Hydrol., 23: 79 - 89.

Gat, J.R., 1980. The isotopes of oxygen and hydrogen in precipitation. In: Fritz, P., Fontes, J.Ch. (Eds.). Handbook of Environmental Isotope Geochemistry, 1. Elsevier, New York, pp. 27 - 47.

Gat, J.R., 1971. Comments on the stable isotope method in regional groundwater investigation. Wat. Resour. Res. 7: 980 - 993.

Gat, J.R., Matsui, E., 1991. Atmospheric water balance in the Amazon Basin: an isotopic evapo-transpiration model. Journal of Geophysical Research 96, 13179 - 13188.

Gat, J.R., Bowser, C.J., Kendall, C., 1994. The contribution of evaporation from the Great Lakes to the continental atmosphere: estimate based on stable isotope data. Geophysical Research Letters 21 (7), 557 - 560.

Gonfiantini, R., 1986. Environmental isotopes in lake studies. In: Fritz, P., Fontes, J.Ch. (Eds.). Handbook of Environmental Isotope Geochemistry, 3. Elsevier, New York, pp. 113 - 168.

Harvey, F.E., 2001. Use of NADP archive samples to determine the isotope composition of precipitation: characterizing the meteoric input function for use in ground water studies. Ground Water 39, 380 - 390.

Hamada, Y,,Yabusaki, S, Tase, N, and Taniyama, S., 2002. Stable isotope ratios of hydrogen and oxygen in paddy water affected by evaporation. In Rice is life: scientific perspectives for the 21st century.

Jouzel, J., Merlivat, L., 1984. Deuterium and oxygen-18 in precipitation: modelling of the isotopic effect during snow formation. Journal of Geophysical Research 89, 11749 - 11757.

Kendall, C., Coplen, T.B., 2001. Distribution of oxygen-18 and deuterium in river waters across the United States. Hydrological Processes 15, 1363 - 1393.

Merlivat, L., Jouzel, J., 1979. Global climatic interpretation of the deuterium–oxygen 18 relationship for precipitation. Journal of Geophysical Research 84, 5029 - 5033.

Rozanski, K., Aragua´s-Aragua´s, L.,Gonfiantini R., 1993. Isotopic patterns in modern global precipitation. In: Continental Isotope Indicators of Climate, American Geophysical Union Monograph.

Simpkins, W.W., 1995. Isotopic composition of precipitation in central Iowa. Journal of Hydrology 172, 185 - 207.

Simpson, H. J., Hamza, M. S., White, J. W. C , Nada, A. & Awad, M. A., 1987. Evaporative enrichment of deuterium and 1S0 in arid zone irrigation. In: Isotope Techniques In Water Resources Development. IAEA-SM-299/125, 241 - 256

Wohling, D., 2007. Minimising Salt Accession to the South East of South Australia. The Border Designated Area and Hundred of Stirling Salt Accession Projects. Volume 2 - Analytical Techniques, Results and Management Implications, DWLBC Report 2007, Government of South Australia, through Department of Water, Land and Biodiversity Conservation, Adelaide.

APPENDIX A

Meteorological Data

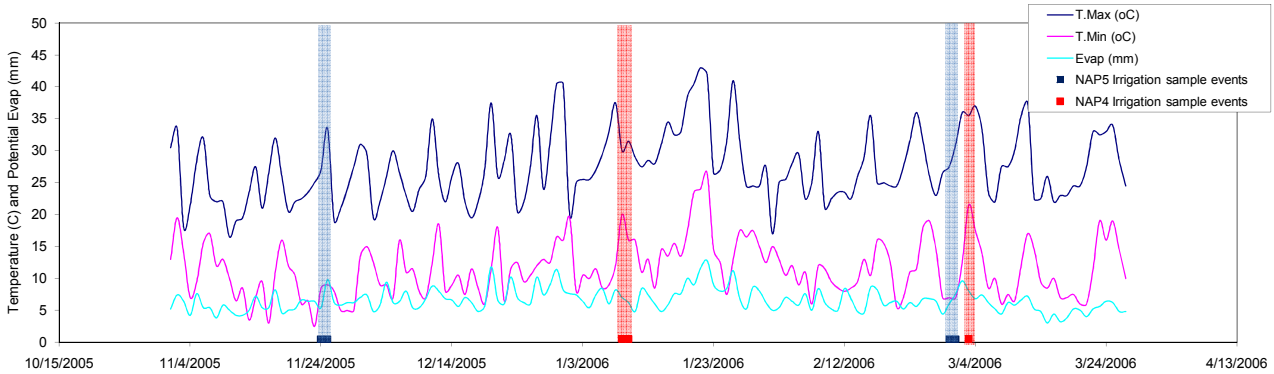

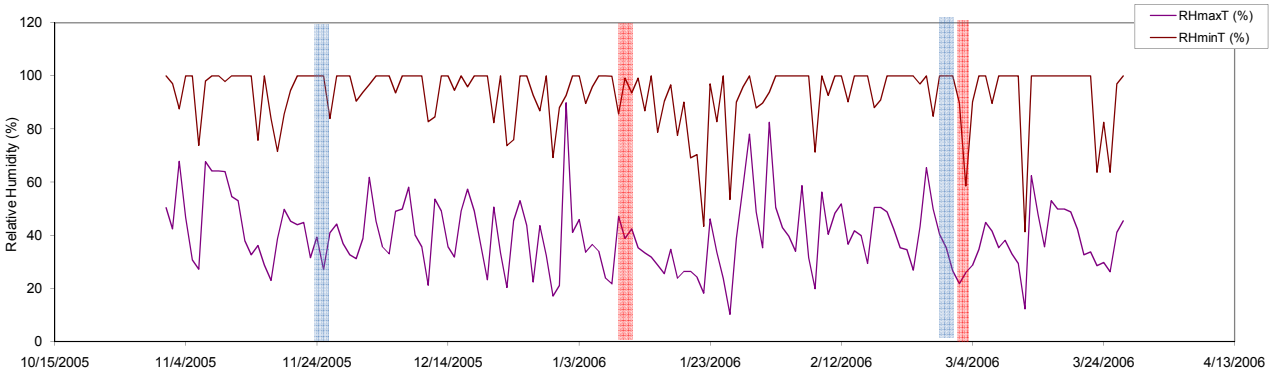

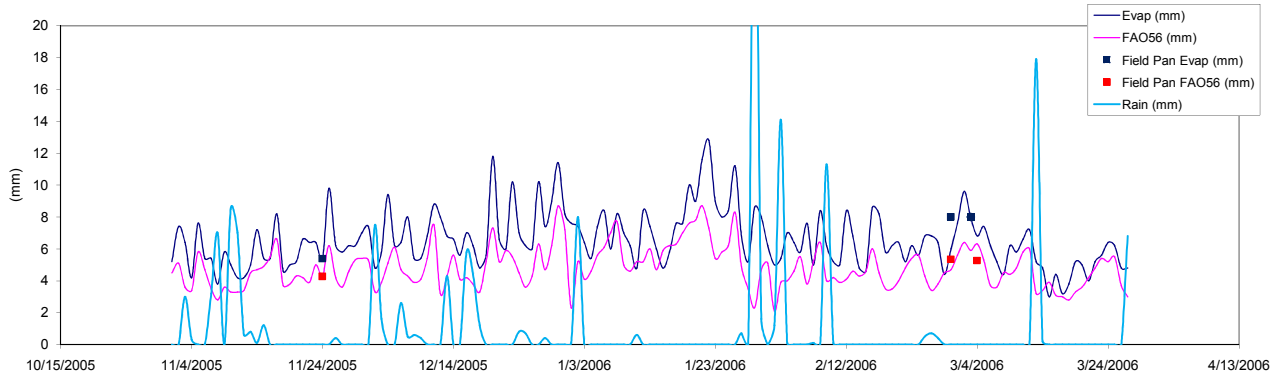

BOM Padthaway Weather Station (26089) data

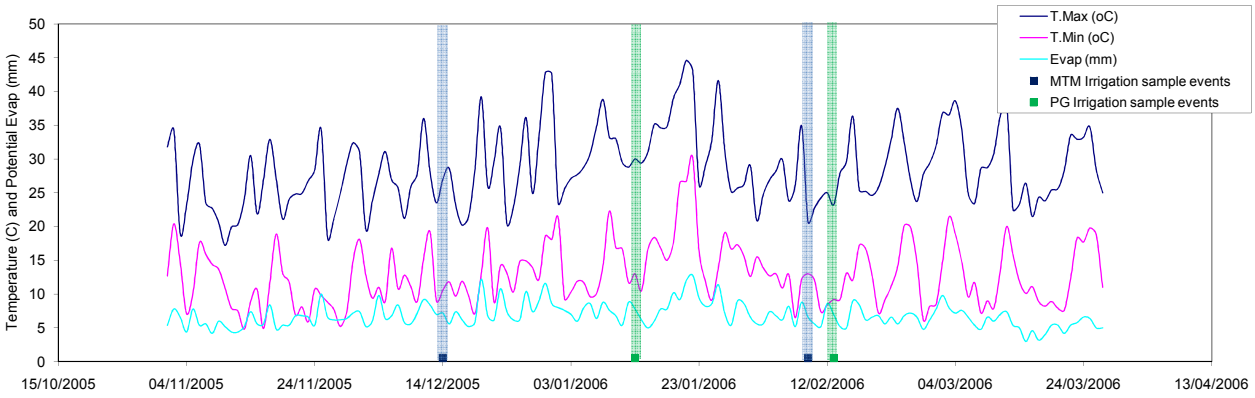

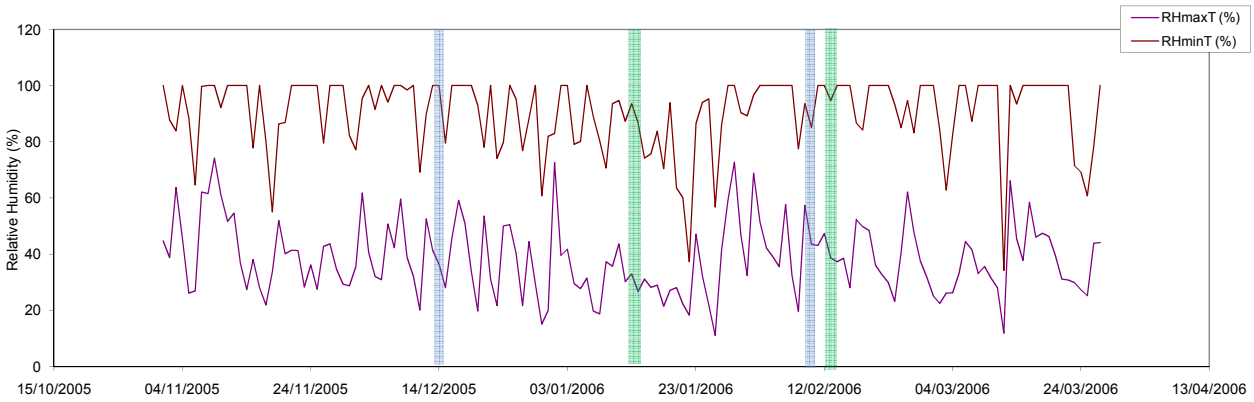

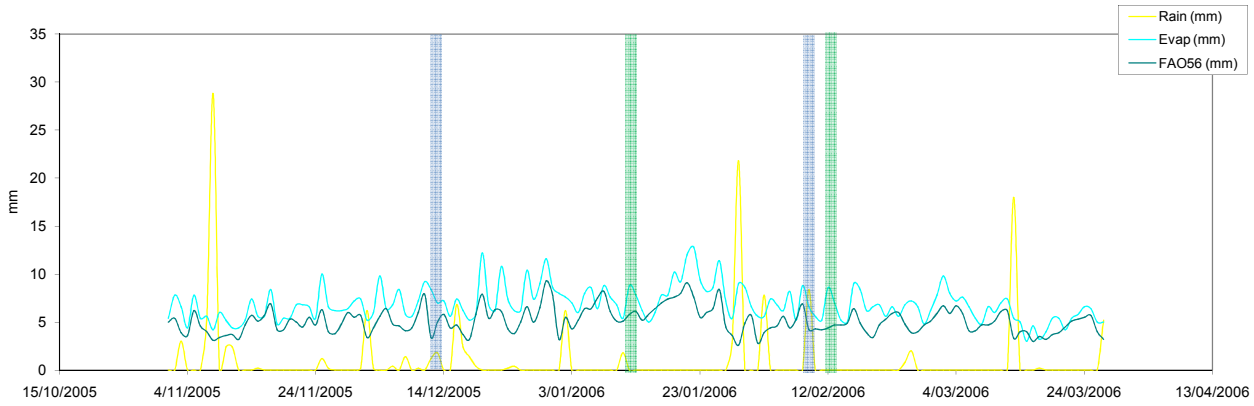

BOM Keith Weather Station (25507) data

APPENDIX B

Stable isotope and chloride data

NAP5 NOVEMBER

DATE	TIME	PONDING TIME	SAMPLE ID	δ O18 (‰)	δD (‰)	CHLORIDE (mg/l)	EC (u/cm)	TDS (mg/l)	% Evap ^{18}O (x_c)	% Evap ^{2}H (x_c)	Average % evap
24/11/2005	10:11AM		BORE	-4.27	-23.8	1188	3.400	1889	0.00	0.00	0.00
24/11/2005			NAP5 A								
24/11/2005	10:30 AM		NAP5 B								
24/11/2005	10:30 AM		NAP5 C								
24/11/2005	10:40 AM		NAP5 D								
24/11/2005	10:44 AM		NAP5 E	-4.32	-23.6	1144	3.377	1872	0.00	0.22	0.11
24/11/2005	11:10AM		NAP5 F								
24/11/2005	3:30PM		NAP5 E1								
24/11/2005	3:30PM		NAP5 F1								
24/11/2005	3:30PM		NAP5 G	-4.25	-24.1	1148	3.347	1860	0.32	0.00	0.16
24/11/2005	3:30PM		NAP5 G1								
24/11/2005	4:50PM	0	NAP5 H								
25/11/2005	8:30AM	13	NAP5 F3								
25/11/2005	8:30AM	13	NAP5 G3	-4.1	-23.2	1174	3.583	1990	1.00	0.66	0.83
25/11/2005	8:30AM	13	NAP5 H3								
25/11/2005	8:30AM	13	NAP5 I3	-4.11	-21.7	1153	3.533	1962	0.95	2.30	1.63
25/11/2005	8:30AM	13	NAP5 J3	-3.84		1165	3.754	2086	2.18		2.18
25/11/2005	3:00PM	19	NAP5 F4	-3.06		1291	4.177	2329	5.73		5.73
25/11/2005	3:10PM	19.6	NAP5 G4	-3.11	-18.3	1175	3.760	2091	5.50	6.01	5.76
25/11/2005	3:15PM	19.6	NAP5 I4	-2.71	-17.3	1223	3.840	2137	7.32	7.11	7.21
25/11/2005	3:20PM		NAP5 SOUTH 0.35m	-4.09	-26.4	1170	3.542	1967	1.05	-2.84	-0.90
25/11/2005			NAP5 SOUTH 1.4m	-3.79	-23.5	1480	4.347	2420	2.41	0.33	1.37
25/11/2005			NAP5SOUTH 2.4m	-3.7	-23.9	1780	4.893	2732	2.82	-0.11	1.35
25/11/2005			NAP5 SOUTH 2.9m	-3.68	-23.6	1650	4.588	2567	2.91	0.22	1.56
25/11/2005			NAP5 SOUTH Piezo	-3.74	-22.7	1410	4.000	2227	2.64	1.20	1.92
25/11/2005			NAP5 NORTH 0.35m	-3.79	-21.3	1390	4.240	2363	2.41	2.73	2.57
25/11/2005			NAP5 NORTH 1.4m	-3.82	-21.3	1470	4.212	2346	2.27	2.73	2.50
25/11/2005			NAP5 NORTH 2.4m	-3.78	-20.4	1490	4.148	2312	2.45	3.72	3.09
25/11/2005	4:00PM		NAP5 NORTH 2.9m	-3.77	-21.3	1400	3.884	2159	2.50	2.73	2.62

DATE	TIME	TIME (h)	SAMPLE ID	δ O18	δD	CHLORIDE	EC	TDS	DTW (mm)	Epan*Cp	% Loss (x_m)
24/11/2005	10:11AM	0	BORE	-4.27	-23.8	1188	3.403	1889	0	0	0.00
24/11/2005	3:20PM	5	PAN 1	-4.15		1159	3.695	2052	2	1.6	0.73
25/11/2005	9:00AM	23	PAN 2	-3.77	-22.4	1190	3.545	1970	5.4	4.26	1.94
25/11/2005	4:00PM	30	PAN 3	-3.31	-20.4	1180	3.640	2024	windy	7	3.18
28/11/2005	nikki	48	PAN 4							10.5	4.77

^{18}O Enrichment F	0.22
^{2}H Enrichment F	0.9144

Average % Evap	
During Irrigation application only	0.134
During irrigation application and ponding	2.950
During ponding only	3.889

NAP5 MARCH

DATE	TIME	PONDING TIME	SAMPLE ID	δ O18 (‰)	δD (‰)	CHLORIDE (mg/l)	EC (u/cm)	TDS (mg/l)	% Evap ^{18}O (x_c)	% Evap ^{2}H (x_c)	Average % evap
28/02/2006			BORE	-4.26	-27.5	1188	3.80	2144	0	0	0
28/02/2006	11:30AM		NAP5 A								
28/02/2006	11:30AM		NAP5 B								
28/02/2006	11:30AM		NAP5 C								
28/02/2006	4:30PM		NAP5 B1								
28/02/2006	4:30PM		NAP5 C1	-4.02	-26.7	1202	3.78	2103	1.09	0.85	0.97
28/02/2006	4:30PM		NAP5 D1								
28/02/2006	4:30PM		NAP5 E1	-3.95	-27.2	1205	3.82	2125	1.41	0.32	0.86
28/02/2006	4:30PM		NAP5 Ea								
01/03/2006	9:30AM	14	NAP5 B2								
01/03/2006	9:30AM	14	NAP5 C2	-4.09	-25.1	1212	3.82	2125	0.77	2.55	1.66
01/03/2006	9:30AM	14	NAP5 D2								
01/03/2006	9:30AM	14	NAP5 E2	-3.76	-24.8	1208	3.84	2137	2.27	2.87	2.57
01/03/2006	9:30AM	14	NAP5 F2	-3.5		1254	3.85	2142	3.45		3.45
01/03/2006	1:30PM	18	NAP5 B3								
01/03/2006	1:30PM	18	NAP5 C3								
01/03/2006	1:30PM	18	NAP5 E3	-3.28	-22.5	1251	3.94	2193	4.45	5.32	4.89
01/03/2006	1:30PM	18	NAP5 F3	-3.18		1251	3.919	2182	4.91		4.91
01/03/2006	4:00PM	22.5	NAP5 B4								
01/03/2006	4:00PM	22.5	NAP5 C4	-2.92	-20.9	1291	4.084	2272	6.09	7.02	6.56
01/03/2006	4:00PM	22.5	NAP5 E4	-2.31	-20	1118	4.116	2295	8.86	7.98	8.42
01/03/2006	4:00PM	22.5	NAP5 F4	-2.46		1206	3.986	2221	8.18		8.18
01/03/2006	6:00PM		NAP5 SOUTH 0.35m	-4.22	-23	1344	3.98	2216	0.18	4.79	2.48
01/03/2006			NAP5 SOUTH 1.4m	-3.98	-26.5	1621	4.68	2613	1.27	1.06	1.17
01/03/2006			NAP5SOUTH 2.4m	-3.84	-20.1	1847	5.08	2852	1.91	7.87	4.89
01/03/2006			NAP5 SOUTH 2.9m	-3.83	-19.9	1712	4.91	2743	1.95	8.09	5.02
01/03/2006			NAP5 NORTH 0.35m	-3.68	-15.8	1480	4.32	2408	2.64	12.45	7.54
01/03/2006			NAP5 NORTH 1.4m	-3.64	-25.5	1570	4.52	2522	2.82	2.13	2.47
01/03/2006			NAP5 NORTH 1.4m A								
01/03/2006			NAP5 NORTH 2.4m	-3.68	-24.3	1471	4.41	2459	2.64	3.40	3.02
01/03/2006	4:00PM		NAP5 NORTH 2.9m	-3.73	-26	1451	4.50	2510	2.41	1.60	2.00
02/03/2006	4:00PM		NAP5 SOUTH 0.35m	-3.66	-24.2	1311	4.2	2340	2.73	3.51	3.12
02/03/2006			NAP5 SOUTH 1.4m	-3.73	-22.6	1702	5.065	2852	2.41	5.21	3.81
02/03/2006			NAP5SOUTH 2.4m	-3.69	-22.9	1810	5.252	2909	2.59	4.89	3.74
02/03/2006			NAP5 SOUTH 2.9m	-3.71	-22	1656	5.03	2795	2.50	5.85	4.18
02/03/2006			NAP5 SOUTH Piezo	-3.71	-22.3	1506	4.554	2539		5.53	2.77
02/03/2006			NAP5 NORTH 0.35m								
02/03/2006			NAP5 NORTH 1.4m								
02/03/2006			NAP5 NORTH 2.4m								
02/03/2006	5:00PM		NAP5 NORTH 2.9m								
08/03/2006	9:30AM		NAP5 SOUTH 0.35m	-3.79	-21.7	1428	-	2430	2.14	6.17	4.15
08/03/2006			NAP5 SOUTH 1.4m	-3.79	-23.2	1907	5.497	3080	2.14	4.57	3.36
08/03/2006			NAP5SOUTH 2.4m	-3.75	-22.4	1814	5.24	2909	2.32	5.43	3.87
08/03/2006			NAP5 SOUTH 2.9m	-3.67	-23.2	1580	4.832	2698	2.68	4.57	3.63
08/03/2006			NAP5 NORTH 0.35m								
08/03/2006			NAP5 NORTH 1.4m								
08/03/2006			NAP5 NORTH 2.4m								
08/03/2006	10:30AM		NAP5 NORTH 2.9m								

DATE	TIME	TIME (h)	SAMPLE ID	δ O18	δD	CHLORIDE	EC	TDS	DTW (mm)	Epan*Cp	% Loss (x_m)
2/28/2006	11:00AM	0.00	PAN1	-4.26	-27.5	1188	3.80	2144	0	0.00	0.00
28/02/2006	4:00PM	5.00	PAN2								
28/02/2006	5:30PM	6.50	PAN3	-3.92		1199	3.909	2176	3	2.35	1.36
01/03/2006	9:00AM	22.00	PAN4	-3.59	-23.3	1238	3.86	2148	8	5.36	3.64
01/03/2006	1:15PM	26.00	PAN5	-3.45	-21.8	1243	3.87	2154	10	6.70	4.55
01/03/2006	6:00PM	32.00	PAN6	-3.28	-23.2	1264	3.90	2171	12	8.04	5.45
3/2/2006	5:00PM	55.00	PAN8	-2.16		1308	4.226	2352	21	15.48	9.55

^{18}O Enrichment F	0.22
^{2}H Enrichment F	0.94

Average % Evap	
During Irrigation application only	0.918
During irrigation application and ponding	4.248
During Ponding only	5.080

NAP4 JANUARY

DATE	TIME	PONDING TIME (h)	SAMPLE ID	δ O18 (‰)	δD (‰)	CHLORIDE (mg/l)	EC (u/cm)	TDS (mg/l)	% Evap ^{18}O (x_c)	% Evap ^{2}H (x_c)	Average % evap
			BORE	-4.75	-28.2	697		1434	0.00	0	0
09/01/2006	3:15PM		NAP4 A								
09/01/2006	3:30PM		NAP4 B								
09/01/2006	8:00PM		NAP4 A1								
09/01/2006	8:10PM		NAP4 B1	-4.78	-27.4	639	2.429	1345	-0.12	0.88	0.32
09/01/2006	8:15PM		NAP4 C1								
09/01/2006	8:15PM		NAP4 D1	-4.75	-25.1	674	2.614	1445	0.00	3.41	1.70
10/01/2006	8:40AM	11	NAP4 A2								
10/01/2006	8:40AM	11	NAP4 B2	-4.65	-26.1	652	2.542	1406	0.40	2.31	1.55
10/01/2006	8:45AM	11	NAP4 C2								
10/01/2006	8:50AM	11	NAP4 D2	-4.54		651	2.461	1361	0.84		0.84
10/01/2006	8:50AM	11	NAP4 E2	-4.51	-26.1	691	2.664	1473	0.96	2.31	2.11
10/01/2006	8:55AM	11	NAP4 F2								
10/01/2006	12:45PM	15	NAP4 A3								
10/01/2006	12:45PM	15	NAP4 B3	-4.74	-27.5	656	2.535	1400	0.04	0.77	0.42
10/01/2006	12:45PM	15	NAP4 C3								
10/01/2006	12:45PM	15	NAP4 D3	-4.69		661	2.351	1300	0.24		0.24
10/01/2006	12:45PM	15	NAP4 E3	-4.15	-26.4	707	2.732	1512	2.40	1.98	3.39
10/01/2006	1:00PM		NAP4 EAST 0.30m	-4.82	-29.3	738	2.810	1552	-0.28	0.00	0.00
10/01/2006			NAP4 EAST 1.4m	-4.7	-27.3	783	2.959	1664	0.20	0.99	0.69
10/01/2006			NAP4 EAST 2.4m	-4.2	-23.2	668	2.852	1608	2.20	5.49	4.95
10/01/2006			NAP4 EAST 3.4m	-4.48	-25.1	813	2.899	1608	1.08	3.41	2.78
10/01/2006			NAP4 EAST PIEZO	-4.2	-24.9	984	3.459	1945	2.20	3.63	4.01
10/01/2006			NAP4 WEST 0.35m	-4.24	-27.8	1130	3.848	2144	2.04	0.44	2.26
10/01/2006			NAP4 WEST 1.4m	-4.58	-31.1	928	3.196	1776	0.68	0.00	0.68
10/01/2006			NAP4 WEST 2.4m	-4.09	-25.2	1198	3.887	2171	2.64	3.30	4.29
10/01/2006	3:00PM		NAP4 WEST 3.4m	-4.38	-25.4	878	3.288	1832	1.48	3.08	3.02
12/01/2006	5:00pm		NAP4 EAST 0.30m	-4.6	-24.4	671			0.60	4.18	2.69
12/01/2006			NAP4 EAST 1.4m	-4.72	-27.4	803	3.00	1664	0.12	0.88	0.56
12/01/2006			NAP4 EAST 2.4m	-4.43	-23.7	632	2.73	1512	1.28	4.95	3.75
12/01/2006	6:00pm		NAP4 EAST 3.4m	-4.42	-25.2	679			1.32	3.30	2.97

DATE	TIME	TIME (h)	SAMPLE ID	δ O18	δD	CHLORIDE	EC	TDS	DTW (mm)	Epan*Cp	% Loss (x_m)
09/01/2006	2:50PM	0	EPAN 1	-4.75	-28.2	697	2.592	1434	0.00	0	0.00
09/01/2006	8:00PM	5	EPAN 2	-4.51		722	2.526	1400	2.00	1.88	0.91
10/01/2006	9:00AM	13	EPAN 3	-4.25	-25.8	723	2.624	1451		0	0.00
10/01/2006	1:00PM	18	EPAN 4	-4.14		730	2.531	1400	5.00	3.55	2.27
10/01/2006	3:00PM	20	EPAN 5	-4.22	-26	733	2.715	1503	5.50	3.905	2.50
12/01/2006	5:30PM	74	EPAN 6	-2.21		777	2.979	1653	22.00	15.62	10.00

^{18}O Enrichment F	0.25
^{2}H Enrichment F	0.91

Average % Evap	
During Irrigation application and pon	1.323
During Ponding only	1.427

NAP4 MARCH

DATE	TIME	PONDING TIME (h)	SAMPLE ID	δ O18 (‰)	δD (‰)	CHLORIDE (mg/l)	EC (u/cm)	TDS (mg/l)	% Evap ^{18}O (x_c)	% Evap ^{2}H (x_c)	Average % evap
03/03/2006	9:30AM	1.5	NAP4 A	-4.82	-28.8			1384	0.00	0.00	0
03/03/2006	9:30AM	1.5	NAP4 B	-4.73	-29.6	649	2.532	1400	0.41	0.00	0.20
03/03/2006	9:30AM	1.5	NAP4 C								
03/03/2006	9:30AM	1.5	NAP4 D	-4.43	-27.8	715	2.770	1534	1.77	1.43	1.60
03/03/2006	9:30AM	1.5	NAP4 E	-4.52					1.36		1.36
03/03/2006	9:30AM	1.5	NAP4 EAST								
03/03/2006	9:30AM	1.5	NAP4 WEST								
03/03/2006	2:30PM	6.5	NAP4 A1								
03/03/2006	2:30PM	6.5	NAP4 B1	-4.19	-27.8	666	2.579	1428	2.86	1.43	2.15
03/03/2006	2:30PM	6.5	NAP4 C1								
03/03/2006	2:30PM	6.5	NAP4 D1	-4.5	-30.7	678	2.640	1462	1.45	0.00	0.73
03/03/2006	2:30PM	6.5	NAP4 E1	-3.92	-25.4	705	2.705	1498	4.09	4.86	4.47
03/03/2006	2:30PM	6.5	NAP EAST1								
03/03/2006	2:30PM	6.5	NAP WEST1								
03/03/2006	7:00PM	11	NAP4 A2								
03/03/2006	7:00PM	11	NAP4 B2	-4.58	-26.5	666	2.583	1428	1.09	3.29	2.19
03/03/2006	7:00PM	11	NAP4 C2								
03/03/2006	7:00PM	11	NAP4 D2	-4.49	-29.8	692	2.674	1480	1.50	0.00	0.75
03/03/2006	7:00PM	11	NAP4 E2	-2.98	-22.9	773	2.850	1580	8.36	8.43	8.40
03/03/2006	7:00PM	11	NAP EAST 2								
03/03/2006	7:00PM	11	NAP WEST 2								
04/03/2006	8:30 AM	23.5	NAPA3								
04/03/2006	9:30 AM	23.5	NAPC3								
04/03/2006	10:30 AM	23.5	NAPD3								
04/03/2006	11:30 AM	23.5	NAPE3								
04/03/2006	8:00AM		NAP4 EAST 0.30m	-4.29	-26.9	723	2.719	1507	2.41	2.71	2.56
04/03/2006			NAP4 EAST 1.4m	-4.37	-26.8	805	2.911	1613	2.05	2.86	2.45
04/03/2006			NAP4 EAST 2.4m	-4.45	-26.7	789	2.720	1507	1.68	3.00	2.34
04/03/2006			NAP4 EAST 3.4m	-4.46	-26.5	712	2.781	1540	1.64	3.29	2.46
04/03/2006			NAP4 WEST 0.35m	-3.87	-23.1	1427	4.391	2448	4.32	8.14	6.23
04/03/2006			NAP4 WEST 1.4m	-4.15	-26.8	1260	4.009	2227	3.05	2.86	2.95
04/03/2006			NAP4 WEST 2.4m	-4.37	-24.7	955	3.536	1962	2.05	5.86	3.95
04/03/2006	9:00PM		NAP4 WEST 3.4m	-4.38	-26.8	897	3.309	1838	2.00	2.86	2.43
03/03/2006			NAP4 BORE								
06/03/2006	6:00PM		NAP4 EAST 0.30m	-4.32	-21.7	727	3.099	1720	2.27	10.14	6.21
06/03/2006			NAP4 EAST 1.4m	-4.34	-25.2	834	3.271	1815		5.14	2.57
06/03/2006			NAP4 EAST 2.4m	-4.26	-26.9	804		1665	2.55	2.71	2.63
06/03/2006			NAP4 EAST 3.4m	-4.48	-26.7	715		1531	1.55	3.00	2.27
06/03/2006			NAP4 EAST PIEZO	-4.35	-25.9	977	3.558	1979	2.14	4.14	3.14
06/03/2006			NAP4 WEST 0.35m								
06/03/2006			NAP4 WEST 1.4m								
06/03/2006			NAP4 WEST 2.4m								
06/03/2006	5:00PM		NAP4 WEST 3.4m								
08/03/2006	10:30		NAP4 EAST 0.30m	-4.24	-27.5	753	2.97	1647	2.64	1.86	2.25
08/03/2006			NAP4 EAST 1.4m	-4.45	-26.9	851		1721	1.68	2.71	2.20
08/03/2006			NAP4 WEST 0.35m								
08/03/2006			NAP4 WEST 1.4m								
08/03/2006			NAP4 WEST 2.4m								
08/03/2006	11:30		NAP4 WEST 3.4m								

^{18}O Enrichment F	0.22
^{2}H Enrichment F	0.70

Average % Evap During Ponding	2.427

DATE	TIME	TIME (h)	SAMPLE ID	δ O18	δD	CHLORIDE	EC	TDS	DTW (mm)	Epan*Cp	% Loss (x_m)
03/03/2006	9:00AM	0	NAP4 PAN1	-4.82	-28.8	649	2.499	1384	0	0.00	0.00
03/03/2006	3:00PM	6	NAP4 PAN2	-4.63	-27.3	646	2.573	1378	2	1.84	0.91
03/03/2006	7:30PM	10.5	NAP4 PAN3	-4.37	-26.2	668	2.580	1428	4	3.68	1.82
04/03/2006	9:00AM	24	NAP4 PAN4	-4.04	-26.1	681	2.581	1428	8	7.36	3.64
06/03/2006	5:00PM	56	NAP4 PAN5	-1.99		800		1600	28	21	12.73

Pc
0.92
0.75

PG JANUARY

DATE	TIME	PONDING TIME (h)	SAMPLE ID	δ O18 (‰)	δD (‰)	CHLORIDE (mg/l)	EC (u/cm)	TDS (mg/l)	% Evap ^{18}O (x_c)	% Evap ^{2}H (x_c)	Average % evap
			BORE	-4.99	-31.1	3550	11.340	6498.0	0.00	0.00	0.00
13/01/2006	12:40PM		PG A								
13/01/2006	12:35PM		PG B	-5.06	-31.5	3440	11.280	6464.0	0.00	0.00	0.00
13/01/2006	2:55PM		PG B1	-5.05	-30.6	3540	11.460	6567.0	0.00	0.96	0.48
13/01/2006	3:00PM		PG C1	-4.99		3550	11.290	6470.0	0.00		0.00
13/01/2006	3:05PM		PG D1	-4.99	-31.5	3510	11.400	6533.0	0.00	0.00	0.00
13/01/2006	6:30PM	1.5	PG A2								
13/01/2006			PG B2	-4.98		3520	11.270	6458.0	0.03		0.03
13/01/2006			PG C2	-5	-31.2	3520	11.270	6458.0	0.00	0.00	0.00
13/01/2006			PD D2	-5.05	-32.8	3510	11.310	6481.0	0.00	0.00	0.00
13/01/2006	6:55PM	2	PG E2	-5.04	-30.1	3490	11.310	6481.0	0.00	1.92	0.96
15/01/2006			PG S.L 0.45m	-4.68	-29.7	5360	14.86	8627.0	0.81	2.69	1.75
15/01/2006			PG S.L 0.80m	-4.91	-30.3	4770	13.57	7849.0	0.21	1.54	0.87
15/01/2006			PG S.L 1.45m	-3.58	-21.9	5660	15.94	9288.0	3.67	17.69	10.68
15/01/2006			PG S.L 3.00m	-4.17	-25	6140	18.240	10725	2.13	11.73	6.93
15/01/2006			PG PIEZO	-4.45	-25.3	4300	12.940	7456	1.40	11.15	6.28

DATE	TIME	TIME (h)	SAMPLE ID	d O18	dD	CHLORIDE	EC	TDS	DTW (mm)	Epan*Cp	% Loss
13/01/2006	9:00AM	0	PG PAN1	-4.99	-31.1	3550	11.340	6498	0	0	0.00
13/01/2006	12:45PM	3.75	PG PAN2	-4.87	-32.1	3590	11.430	6550	1	0.84	0.45
13/01/2006	3:20Pm	6.25	PG PAN 3	-4.54	-31.2	3610	11.500	6590	2	1.68	0.91
13/01/2006	6:30PM	9.5	PG PAN 4	-4.32	-30.5	3640	11.530	6619	4	3.36	1.82
14/01/2006		52	PG PAN5						25	21	

^{18}O Enrichment F	0.3847
^{2}H Enrichment F	0.52

Average % Evap	
During Irrigation and ponding	0.184
During Ponding only	0.248

PG FEBRUARY

DATE	TIME	PONDING TIME (h)	SAMPLE ID	δ O18 (‰)	δD (‰)	CHLORIDE (mg/l)	EC (u/cm)	TDS (mg/l)	% Evap ^{18}O (x_c)	% Evap ^{2}H (x_c)	Average % evap
			BORE SAMPLE	-5	-33						
			BORE	-4.84	-31.3	3649	11.270	6458	0.00	0.00	0.00
13/02/2006	12:15PM		PG B								
13/02/2006			PG C	-4.79	-32.2	3700	11.350	6504	0.16	0.00	0.08
13/02/2006	3:10PM		PG C1	-4.88	-32.7	3619	11.210	6424	0.00	0.00	0.00
13/02/2006			PG D	-4.82	-32	3675	11.340	6498	0.06	0.00	0.03
13/02/2006	5:15PM	1.75	PG E	-4.82	-31.7	3633	11.220	6430	0.06	0.00	0.03
13/02/2006	6:00PM	2.5	PG A								
13/02/2006			PG B1								
13/02/2006			PG C2	-4.79	-32.9	3635	11.220	6430	0.16	0.00	0.08
13/02/2006			PG D1	-4.8	-31.4	3636	11.230	6435	0.13	0.00	0.06
13/02/2006	8:00PM	4.5	PG B2								
13/02/2006			PG C3	-4.66	-30.6	3651	11.260	6452	0.58	0.80	0.69
13/02/2006			PG D2	-4.84	-30.7	3672	11.200	6418	0.00	0.68	0.34
13/02/2006			PG E1	-4.75	-29.9	3707	11.260	6452	0.29	1.59	0.94
15/02/2006			PG S.L 0.45m	-4.76	-30.5	6353	17.740	10412	0.26	0.91	0.58
15/02/2006			PG S.L 0.80m	-4.8	-31.3	4350	13.250	7650	0.13	0.00	0.06
15/02/2006			PG S.L 1.45m	-4	-25.8	8045	21.460	12764	2.71	6.25	4.48
15/02/2006			PG S.L 3.00m	-3.8	-26.6	4365	14.660	8511	3.35	5.34	4.35
15/02/2006			PG PIEZO	-4.51	-28.5	4693	14.090	8164	1.06	3.18	2.12

DATE	TIME	TIME (h)	SAMPLE ID	d O18	dD	CHLORIDE	EC	TDS	DTW (mm)	Epan*Cp	% Loss (x_m)
13/02/2006	12:15PM	0	PG PAN 1	-4.84	-31.3	3649	11.270	6458	0	0	0.00
13/02/2006	3:30PM	3.25	PG PAN 2	-4.53	-31.9	3646	11.290	6470	1	0.9	0.45
13/02/2006	6:00PM	5.75	PG PAN 3	-4.32	-31.7	3693	11.330	6493	3	2.7	1.36
13/02/2006	8:00PM	7.75	PG PAN 4	-4.24	-29.4	3667	11.400	6533	4	3.6	1.82
15/02/2006			PG PAN 5	-5.69	-23.5	4023 44	12.210	7023			

^{18}O Enrichment F	0.31
^{2}H Enrichment F	0.88

Average % Evap	
During Irrigation application and ponding	0.20545
During Ponding only	0.42295

MTM DECEMBER

DATE	TIME	PONDING TIME (h)	SAMPLE ID	δ O18 (‰)	δD (‰)	CHLORIDE (mg/l)	EC (u/cm)	TDS (mg/l)	% Evap ^{18}O (x_c)	% Evap ^{2}H (x_c)	Average % evap
			BORE	-4.22	-26.4	2722	8.60	4874	0	0	0
14/12/2005	12:42 PM		MTM A	-4.18	-27.7	2776	8.40	4757	0.11	0.00	0.05
14/12/2005	1:00 PM		MTM B	-4.05	-26.1	2784	8.59	4868	0.45	0.32	0.38
14/12/2005	1:05 PM		MTM C								
14/12/2005			MTM D	-4.1	-24.5	2806	8.63	4893	0.32	2.02	1.17
14/12/2005			MTM E	-3.94	-25	2802	8.57	4857	0.74	1.49	1.11
14/12/2005	3:00 PM	2.00	MTM C1								
14/12/2005	3:00 PM	2.00	MTM D1	-3.84	-24.9	2820	8.59	4868	1.00	1.60	1.30
14/12/2005	3:00 PM	2.00	MTME1	-3.94	-26.6	2786	8.51	4823	0.74	0.00	0.37
14/12/2005	5:00 PM	4.00	MTM C2	-2.88	-23	2944	8.93	5069	3.53	3.62	3.57
14/12/2005		4.00	MTM D2	-3.01	-20.1	2970	9.05	5139	3.18	6.70	4.94
14/12/2005		4.00	MTM E2	-3.44	-21.5	2885	8.75	4963	2.05	5.21	3.63
14/12/2005		4.00	MTM S1								
14/12/2005		4.00	MTM S2	-3.88	-23.2	2761	8.62	4888	0.89	3.40	2.15
14/12/2005	5:30PM	4.50	MTM S3	-3.69	-21.6	2793	8.70	4933	1.39	5.11	3.25
15/12/2005	time?		MTM S.L 1m	-3.77	-22.2	4060	12.10	6889	1.18	4.47	2.83
15/12/2005			MTM S.L 2m	-3.77	-22.4	6130	17.00	9942	1.18	4.26	2.72
15/12/2005			MTM S.L 3m	-3.8	-23	4600	13.40	7794	1.11	3.62	2.36
15/12/2005			Piezo	-4.09	-23.9	2730	9.00	5108	0.34	2.66	1.50

DATE	TIME	TIME (h)	SAMPLE ID	d O18	dD	CHLORIDE	EC	TDS	DTW (mm)	Epan*Cp	% Loss (x_m)
14/12/2005	12:30 PM	0	BORE PAN 1	-4.22	-26.4	2722	8.550	4845	0	0	0.00
14/12/2005	3:00 PM	1.5	MTM PAN 2	-4.32	-28.1	2781	8.380	4746	1	0.76	0.45
14/12/2005	5:30 PM	4	MTM PAN 3	-3.88	-25	2837	8.740	4957	2	1.52	0.91
15/12/2005	time?	7.75	MTM PAN 4	-3.44	-20.8	2845	8.97	4991	5	3.8	2.27

Cp 0.76

SLUICE GATE OPEN	10:30 AM	12/14/2005
SLUICE GATE CLOSE	12:55 PM	12/14/2005

^{18}O Enrichment F	0.38
^{2}H Enrichment F	0.94

Average % Evap	
During Irrigation and ponding	1.994
During Ponding only	2.745

MTM FEBRUARY

DATE	TIME	PONDING TIME (h)	SAMPLE ID	δ O18 (‰)	δD (‰)	CHLORIDE (mg/l)	EC (u/cm)	TDS (mg/l)	% Evap ^{18}O (x_c)	% Evap ^{2}H (x_c)	Average % evap
09/02/2006	12:15PM		MTM A	-4.19	-25.5	2528	8.07	4565	0	0	0
09/02/2006	1:45PM		MTM B								
09/02/2006	1:45PM		MTM C								
09/02/2006	2:30PM		MTM D	-4.19	-25.7	2538	8.07	4565	0.00	0.00	0.00
09/02/2006	4:00PM	0.5	MTM E	-4.24	-26.1	2516	8.15	4612	0.00	0.00	0.00
09/02/2006	5:00PM	1.5	A1								
09/02/2006	5:00PM	1.5	B1								
09/02/2006	5:00PM	1.5	C1	-4.18	-24.3	2527	8.12	4595	0.05	1.28	0.66
09/02/2006	5:00PM	1.5	D1								
09/02/2006	5:00PM	1.5	E1	-2.55	-24.1	2542	8.13	4600	8.63	1.49	5.06
09/02/2006	7:00PM	2.5	B2								
09/02/2006	7:00PM	2.5	C2	-4.19	-25.1	2535	8.17	4623	0.00	0.43	0.21
09/02/2006	7:00PM	2.5	D2	-4.08	-24.7	2507	8.11	4589	0.58	0.85	0.72
09/02/2006	7:00PM	2.5	E2	-3.94	-26.1	2511	8.16	4617	1.32	0.00	0.66
12/02/2006			MTM S.L 1m	-4	-27.1	4999	14.05	7000	1.00	1.00	1.00
12/02/2006			MTM S.L 2m	-3.79	-25.3	6481	16.960	9919	2.11	2.00	2.05
12/02/2006			MTM S.L 3m	-3.81	-24.9	4717	12.660	7295	2.00	3.00	2.50
12/02/2006			Piezo	-4.03	-25.4	2773	8.580	4863	0.84	4.00	2.42

^{18}O Enrichment F	0.19
^{2}H Enrichment F	0.94

Average % Evap	
During Irrigation application and ponc	0.220
During Ponding only	0.623

Excludes cell L11

DATE	TIME	TIME (h)	SAMPLE ID	d O18	dD	CHLORIDE	EC	TDS	DTW (mm)	Epan*Cp	% Loss (x_m)
09/02/2006	10AM	0	PAN1	-4.11	-23.2	2527	8.13	4600	0.0	0.00	0.00
09/02/2006	12:30PM	2.5	PAN2	-4.09	-23.3	2536	8.17	4623	1.0	0.76	0.45
09/02/2006	2:30PM	4.5	PAN3	-4.02	-24.4	2550	8.15	4612	3.0	2.28	1.36
09/02/2006	5:15PM	7.25	PAN4	-3.83	-27	2570	8.22	4654	5.0	3.80	2.27
09/02/2006	7:00PM	9	PAN5	-3.75	-22.6	2568	8.21	4648	6.0	4.56	2.73
10/02/2006	9:00AM	23	BOM						12.1		5.50
10/02/2006			PAN6								
13/02/2006	12:00PM	76	PAN7	-1.59	-17.9	2835	8.45	4757	29	22.04	13.18

Cp = 0.76

gate shut at 3:30pm

APPENDIX C

Pan calibration and evaporation calculations

Pan calibration NAP4 - January 2006

	δs	δi	h	δ_A	x	Δe	e	enrichment f
$\delta^{18}O$	-4.75	-2.21	0.94	-26.0093	1.0093	14.2(1-h)	x-1	1.8613
						0.852	0.0093	
$\delta^{2}H$	-28.2	-26	0.94	-151.09	1.09	12.5(1-h)		13.59
						12.5	0.09	

	f	%E calulated	% E measured from Epan
$\delta^{18}O$	0.0998	9.98	10
$\delta^{2}H$	0.0604	6.04	2.5

Estimation of δ_A

$\delta^{18}O_A$	-25
$\delta^{2}H_A$	-150

Estimations of δ_A and h which produce a close fit

h	$\delta^{18}O_A$	$\delta^{2}H_A$
0.9	-36	-270
0.87	-46	-340

% evaporation (calculation based on 18O)

Irrigation volume (Ml)	Pomding Time (h)	Location	δs	δi	f	% E Gonfiantini	%E Simpson	Evap (mm)
		BORE	-4.75	-4.75	0.00	0.00	0.00	0.00
1.79		A						
1.79		B						
4.40		A1						
4.49		B1	-4.78	-4.78	0.00	-0.12	0.32	0.00
4.54		C1						
4.54		D1	-4.75	-4.75	0.00	0.00	1.70	0.89
	11	A2						
	11	B2	-4.65	-4.65	0.00	0.39	1.55	1.02
	11	C2						
	11	D2	-4.54	-4.54	0.01	0.83	0.84	0.87
	11	E2	-4.51	-4.51	0.01	0.94	2.11	1.60
	11	F2						
	15	A3						
	15	B3	-4.74	-4.74	0.00	0.04	0.42	0.24
	15	C3						
	15	D3	-4.69	-4.69	0.00	0.24	0.24	0.25
	15	E3	-4.15	-4.15	0.02	2.36	3.39	3.02
Averages (ponding)						0.80	1.43	1.17

% evaporation of Epan water (calculation based on $\delta^{18}O$)

δ18O pan	f	E% Caculated (Gonfiantini)	E% Measured
-4.75	0.00	0.00	0.00
-4.51	0.01	0.94	0.91
-4.25	0.02	1.96	
-4.14	0.02	2.40	2.27
-4.22	0.02	2.08	2.50
-2.21	0.10	9.98	10

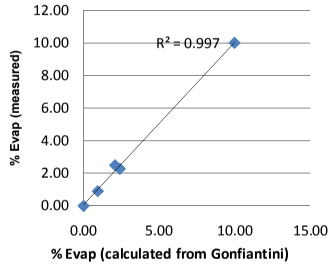

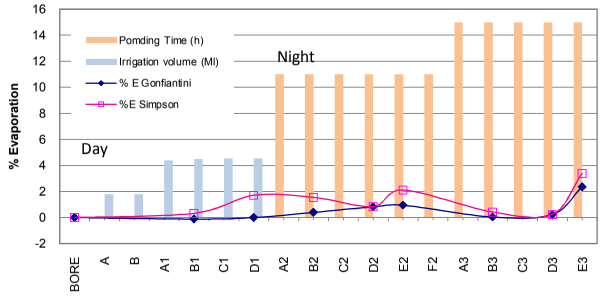

Pan calibration NAP4 - March 2008

	δs	δi	h	δ_A	x	Δe	e	enrichment f
$\delta^{18}O$	-4.82	-1.99	0.955	-19.0093	1.0093	14.2(1-h)	x-1	1.6483
						0.639	0.0093	
$\delta^{2}H$	-28.8	-26.1	0.955	-131.09	1.09	12.5(1-h)		13.59
						12.5	0.09	

	f	%E calulated	% E measured from Epan
$\delta^{18}O$	0.1208	12.08	12
$\delta^{2}H$	0.0757	7.57	3

Estimation of δ_A

$\delta^{18}O_A$	-18
$\delta^{2}H_A$	-130

Estimations of δ_A and h which produce a close fit

h	$\delta^{18}O_A$	$\delta^{2}H_A$
0.9	-36	-270
0.87	-46	-340

% evaporation (calculation based on 18O)

Pomding Time (h)	Location	δs	δi	f	% E Gonfiantini (eq 2)	%E Simpson (eq 3)	Evap (mm)
1.5	A	-4.82	-4.82	0.00	0.00	0.00	
1.5	B		-4.73	0.00	0.38	0.41	0.60
1.5	C						
1.5	D		-4.43	0.02	1.66	1.77	2.60
1.5	E		-4.52	0.01	1.28	1.36	2.00
6.5	A1						
6.5	B1		-4.19	0.03	2.69	2.86	4.19
6.5	C1						
6.5	D1		-4.50	0.01	1.37	1.45	2.13
6.5	E1		-3.92	0.04	3.84	4.09	5.99
11	A2						
11	B2		-4.58	0.01	1.02	1.09	1.60
11	C2						
11	D2		-4.49	0.01	1.41	1.50	2.20
11	E2		-2.98	0.08	7.85	8.36	12.24
Averages (Ponding)					3.03	3.23	4.72

% evaporation of Epan water (calculation based on $\delta^{18}O$)

δ18O pan	f	E% Caculated (Gonfiantini)	E% Measured
-4.82	0.00	0.00	0.00
-4.63	0.01	0.81	0.91
-4.37	0.02	1.92	1.82
-4.04	0.03	3.33	3.64
-1.99	0.12	12.08	12.73

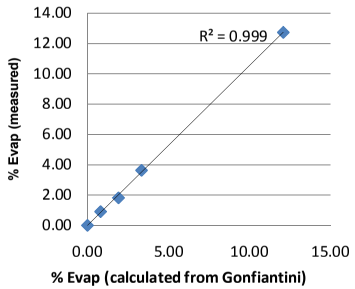

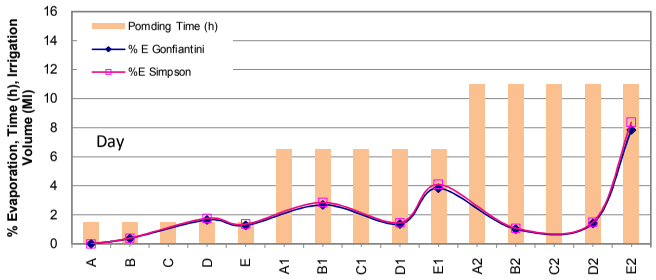

Pan calibration NAP5 - November 2005

	δs	δi	h	δ_A	x	Δe	e	enrichment f
$\delta^{18}O$	-4.27	-3.31	0.923	-34.0093	1.0093	14.2(1-h)	x-1	2.1027
						1.0934	0.0093	
$\delta^{2}H$	-23.8	-20.4	0.8	-261.09	1.09	12.5(1-h)		13.59
						12.5	0.09	

	f	%E calulated	% E measured from Epan
$\delta^{18}O$	0.0362	3.62	3.64
$\delta^{2}H$	0.0906	9.06	3.64

Estimation of δ_A

$\delta^{18}O_A$	-33
$\delta^{2}H_A$	-260

Estimations of δ_A and h which produce a close fit

h	$\delta^{18}O_A$	$\delta^{2}H_A$

% evaporation of flood irrigation water (calculation based on $\delta^{18}O$)

Volume applied (Ml)	Ponding time (h)	Location	δs	δi	f	% E Gonfiantini	%E Simpson	Evap (mm)
0.3	0	BORE	-4.27	-4.27	0.00	0.00	0.00	0.00
0.53	0	A		-4.32	0.00	-0.19	0.00	0.00
0.53	0	B						
0.53	0	C						
0.53	0	B1						
0.53	0	C1						
0.53	0	D1						
2.76	0	E1		-4.25	0.00	0.08	0.28	0.26
2.76	0	B2						
	13	C2		-4.10	0.01	0.64	0.88	1.13
	13	D2						
	13	E2		-4.11	0.01	0.60	0.84	1.07
	13	F2		-3.84	0.02	1.62	1.92	2.62
	13	B3						
	13	C3						
	13	E3						
	13	F3						
	13	B4						
	19	C4		-3.06	0.05	4.56	5.04	7.10
	19.6	E4		-3.11	0.04	4.37	4.84	6.82
	19.6	F4		-2.71	0.06	5.88	6.44	9.12
Averages (Ponding)						2.95	3.33	4.64

% evaporation of Epan water (calculation based on $\delta^{18}O$)

δ18O pan	f	E% Caculated (Gonfiantini)	E% Measured
-4.27	0.000	0.00	0.00
-4.15	0.005	0.45	0.91
-3.77	0.019	1.88	2.45
-3.31	0.036	3.62	3.64

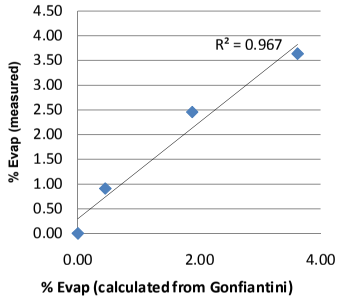

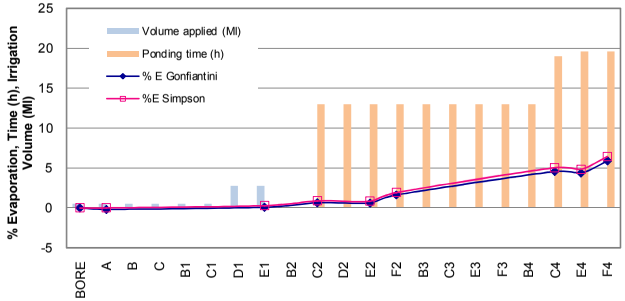

Pan calibration NAP5 - March 2006

	δs	δi	h	δ_A	x	Δe	e	enrichment f
$\delta^{18}O$	-4.26	-3.28	0.935	-20.0093	1.0093	14.2(1-h)	x-1	1.9323
						0.923	0.0093	
$\delta^{2}H$	-23.8	-22.5	0.935	-141.09	1.09	12.5(1-h)		13.59
						12.5	0.09	

	f	%E calulated	% E measured from Epan
$\delta^{18}O$	0.0545	5.45	5.45
$\delta^{2}H$	0.0412	4.12	2

Estimation of δ_A

$\delta^{18}O_A$	-19
$\delta^{2}H_A$	-140

Estimations of δ_A and h which produce a close fit

h	$\delta^{18}O_A$	$\delta^{2}H_A$
0.9	-28	-210
0.88	-34	-250
0.835	-49	-349
0.864	-38.6	-290

% evaporation of flood irrigation water (calculation based on $\delta^{18}O$)

Volume applied (Ml)	Ponding time (h)	Location	δs	δi	f	% E Gonfiantini	%E Simpson	Evap (mm)
		BORE	-4.26	-4.26	0.00	0.00	0.00	0.00
0.92		A						
0.92		B						
0.92		C						
3.22		B1						
3.22		C1		-4.02	0.01	1.33	0.97	1.26
3.22		D1						
3.22	14	E1		-3.95	0.02	1.72	0.86	1.12
3.22	14	B2						
	14	C2		-4.09	0.01	0.95	1.66	2.16
	14	D2						
	14	E2		-3.76	0.03	2.78	2.57	3.34
	18	F2		-3.50	0.04	4.23	3.45	4.49
	18	B3						
	18	C3						
	18	E3		-3.28	0.05	5.45	4.89	6.35
	22.5	F3		-3.18	0.06	6.01	4.91	6.38
	22.5	B4						
	22.5	C4		-2.92	0.07	7.45	6.56	8.52
	22.5	E4		-2.31	0.11	10.85	8.42	10.95
	22.5	F4		-2.46	0.10	10.01	8.18	10.64
Averages (ponding)						5.49	4.17	6.00

% evaporation of Epan water (calculation based on $\delta^{18}O$)

δ18O pan	f	E% Caculated (Gonfiantini)	E% Measured
-4.26	0.00	0.00	0.00
-3.92	0.02	1.89	1.36
-3.59	0.04	3.73	3.64
-3.45	0.05	4.50	4.55
-3.28	0.05	5.45	5.45
-2.16	0.12	11.68	9.55

$$\%E = \frac{(\delta s-\delta i)(1-h+\Delta\epsilon)}{(\delta s+1)(\Delta\epsilon+\epsilon/\epsilon^{*})+h(\delta_A-\delta s)}$$

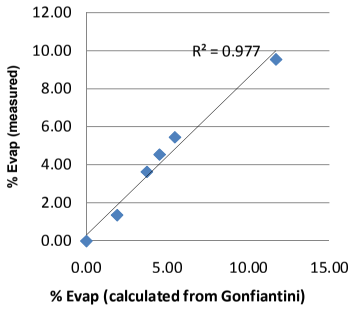

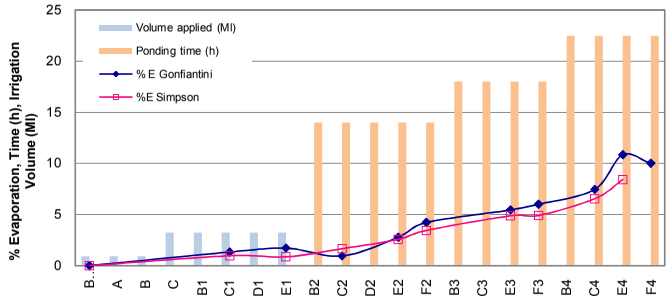

Pan calibration PG - January 2006

	δs at t_o	δi at t_1	h	δ_A	x	Δe	e	enrichment f
$\delta^{18}O$	-4.99	-4.32	0.95	-31.0093	1.0093	14.2(1-h)	x-1	1.7193
						0.71	0.0093	
$\delta^{2}H$	-31.3	-30.5	0.95	-171.09	1.09	12.5(1-h)		13.59
						12.5	0.09	

	f	%E calulated	% E measured from Epan
$\delta^{18}O$	0.0185	1.85	1.82
$\delta^{2}H$	0.0195	1.95	1.82

Estimation of δ_A

$\delta^{18}O_A$	-30
$\delta^{2}H_A$	-170

Estimations of δ_A and h which produce a close fit

h	$\delta^{18}O_A$	$\delta^{2}H_A$
0.95	-31.0093	-171.09

% evaporation (calculation based on 18O)

Volume applied (Ml)	Ponding time (h)		δs at to	δi at t1	f	% E Gonfiantini	%E Simpson
0		BORE	-4.99	-4.99	0.00	0.00	0.00
0.83		A					
0.83		B		-5.06	0.00	-0.19	0.00
1.65		B1		-5.05	0.00	-0.17	0.00
2.20		C1		-4.99	0.00	0.00	0.00
2.20		D1		-4.99	0.00	0.00	0.00
	1.5	A2					
	1.5	B2		-4.98	0.00	0.03	0.03
	2	C2		-5	0.00	-0.03	0.00
	2	D2		-5.05	0.00	-0.17	0.00
	2	E2		-5.04	0.00	-0.14	0.00

% evaporation of Epan water (calculation based on $\delta^{18}O$)

δ18O pan	f	E% Caculated (Gonfiantini)	E% Measured
-4.99	0.00	0.00	0.00
-4.87	0.00	0.33	0.45
-4.54	0.01	1.24	0.91
-4.32	0.02	1.85	1.82

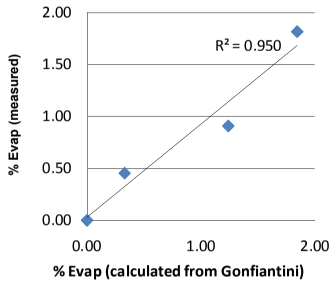

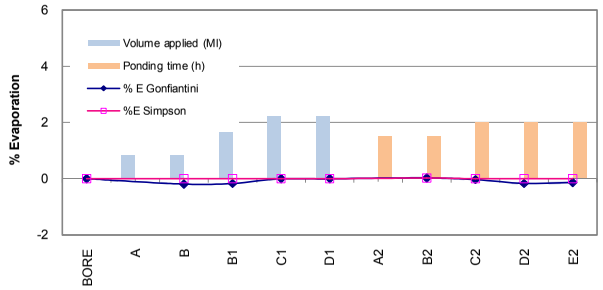

Pan calibration PG - February 2006

	δs at t_o	δi at t_1	h	δ_A	x	Δe	e	enrichment f
$\delta^{18}O$	-4.84	-4.24	0.95	-26.0093	1.0093	14.2(1-h)	x-1	1.7193
						0.71	0.0093	
$\delta^{2}H$	-31.3	-29.4	0.95	-171.09	1.09	12.5(1-h)		13.59
						12.5	0.09	

	f	%E calulated	% E measured from Epan
$\delta^{18}O$	0.0199	1.99	1.82
$\delta^{2}H$	0.0464	4.64	1.82

Estimation of δ_A

$\delta^{18}O_A$	-25
$\delta^{2}H_A$	-170

Estimations of δ_A and h which produce a close fit

h	$\delta^{18}O_A$	$\delta^{2}H_A$
0.95	-25	-170

% evaporation (calculation based on 18O)

Volume applied (Ml)	Ponding time (h)	Location	δs at to	δi at t1	f	% E Gonfiantini	%E Simpson	Evaporation (mm)
0	-	BORE	-4.84	-5	-0.01	-0.53		
1.51	-	A		-4.84	0.00	0.00	0.00	
1.51	-	B						
1.51	-	B1		-4.79	0.00	0.17	0.08	0.19
3.12	-	C1		-4.88	0.00	-0.13	0.00	
3.12	-	D1		-4.82	0.00	0.07	0.03	0.08
3.30	1.75	E1		-4.82	0.00	0.07	0.03	0.08
_	2.50	B2						
-	2.50	C2						
-	2.50	D2		-4.79	0.00	0.17	0.08	0.19
-	2.50	E2		-4.8	0.00	0.13	0.06	0.15
-	4.50	B3						
-	4.50	C3		-4.66	0.01	0.60	0.69	1.00
-	4.50	D3		-4.84	0.00	0.00	0.34	0.26
-	4.50	E3		-4.75	0.00	0.30	0.94	0.96
Averages (Ponding)						0.15	0.25	0.36

% evaporation of Epan water (calculation based on $\delta^{18}O$)

δ18O pan	f	E% Caculated (Gonfiantini)	E% Measured
-4.84	0.00	0.00	0.00
-4.53	0.01	1.03	0.45
-4.32	0.02	1.73	1.36
-4.24	0.02	1.99	1.82
-5.69			

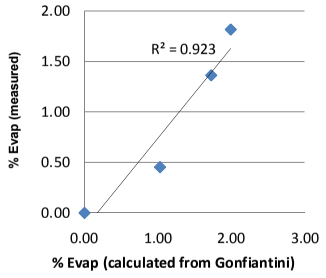

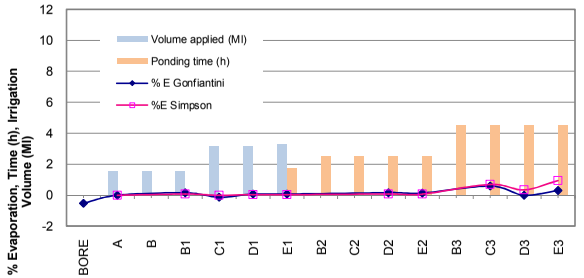

Pan calibration MTM - December 2005

	δs at t_o	δi at t_1	h	δ_A	x	Δe	e	enrichment f
$\delta^{18}O$	-4.22	-3.44	0.97	-19.0093	1.0093	14.2(1-h)	x-1	1.4353
						0.426	0.0093	
$\delta^{2}H$	-26.4	-25.1	0.97	-121.09	1.09	12.5(1-h)		13.59
						12.5	0.09	

	f	%E calulated	% E measured from Epan
$\delta^{18}O$	0.0226	2.26	2.3
$\delta^{2}H$	0.0396	3.96	0.9

Estimation of δ_A

$\delta^{18}O_A$	-18
$\delta^{2}H_A$	-120

Estimations of δ_A and h which produce a close fit

h	$\delta^{18}O_A$	$\delta^{2}H_A$
0.91	-45	-350
0.95	-25	-185

% evaporation (calculation based on 18O)

Volume applied (Ml)	Ponding time (h)	Location	δs at to	δi at t1	f	% E Gonfiantini	%E Simpson	Evaporation (mm)
		BORE	-4.22	-4.22	0.00	0.00	0.00	0.00
1.03		A		-4.18	0.00	0.12	0.05	0.15
1.2		B		-4.05	0.00	0.49	0.38	0.81
1.2		C						
1.2		D		-4.10	0.00	0.35	1.17	1.39
1.2		E		-3.94	0.01	0.81	1.11	1.77
	2.00	C1						
	2.00	D1		-3.84	0.01	1.10	1.30	2.21
	2.00	E1		-3.94	0.01	0.81	0.37	1.08
	4.00	C2		-2.88	0.04	3.88	3.57	6.86
	4.00	D2		-3.01	0.04	3.50	4.94	7.77
	4.00	E2		-3.44	0.02	2.26	3.63	5.42
	4.00	S1						
	4.00	S2		-3.88	0.01	0.98	2.15	2.88
	4.50	S3		-3.69	0.02	1.53	3.25	4.40
Averages (Ponding)						2.01	2.74	4.37

% evaporation of Epan water (calculation based on $\delta^{18}O$)

δ18O pan	f	E% Caculated (Gonfiantini)	E% Measured
-4.22	0.00	0.00	0.00
-4.32	0.00		0.45
-3.88	0.01	0.98	0.91
-3.44	0.02	2.26	2.27

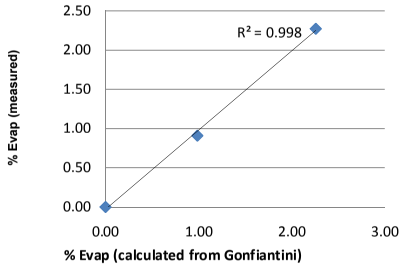

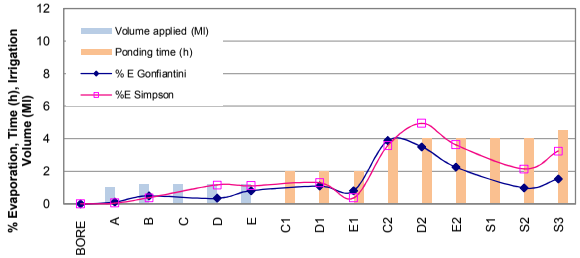

Pan calibration MTM - February 2006

	δs at t_0	δi at t_1	h	δ_A	x	Δe	e	enrichment f
$\delta^{18}O$	-4.11	-1.59	0.91	-28.5093	1.0093	14.2(1-h)	x-1	2.2873
						1.278	0.0093	
$\delta^{2}H$	-23.2	-17.9	0.95	-171.09	1.09	12.5(1-h)		13.59
						12.5	0.09	

	f	%E calulated	% E measured from Epan
$\delta^{18}O$	0.1315	13.15	13.18
$\delta^{2}H$	0.1584	15.84	13.18

Estimation of δ_A

$\delta^{18}O_A$	-27.5
$\delta^{2}H_A$	-170

Estimations of δ_A and h which produce a close fit

h	$\delta^{18}O_A$	$\delta^{2}H_A$
0.91	-28.5093	-171.09

% evaporation (calculation based on 18O)

Volume applied (Ml)	Ponding time (h)	Location	δs at to	δi at t1	f	% E Gonfiantini	%E Simpson	Evap (mm)
		BORE	-4.22	-4.22	0.00	0.00	0.00	0.00
0		A		-4.19	0.00	0.16	0.00	0.41
0.72		B						
0.72		C						
1.08		D		-4.19	0.00	0.16	0.00	0.41
1.8	0.5	E		-4.24	0.00	-0.10	0.00	0.00
	1.50	A1						
	1.50	B1						
	1.50	C1		-4.18	0.00	0.21	0.66	1.41
	1.50	D1						
	1.50	E1		-2.55	0.09	8.70	5.06	
	2.50	B2						
	2.50	C2		-4.19	0.00	0.16	0.21	0.68
	2.50	D2						
	2.50	E2		-3.94	0.01	1.46	0.66	4.65
Averages (ponding)						2.08	1.32	0.70

% evaporation of Epan water (calculation based on $\delta^{18}O$)

δ18O pan	f	E% Caculated (Gonfiantini)	E% Measured
-4.11	0.01	0.57	0.00
-4.09	0.01	0.68	0.45
-4.02	0.01	1.04	1.36
-3.83	0.02	2.03	2.27
-3.75	0.02	2.45	2.73
-1.59	0.14	13.71	13.18